



POLITECNICO
MILANO 1863

Iran First International Combustion School (ICS2019)
Tehran, 24-26 August 2019

Combustion modeling

3. Numerical methods for 1D and multi-dimensional flames

Alberto Cuoci

References

[Bisetti2015] **F. Bisetti**, *Short Course on Reactive Flow Modelling*, International CI Summer School 2015, Procida (Italy)

[Cuoci2019] **A. Cuoci**, *Numerical modeling of reacting systems with detailed kinetic mechanisms*, *Computer Aided Chemical Engineering*, 45, p. 675-721 (2019)

[Kee2017] **R.J. Kee, M.E. Coltrin, P. Glarborg**, *Chemically Reacting Flow: Theory and Practice*, Wiley, 2 edition, 2017

[Oran2001] **E. Oran, J.P. Boris**, *Numerical simulation of reactive flows*, Cambridge University Press (2001)

[RD2000] **Reaction Design**, *CHEMKIN, A software package for the analysis of gas-phase chemical and plasma kinetics*, CK-TUT-10112-1112-UG-1, CHE-036-1, CHEMKIN Collection Release 3.6, September 2000,
<https://www3.nd.edu/~powers/ame.60636/chemkin2000.pdf>

1. Introduction

Combustion and transport phenomena & laminar flames

2. Numerical solution of 1D flames

- a) Premixed laminar flames
 - i. Burner stabilized unstretched (or flat) flame
 - Governing equations and modeling aspects
 - Numerical solution
 - ii. Freely-propagating unstretched (or flat) flame
 - Governing equations and modeling aspects
- b) Counterflow diffusion flames

3. Multidimensional flames

- a) Introduction and examples
- b) Governing equations
- c) Numerical algorithms for multidimensional flames
- d) The operator-splitting method

1. Introduction

Combustion and transport phenomena & laminar flames.

2. Numerical solution of 1D flames

- a) Premixed laminar flames
 - i. Burner stabilized unstretched (or flat) flame
 - Governing equations and modeling aspects
 - Numerical solution
 - ii. Freely-propagating unstretched (or flat) flame
 - Governing equations and modeling aspects
- b) Counterflow diffusion flames

3. Multidimensional flames

- a) Introduction and examples
- b) Governing equations
- c) Numerical algorithms for multidimensional flames
- d) The operator-splitting method

Transport phenomena in reacting flows

- Chemical production and destruction is not only chemistry, but it also depends on **heat and mass transport** due to convection, diffusion, conduction.
- In ideal cases such as homogeneous ideal reactors, composition and temperature fields are only kinetically limited. In general, kinetic models developed in these simulations are later used for more complex flow conditions, including **laminar 1D or 2D flames**.
- In laminar flames, as well as in non homogeneous reactors, heat and mass transport can become rate limiting.
- It is necessary to characterize the **molecular transport** of species, momentum, and energy in a multicomponent gaseous mixture.
- The corresponding numerical problem requires the **solution of PDE systems** using proper numerical methods.

Examples of Laminar Flames and devices

3D laminar flames

They require computationally expensive CFD simulations

2D laminar flames

- Laminar coflow flames
- Slot burners

1D flames

- Counterflow (premixed/partially premixed/diffusive/pool flames)
- Premixed flat flames (burner stabilized or freely propagating flames)
- Conical or 2D Bunsen burner, stagnation flames, Tsuji burner
- Isolated fuel droplet in microgravity

The flames that can be modeled using a 1D model are **extremely useful** for studying the kinetics of combustion at high temperature and in presence of diffusion of heat and mass:

- Ignition experiments
- Extinction experiments
- Flame speed measurements
- Composition profiles (speciation)
- Dynamic response of flames to forced oscillations

1. Introduction

Combustion and transport phenomena & laminar flames.

2. Numerical solution of 1D flames

a) Premixed laminar flames

- i. Burner stabilized unstretched (or flat) flame
 - Governing equations and modeling aspects
 - Numerical solution
- ii. Freely-propagating unstretched (or flat) flame
 - Governing equations and modeling aspects

b) Counterflow diffusion flames

3. Multidimensional flames

- a) Introduction and examples
- b) Governing equations
- c) Numerical algorithms for multidimensional flames
- d) The operator-splitting method

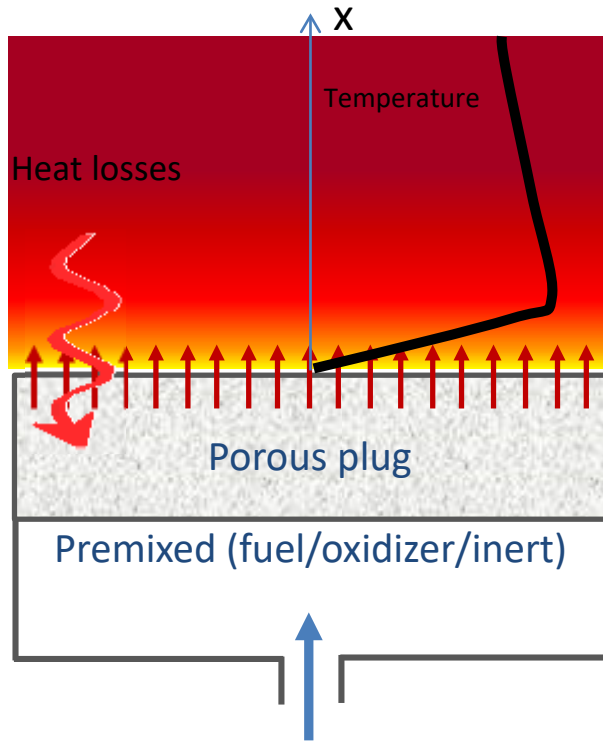
Why studying laminar 1D flames?

- It is one of the “canonical” problems in combustion, which allows for a comparison between theory, experiment, and computations
- May be used to assess the “quality” of combustion models (thermodynamics, kinetics, and transport models)
- Laminar flames are viewed in many turbulent combustion models as “building blocks” for turbulent combustion closures
- Numerical algorithms for multi-dimensional flames can be developed/optimized/assessed on 1D flames

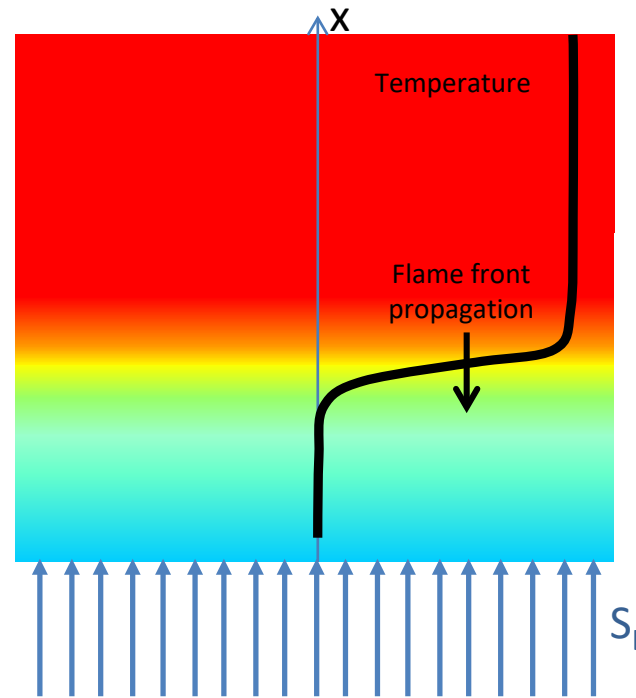
In the following we will focus on the numerical solution of 1D laminar flames with complex chemical kinetics, thermodynamics, and transport models

Premixed 1D flames

1. Burner Stabilized



2. Freely propagating unstretched flame

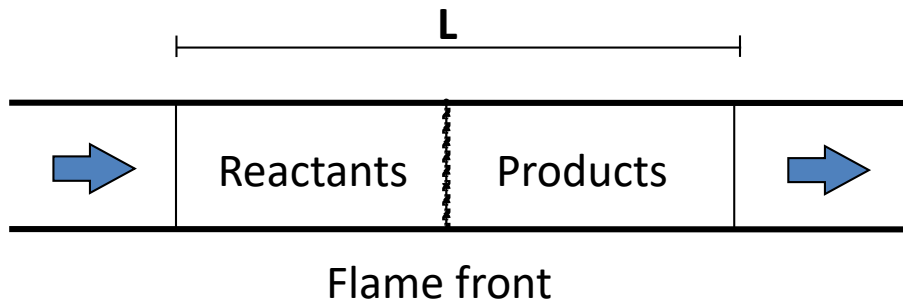


The propagation speed of the premixed flame with respect to the unburned gases is called the burning velocity or laminar flame speed S_L

The conservation equations are the same, but the **boundary conditions differ**:

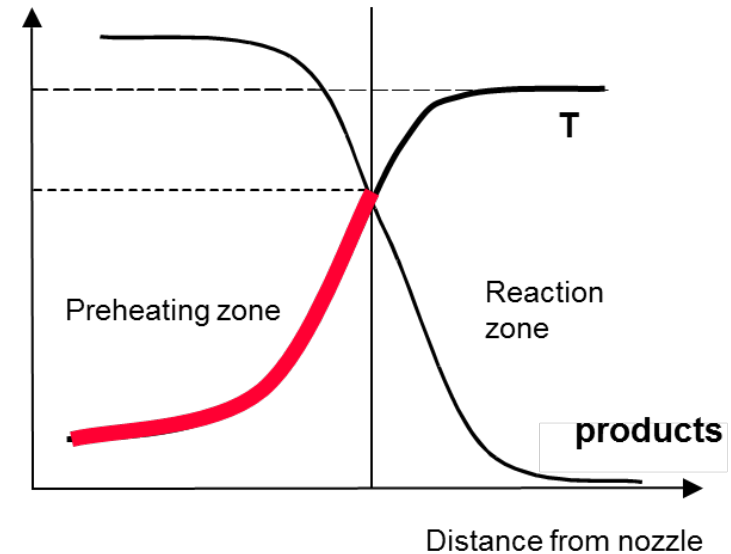
- For burner-stabilized flames the cold flow velocity (or mass flow rate) and composition are known, and vanishing gradients are imposed at the hot boundary.
- For freely propagating flames it is an eigenvalue and must be determined as part of the solution [Smooke et al., Comb Sci and Tech 34:79 (1983)]

Governing equations



Differential equations with boundary conditions (BVP)

$$NE = NC + 1$$



$$\dot{m} = \rho u = \dot{m}_0 \quad \text{Mass conservation equation}$$

$$\dot{m} \frac{\partial Y_k}{\partial x} = - \frac{\partial}{\partial x} (\rho Y_k u_k) + \dot{\Omega}_k \quad k = 1, \dots, N$$

$$\dot{m} \frac{\partial T}{\partial x} = \frac{1}{C_P} \frac{\partial}{\partial x} \left(\lambda \frac{\partial T}{\partial x} \right) - \frac{\rho}{C_P} \sum_{k=1}^{N_S} C_{P,k} Y_k V_k \frac{\partial T}{\partial x} + \frac{\dot{Q}}{C_P}$$

Species transport equation

Energy transport equation

1. Introduction

Combustion and transport phenomena & laminar flames.

2. Numerical solution of 1D flames

a) Premixed laminar flames

i. Burner stabilized unstretched (or flat) flame

- Governing equations and modeling aspects
- Numerical solution

ii. Freely-propagating unstretched (or flat) flame

- Governing equations and modeling aspects

b) Counterflow diffusion flames

3. Multidimensional flames

a) Introduction and examples

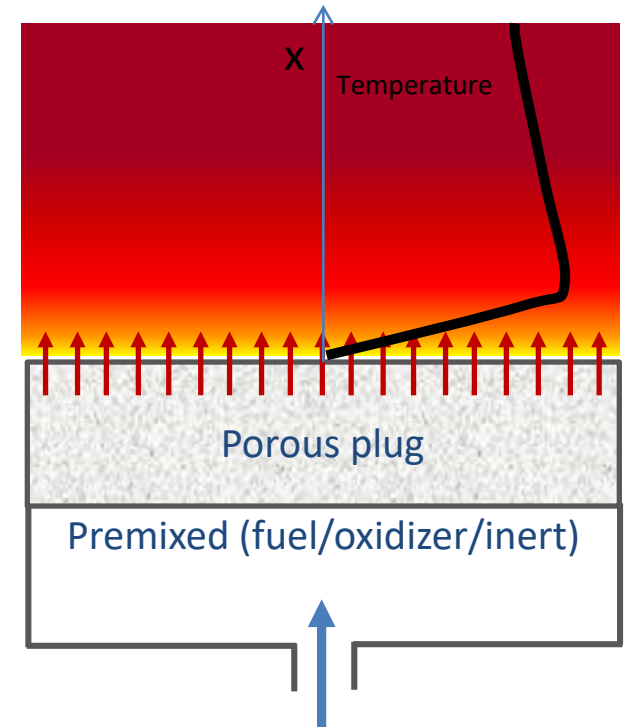
b) Governing equations

c) Numerical algorithms for multidimensional flames

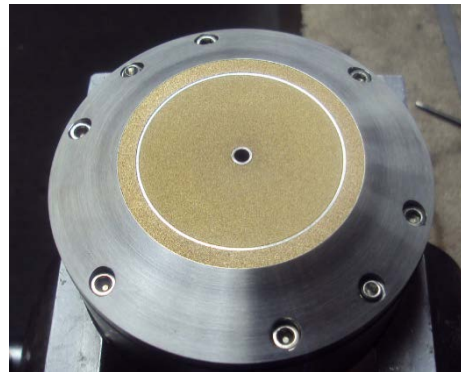
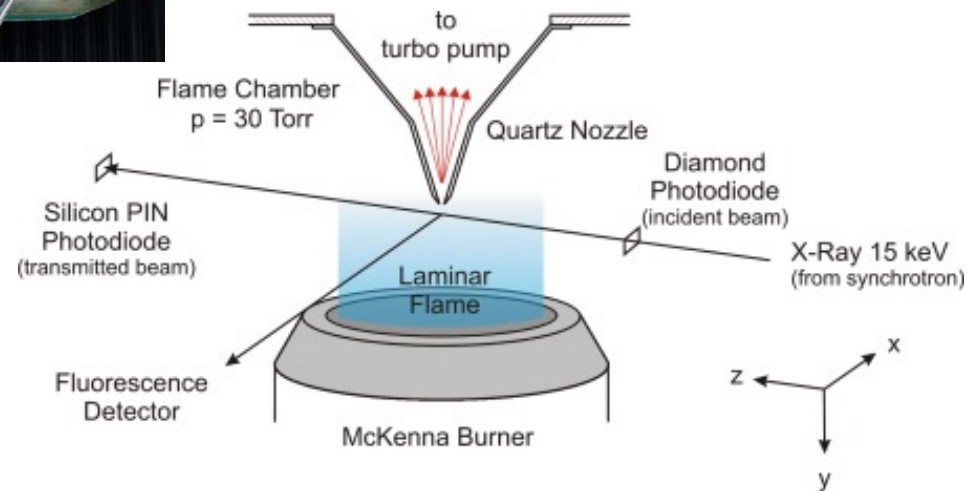
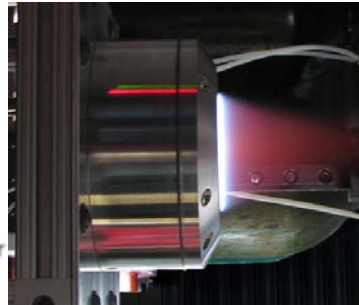
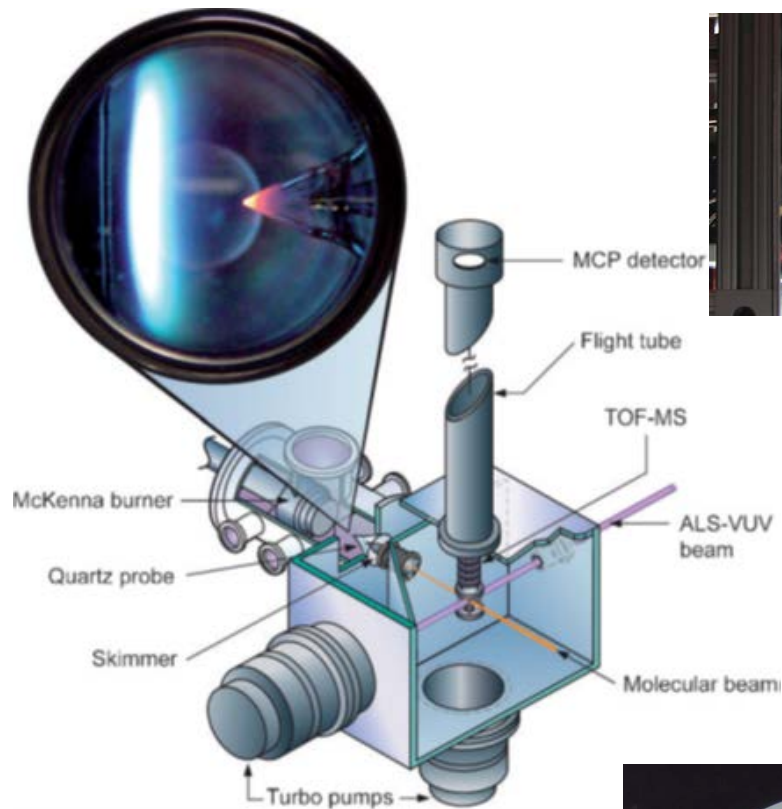
d) The operator-splitting method

Burner Stabilized Flat Flame: modeling aspects

- The Burner-Stabilized Flame Model is often used for analyzing species profiles in flame experiments.
- The mass flow rate through the burner is **known** and it is lower than the flame speed of the mixture. Therefore, **a flame is stabilized** over the burner surface, which is heated by the flame.
- Because of the significant heat losses (difficult to estimate) in the premixed burner-stabilized flames, the **measured temperature profile** is usually used as input in the numerical simulations. As a consequence, the energy conservation equation is not included in the system of equations.
- Comparing the results of simulations using assigned and calculated temperatures, can provide some indication of the heat losses to the burner and to the environment (conductive and radiative).

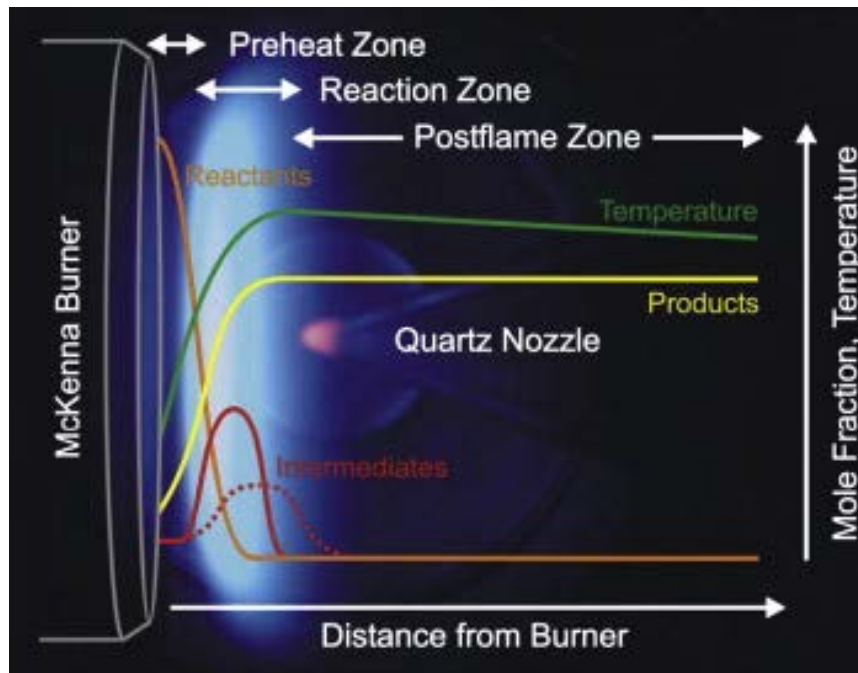


Burner Stabilized Flames: the McKenna burner



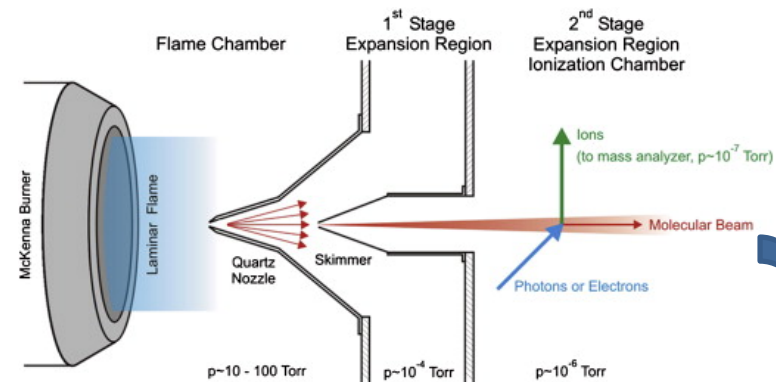
Schematic diagram of an experimental set-up for molecular-beam sampling in low-pressure flat flames.

Burner Stabilized Flame: experimental techniques

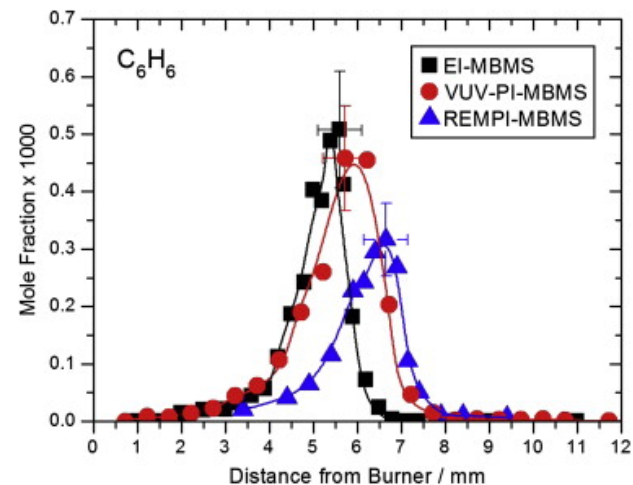


Hansen et al., PECS 35(2) 2009

Photograph and schematic structure of a premixed, laminar, low-pressure flat flame. In the photograph, a widespread reaction (luminous) flame zone and the quartz nozzle used for molecular-beam sampling are seen as well

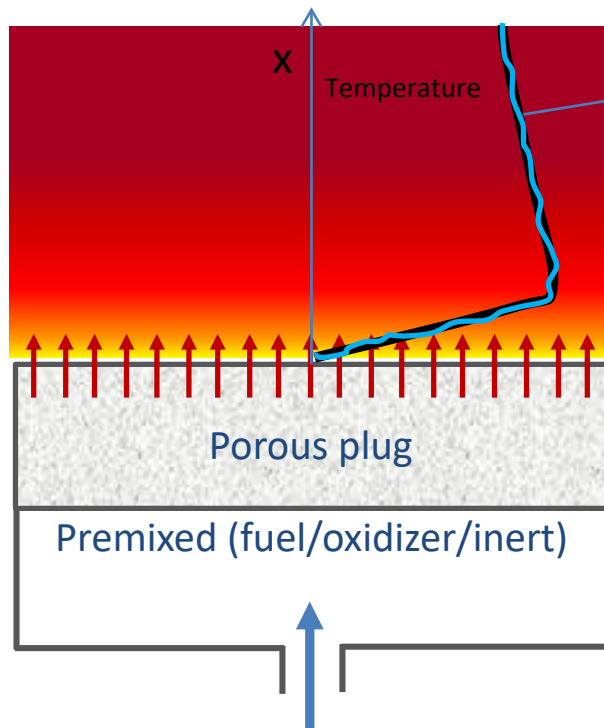


Schematic diagram of an experimental set-up for molecular-beam sampling in low-pressure flat flames.



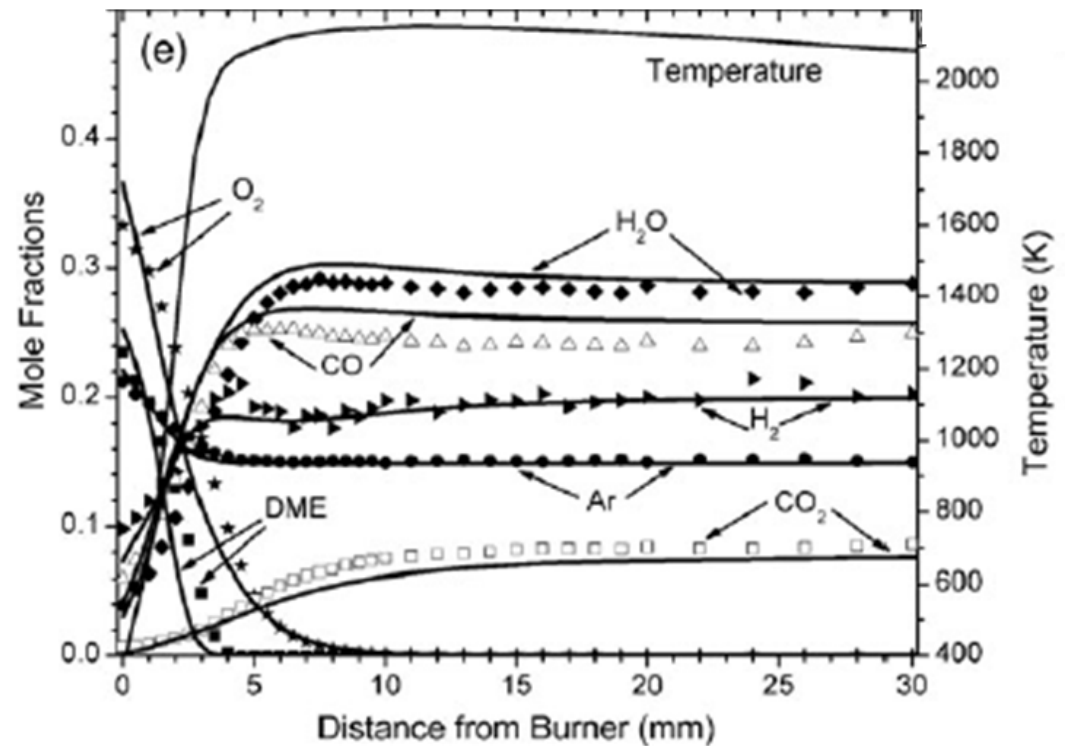
Flame-sampling molecular-beam mass spectrometry employing electron ionization (EI), resonantly enhanced multi-photon ionization (REMPI), and single-photon ionization (SPI)

BSF: modeling difficulties and comparison with exps



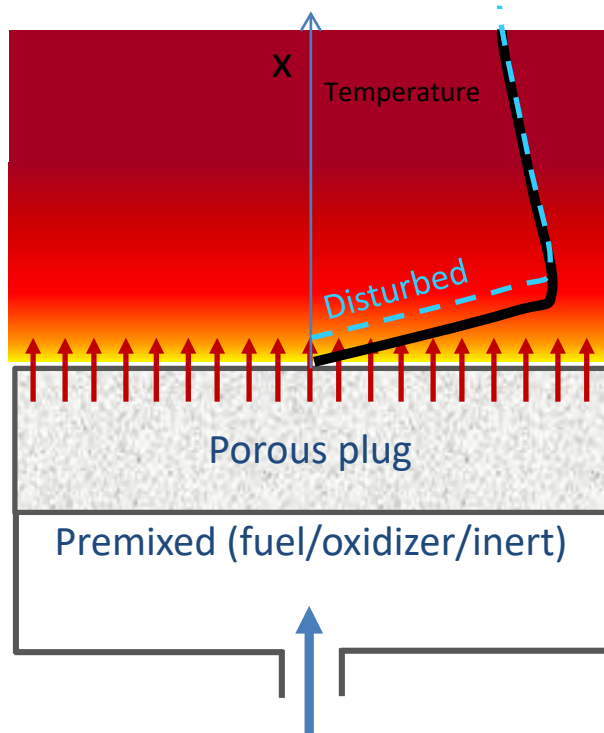
Smoothed experimental temperature profiles are used in calculations to avoid artificial gradients/uncertainties and numerical difficulties.

SHIFT : the “distance from burner” for recorded mole fractions is taken to be 0.9 mm less than the actual separation between the burner and the tip of the sampling cones. This displacement of the data gives good agreement between positions of the maximum mole fraction or key intermediates.



Wang et al., Phys. Chem. Chem. Phys., 2009

Burner Stabilized Flat Flame: modeling difficulties



A **shift** is usually needed to account approximately for the fact that the probe samples gases slightly upstream of the sampling cone orifice and to account for the cooling of the flame by the sampling nozzle.

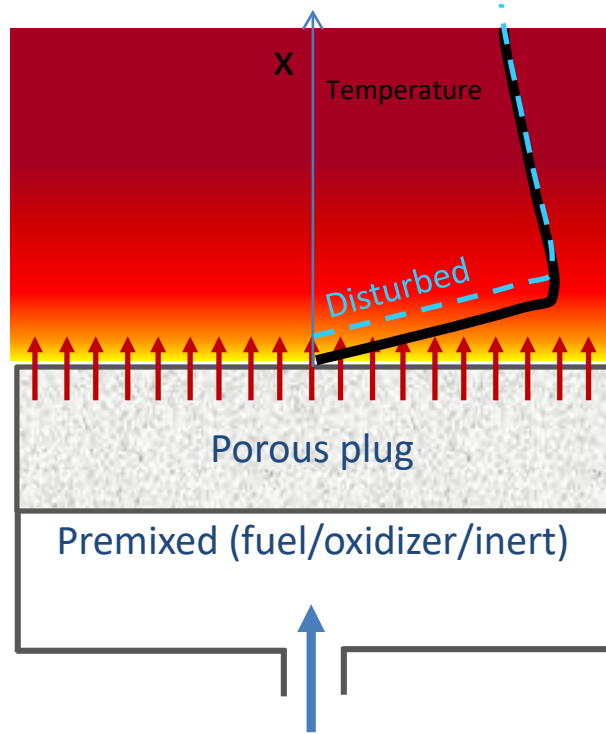
In general, the experimental mole-fraction profiles are shifted by $\sim 1.0 \div 3.0$ mm toward the burner surface for low pressure flames (< 100 mbar).

This shift is greatly reduced if the **disturbed temperature profile** is used in the simulations

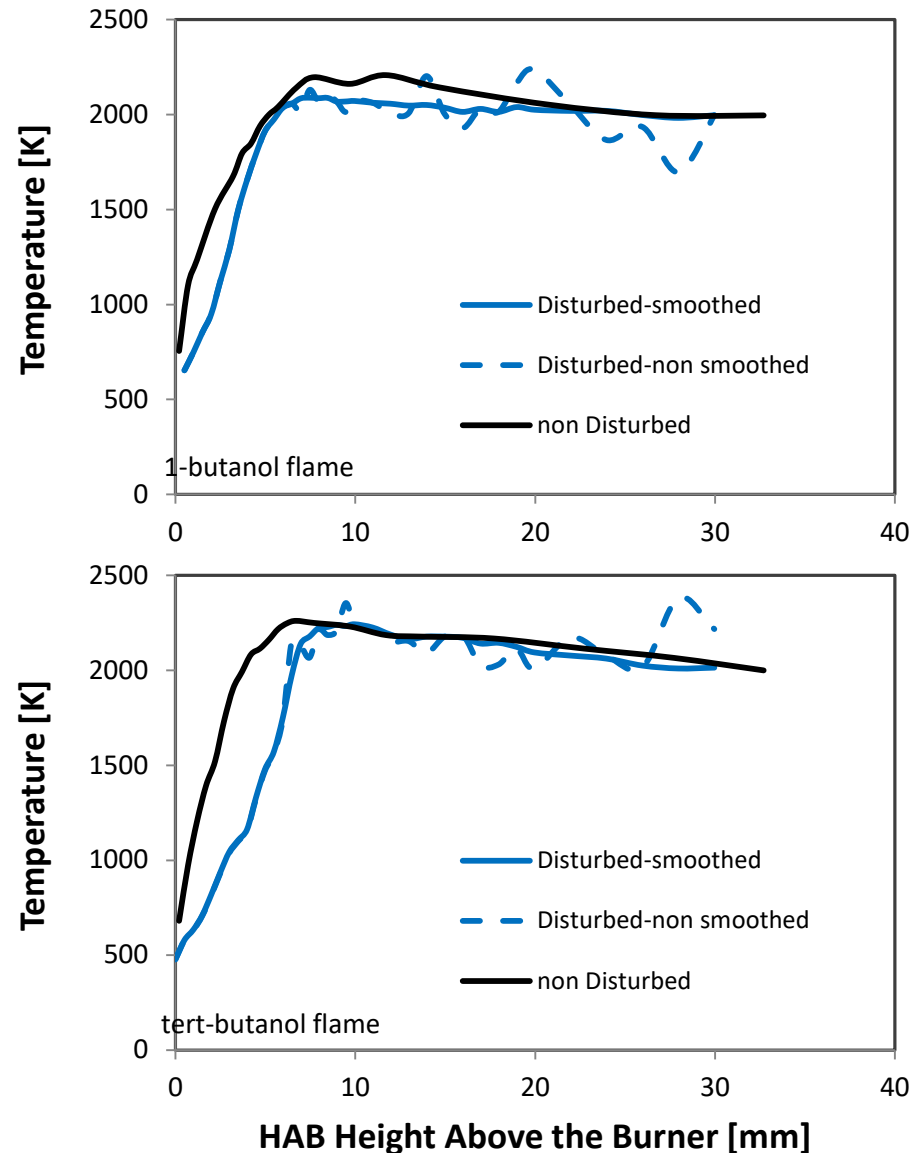
Disturbed temperature profile: the complex disturbance of the flame by the sampling cone can be approximated by the use of a disturbed temperature profile, representing the temperature of the sampled gas at each probed position

Struckmeier et al., *Sampling Probe Influences on Temperature and Species Concentrations in Molecular Beam Mass Spectroscopic Investigations of Flat Premixed Low-pressure Flames*, ZEITSCHRIFT FÜR PHYSIKALISCHE CHEMIE 223(4-5): 503–537 2009.

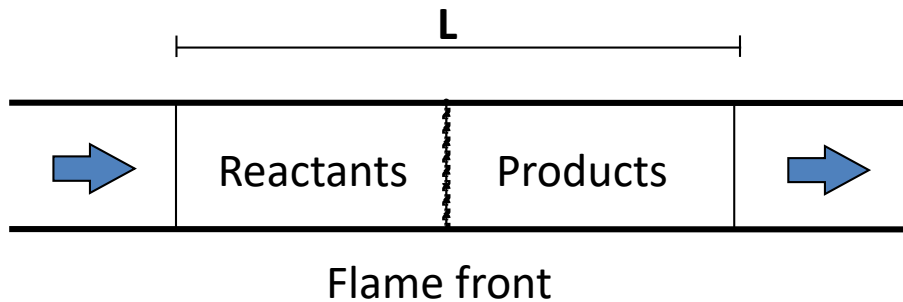
Burner Stabilized Flat Flame: temperature profile



The difference between disturbed and non-disturbed temperature profile corresponds to an axial shift of about 1-3 mm depending on the fuel, pressure and equivalence ratio. The use of the disturbed temperature profile (Struckmeier et al., 2009) allows to better agree with measured values (Frassoldati et al, 2012)

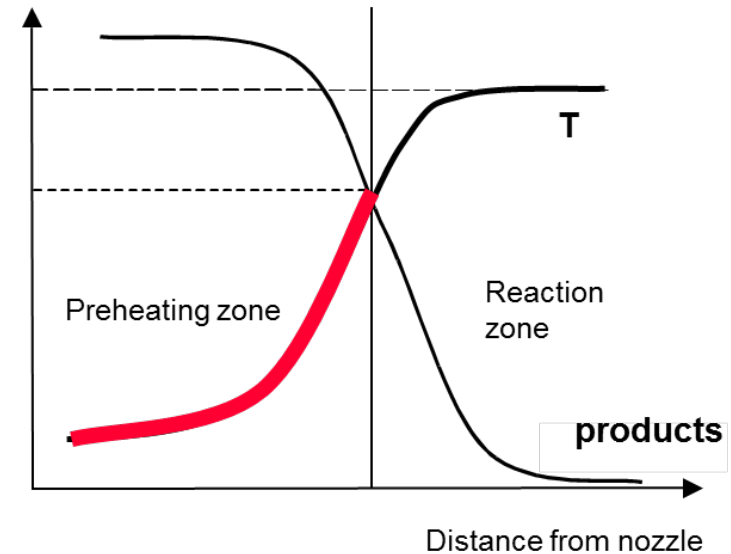


Governing equations: burner stabilized flame (I)



Differential equations with boundary conditions (BVP)

NE = NC



~~$$\dot{m} = \rho u = \dot{m}_0$$~~

Mass conservation equation

$$\dot{m} \frac{\partial Y_k}{\partial x} = - \frac{\partial}{\partial x} (\rho Y_k u_k) + \dot{\Omega}_k \quad k = 1, \dots, N$$

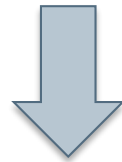
Species transport equation

~~$$\dot{m} \frac{\partial T}{\partial x} = \frac{1}{C_P} \frac{\partial}{\partial x} \left(\lambda \frac{\partial T}{\partial x} \right) - \frac{\rho}{C_P} \sum_{k=1}^{N_S} C_{P,k} Y_k V_k \frac{\partial T}{\partial x} + \frac{\dot{Q}}{C_P}$$~~

Energy transport equation

Governing equations: burner stabilized flame (II)

$$\dot{m} \frac{\partial Y_k}{\partial x} = -\frac{\partial}{\partial x} (\rho Y_k u_k) + \dot{\Omega}_k \quad k = 1, \dots, N$$



Hirschfelder-Curtiss model
for diffusion velocities

$$\dot{m} \frac{\partial Y_k}{\partial x} = \frac{\partial}{\partial x} \left(\rho \mathcal{D}_k \frac{dY_k}{dx} \right) + \dot{\Omega}_k \quad k = 1, \dots, N$$

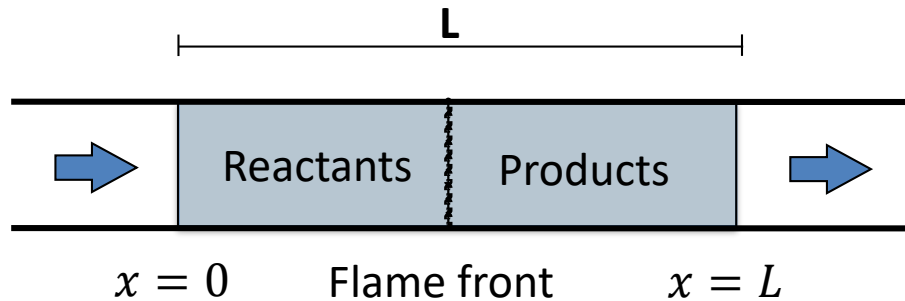
Convection

Diffusion

Reaction

- The features of the system of equations above are very different from ODEs with IC describing 0D systems, despite we still have only 1 independent variable.
- Since we have a second order derivative (the diffusion contribution) we have to specify **2 Boundary Conditions (BCs)** for each variable

Boundary conditions

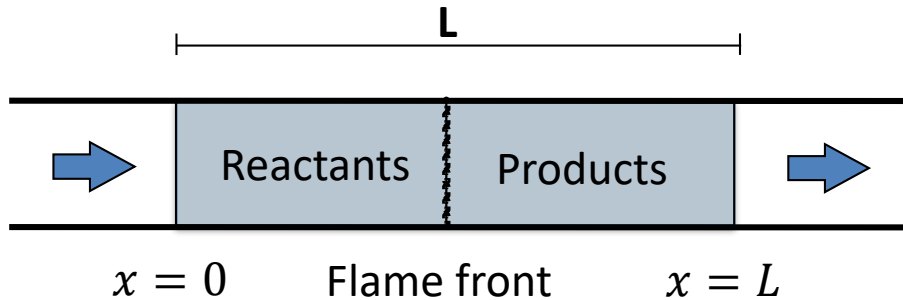


~~$$\begin{cases} Y_k|_{x=0} = Y_k^{inlet} \\ \frac{dY_k}{dx}|_{x=L} = 0 \end{cases}$$~~

At the inlet section it is more appropriate to consider the so-called **Danckwert's boundary conditions**, because what we really know is the mass flow rate of every species $\dot{m}Y_k^{inlet}$, not the inlet mass fraction Y_k^{inlet} (as in the BCs reported above). Because of diffusion, in general $Y_k|_{x=0} \neq Y_k^{inlet}$

Boundary conditions	{	$\dot{m}Y_k^{inlet} = \dot{m}Y_k _{x=0} - \rho\mathcal{D}_k \frac{dY_k}{dx} _{x=0}$	Danckwert's boundary conditions (Robin BC)
		$\frac{dY_k}{dx} _{x=L} = 0$	Negligible gradient at the exit (Neumann BC)

Governing equations: summary



N differential equations with boundary conditions (BVP)

Species equations

$$\left\{ \dot{m} \frac{\partial Y_k}{\partial x} = \frac{\partial}{\partial x} \left(\rho \mathcal{D}_k \frac{dY_k}{dx} \right) + \dot{\Omega}_k \right.$$

Boundary conditions

$$\left\{ \begin{aligned} \dot{m} Y_k^{inlet} &= \dot{m} Y_k \Big|_{x=0} - \rho \mathcal{D}_k \frac{dY_k}{dx} \Big|_{x=0} \\ \frac{dY_k}{dx} \Big|_{x=L} &= 0 \end{aligned} \right.$$

Danckwert's boundary conditions (Robin BC)

Negligible gradient at the exit (Neumann BC)

1. Introduction

Combustion and transport phenomena & laminar flames.

2. Numerical solution of 1D flames

a) Premixed laminar flames

i. Burner stabilized unstretched (or flat) flame

- Governing equations and modeling aspects
- **Numerical solution**

ii. Freely-propagating unstretched (or flat) flame

- Governing equations and modeling aspects

b) Counterflow diffusion flames

3. Multidimensional flames

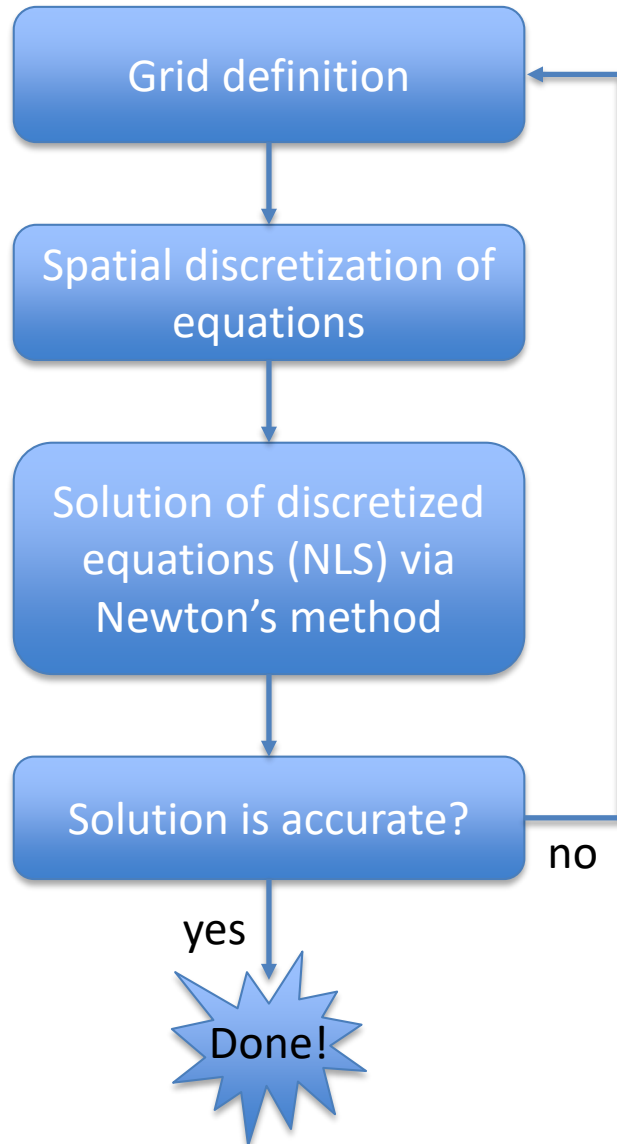
a) Introduction and examples

b) Governing equations

c) Numerical algorithms for multidimensional flames

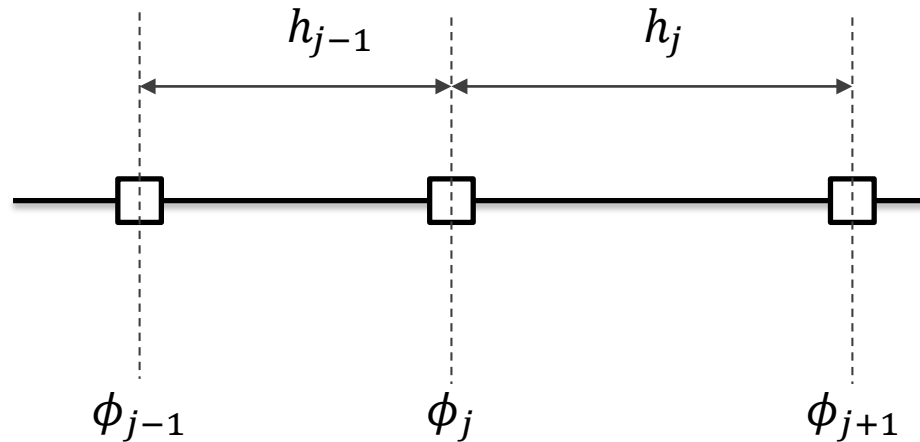
d) The operator-splitting method

Solution strategy



- Once discretized on an appropriate grid, the equations are solved as a **system of nonlinear equations (NLS)**
- The size of the system is $NE = NP \times N$, where NE is the number of unknowns/equations, NP is the number of grid points and N is the number of species. As an example, if $N = 100$ species and $NP = 300$ points, we have $NE = 100 \times 300 = 30,000$ equations/unknowns.
- The method of choice for the solution of the nonlinear system of equations is modified Newton.
- Modified Newton requires (a) Jacobians of the system $o(NE^2)$; (b) solution of linear systems $o(NE^3)$

Discretization of convective term



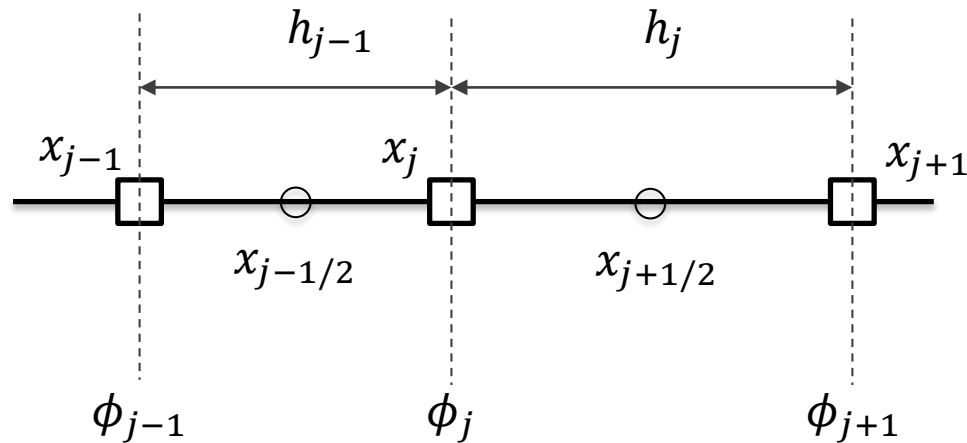
On the convective terms the user has the choice of using either first order upwind differences:

$$\rho u \frac{d\phi}{dx} \approx (\rho u)_j \frac{\phi_j - \phi_{j-1}}{x_j - x_{j-1}} = (\rho u)_j \frac{\phi_j - \phi_{j-1}}{h_{j-1}}$$

Or central differences:

$$\rho u \frac{d\phi}{dx} \approx (\rho u)_j \left(\frac{h_{j-1}}{h_j(h_j + h_{j-1})} \phi_{j+1} + \frac{h_j - h_{j-1}}{h_j h_{j-1}} \phi_j - \frac{h_j}{h_{j-1}(h_j + h_{j-1})} \phi_{j-1} \right)$$

Discretization of diffusion term



The species diffusion term is evaluated with the following difference approximation:

$$\frac{\partial}{\partial x} \left(\rho \mathcal{D}_k \frac{dY_k}{dx} \right) \approx \frac{f_{j+1/2} - f_{j-1/2}}{x_{j+1/2} - x_{j-1/2}} = \frac{\rho \mathcal{D}_k \left. \frac{dY_k}{dx} \right|_{j-1/2} - \rho \mathcal{D}_k \left. \frac{dY_k}{dx} \right|_{j+1/2}}{x_{j+1/2} - x_{j-1/2}}$$

The coefficients at points $j \pm 1/2$ are evaluated using the averages of the dependent variable between the mesh points.

Discretized equations (I)

For each internal point of the grid ($j = 2, \dots, NP - 1$) we have, for each variable (i.e. the mass fraction of each species), a non linear algebraic equation:

$$(\rho u)_j \frac{\phi_j - \phi_{j-1}}{h_{j-1}} = \frac{\rho \mathcal{D}_k \left. \frac{dY_k}{dx} \right|_{j-1/2} - \rho \mathcal{D}_k \left. \frac{dY_k}{dx} \right|_{j+1/2}}{x_{j+1/2} - x_{j-1/2}} + \dot{\Omega}_j$$

The equation above can be written in a more compact form as:

$$A_{j-1}\phi_{j-1} + A_j\phi_j + A_{j+1}\phi_{j+1} = B_j \quad j = 2, \dots, NP$$

Where the coefficients A_{j-1} , A_j , A_{j+1} are functions of the grid spacing (h_{j-1} , h_j , h_{j+1}), mass flux $(\rho u)_j$, diffusion $(\rho \mathcal{D}_{j-1}, \rho \mathcal{D}_j, \rho \mathcal{D}_{j+1})$ and reactions (depending on the kinetic mechanism). In principle, the term B_j is NOT a constant (see next slides).

The key-point is to recognize that equation in point j depends on variables on point j itself and points $j - 1$ and $j + 1$ only

Discretized equations (II)

Let's go back to the equations of mass fractions. The discretized equations for mass fraction of species k are:

$$A_{k,j-1}Y_{k,j-1} + A_{k,j}Y_{k,j} + A_{k,j+1}Y_{k,j+1} = B_{k,j} \quad j = 2, \dots, NP$$

The notation becomes more complicated, because ϕ is replaced by Y_k . A double-index notation is now required: the first index refers to species k , the second index to point j .

On the two points on the boundary we have the boundary conditions, so the whole set of equations for species k becomes:

$$\text{NP algebraic equations} \quad \left\{ \begin{array}{l} A_{k,1}Y_{k,1} + A_{k,2}Y_{k,2} = B_{k,1} \\ A_{k,j-1}Y_{k,j-1} + A_{k,j}Y_{k,j} + A_{k,j+1}Y_{k,j+1} = B_{k,j} \quad j = 2, \dots, NP \\ Y_{k,NP-1} - Y_{k,NP} = 0 \end{array} \right.$$

Non-linearity of discretized equations

$$A_{k,j-1}Y_{k,j-1} + A_{k,j}Y_{k,j} - A_{k,j+1}Y_{k,j+1} = B_{k,j} \quad j = 2, \dots, NP$$

This term is not a constant, but a non-linear function of mass fraction of species in the kinetic mechanism, in point j only, because the reactions are always local
In general, since this term is associated to chemical reaction, it is strongly non-linear

Additional non linearity is included in the convection/diffusion coefficients because the density and the diffusion coefficients are a non linear function of the composition (i.e mass fractions)
However, this non-linearity is usually weaker than the reaction term

Non-linear system (NLS) of algebraic equations

To summarize, at the end of the discretization procedure we have to solve a system of non-linear algebraic equations:

$$\left\{ \begin{array}{l} F_{1,1}(Y_{k,1}, Y_{k,2}) = 0 \\ F_{2,1}(Y_{k,1}, Y_{k,2}) = 0 \\ \dots \\ F_{N,1}(Y_{k,1}, Y_{k,2}) = 0 \\ \hline F_{1,2}(Y_{k,1}, Y_{k,2}, Y_{k,3}) = 0 \\ F_{2,2}(Y_{k,1}, Y_{k,2}, Y_{k,3}) = 0 \\ \dots \\ F_{N,2}(Y_{k,1}, Y_{k,2}, Y_{k,3}) = 0 \\ \hline \dots \\ F_{1,j}(Y_{k,j-1}, Y_{k,j}, Y_{k,j+1}) = 0 \\ F_{2,j}(Y_{k,j-1}, Y_{k,j}, Y_{k,j+1}) = 0 \\ \dots \\ F_{N,j}(Y_{k,j-1}, Y_{k,j}, Y_{k,j+1}) = 0 \end{array} \right.$$

N equations for point 1

N equations for point 2

N equations for point j

Newton's Algorithm for Algebraic Systems (I)

$\mathbf{F}(\mathbf{y}) = \mathbf{0}$ System of N non-linear algebraic equations \mathbf{F} in N unknowns \mathbf{y}

$$\mathbf{F}(\mathbf{y}^{(m+1)}) \approx \mathbf{F}(\mathbf{y}^{(m)}) + \left. \frac{\partial \mathbf{F}}{\partial \mathbf{y}} \right|_{\mathbf{y}^{(m)}} (\mathbf{y}^{(m+1)} - \mathbf{y}^{(m)}) = \mathbf{0}$$

$$\left. \frac{\partial \mathbf{F}}{\partial \mathbf{y}} \right|_{\mathbf{y}^{(m)}} \Delta \mathbf{y}^{(m)} = -\mathbf{F}(\mathbf{y}^{(m)})$$

- The procedure begins with a guess at the solution vector $\mathbf{y}^{(0)}$ and continues until the correction $\Delta \mathbf{y}^{(m)}$ becomes negligibly small
- The Newton's method converges very rapidly (quadratically) if the initial iterate lies within its domain of convergence

$$\mathbf{J}^{(m)} \equiv \left. \frac{\partial \mathbf{F}}{\partial \mathbf{y}} \right|_{\mathbf{y}^{(m)}}$$

Jacobian at the m
iteration

$$\mathbf{J}^{(m)} \Delta \mathbf{y}^{(m)} = -\mathbf{F}(\mathbf{y}^{(m)})$$

$$\Delta \mathbf{y}^{(m)} \equiv (\mathbf{y}^{(m+1)} - \mathbf{y}^{(m)})$$

Correction vector at the
 m iteration

Newton's Algorithm for Algebraic Systems (II)

One method of improving the convergence properties of the Newton's method is to implement a **damping strategy**

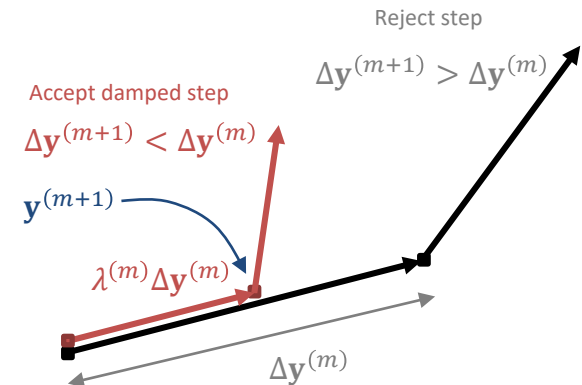
$$\mathbf{J}^{(m)} \Delta \mathbf{y}^{(m)} = -\lambda^{(m)} \mathbf{F}(\mathbf{y}^{(m)})$$

$$0 \leq \lambda^{(m)} \leq 1$$

Damping parameter (to be chosen as large as possible)

1. Each component of the new $\mathbf{y}^{(m+1)}$ must stay within a trust region where the solution is known to exist (for example mass fractions must be greater than 0 and less than unity)
2. The new $\mathbf{y}^{(m+1)}$ is not accepted unless a norm of the next correction vector $\Delta \mathbf{y}^{(m+1)}$ is smaller than the current correction vector $\Delta \mathbf{y}^{(m)}$

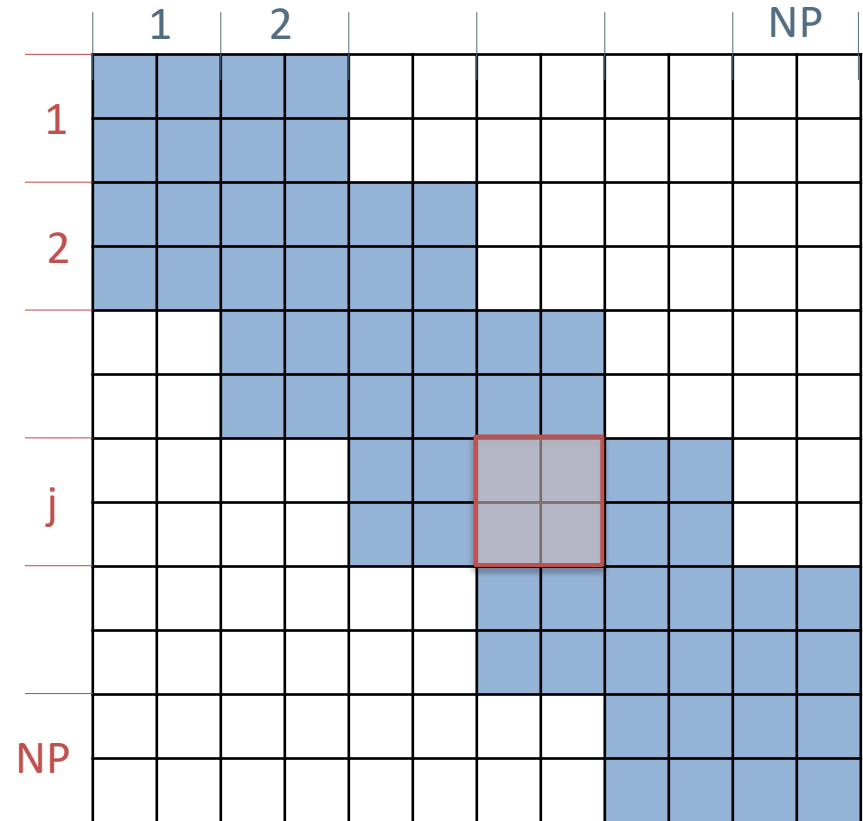
$$\|[\mathbf{J}^{(m)}]^{-1} \mathbf{F}(\mathbf{y}^{(m+1)})\| < \|[\mathbf{J}^{(m)}]^{-1} \mathbf{F}(\mathbf{y}^{(m)})\|$$



The Jacobian matrix (I)

At each iteration, the solution of a large system of linear equations (represented by the Jacobian matrix $\mathbf{J}^{(m)}$) is required by the Newton's method: $\mathbf{J}^{(m)} \Delta \mathbf{y}^{(m)} = -\mathbf{F}(\mathbf{y}^{(m)})$.

$$\begin{array}{l}
 \left. \begin{array}{l}
 1 \\
 2 \\
 \vdots \\
 j
 \end{array} \right\} \begin{array}{l}
 F_{1,1}(Y_{k,1}, Y_{k,2}) = 0 \\
 F_{2,1}(Y_{k,1}, Y_{k,2}) = 0 \\
 \dots \\
 F_{N,1}(Y_{k,1}, Y_{k,2}) = 0
 \end{array} \\
 \\
 \left. \begin{array}{l}
 2 \\
 \vdots \\
 j
 \end{array} \right\} \begin{array}{l}
 F_{1,2}(Y_{k,1}, Y_{k,2}, Y_{k,3}) = 0 \\
 F_{2,2}(Y_{k,1}, Y_{k,2}, Y_{k,3}) = 0 \\
 \dots \\
 F_{N,2}(Y_{k,1}, Y_{k,2}, Y_{k,3}) = 0
 \end{array} \\
 \\
 \left. \begin{array}{l}
 j \\
 \vdots \\
 NP
 \end{array} \right\} \begin{array}{l}
 F_{1,j}(Y_{k,j-1}, Y_{k,j}, Y_{k,j+1}) = 0 \\
 F_{2,j}(Y_{k,j-1}, Y_{k,j}, Y_{k,j+1}) = 0 \\
 \dots \\
 F_{N,j}(Y_{k,j-1}, Y_{k,j}, Y_{k,j+1}) = 0
 \end{array}
 \end{array}$$



Example of sparsity pattern: $N = 2, NP = 6$

The Jacobian matrix (II)

At each iteration, the solution of a large system of linear equations (represented by the Jacobian matrix $\mathbf{J}^{(m)}$) is required by the Newton's method: $\mathbf{J}^{(m)} \Delta \mathbf{y}^{(m)} = -\mathbf{F}(\mathbf{y}^{(m)})$.

Because of the finite-difference discretization formulas, the Jacobian matrix is not full, but very sparse

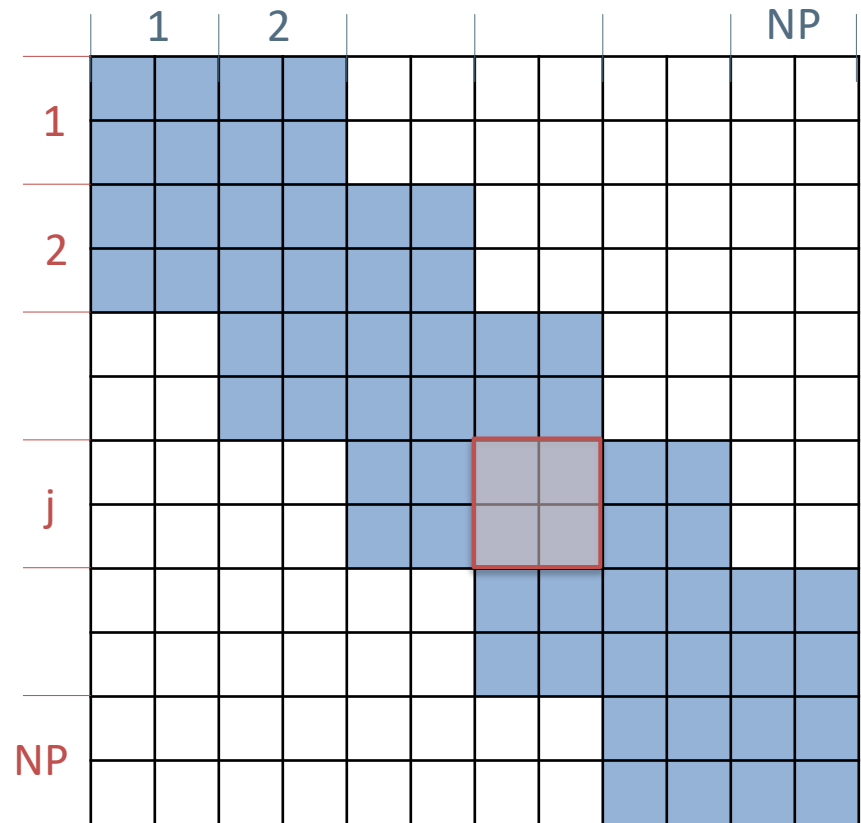
In addition, thanks to the proper ordering of equations, the sparsity is regular (ordered). We have a so called tri-diagonal block matrix

Size of blocks: $N \times N$

Number of blocks: $3NP - 2$

Number of non-zero elements:
 $(3NP - 2) \times N^2$

Sparsity degree: $s \sim \frac{3NP \times N^2}{NP^2 N^2} = \frac{3}{NP}$



Example of sparsity pattern: $N = 2, NP = 6$

The Jacobian matrix (III)

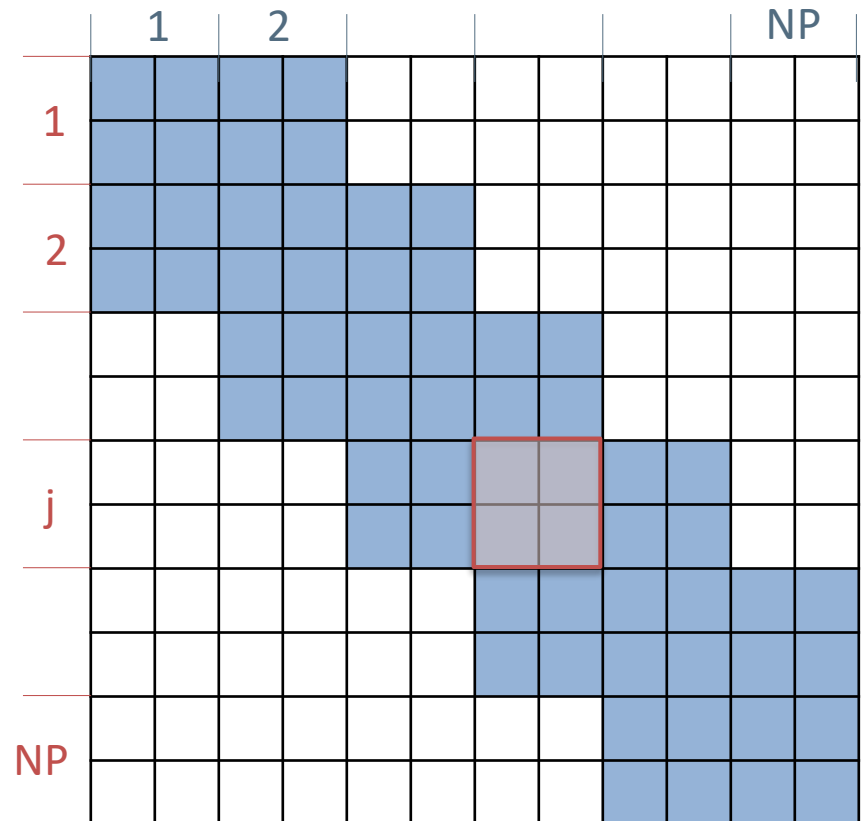
At each iteration, the solution of a large system of linear equations (represented by the Jacobian matrix $\mathbf{J}^{(m)}$) is required by the Newton's method: $\mathbf{J}^{(m)} \Delta \mathbf{y}^{(m)} = -\mathbf{F}(\mathbf{y}^{(m)})$.

Storage and evaluation

The Jacobian matrix must be evaluated by **accounting for the sparsity structure**, i.e. by avoiding to calculate and store the elements which are equal to zero by definition

Factorization

The Jacobian can be factorized using appropriate and **specific algorithms for tridiagonal block matrices**, in order to reduce the computational cost



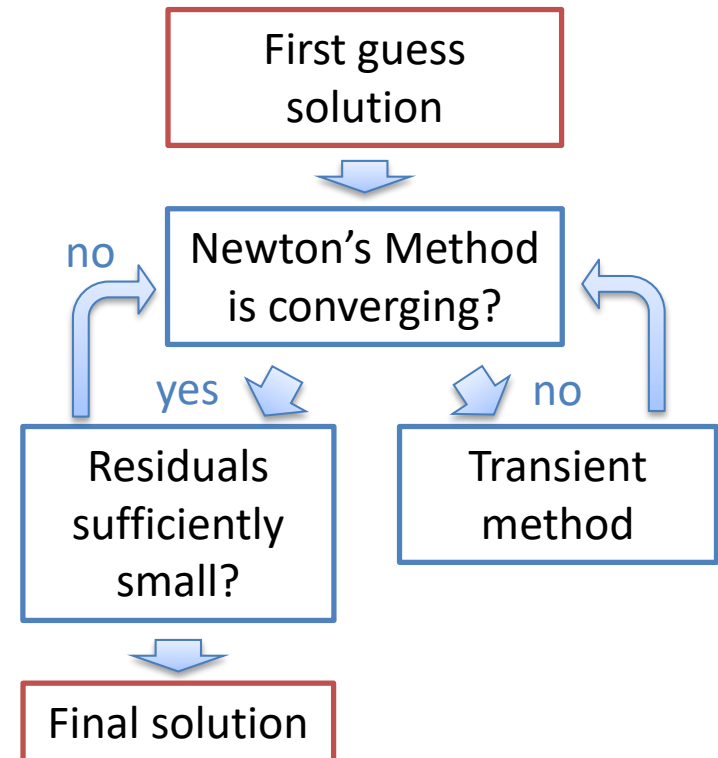
Example of sparsity pattern: $N = 2, NP = 6$

Improving the robustness: transient method (I)

The (modified) Newton's algorithm is an **iterative method** for which a **first-guess solution** must be provided. Convergence of the method is ensured only in case of a good first guess solution.

It may sometimes be difficult to obtain good initial estimates of species mass fractions, especially when complex mechanisms are adopted. For this reason, it is more convenient to approach the problem in the **transient form**, i.e. by adding the unsteady terms to the transport equations.

1. After simulating the transient system for a given amount of time, a new starting estimate for the Newton's algorithm, which is closer to the steady state solution, is obtained, increasing the likelihood of convergence of the Newton's method.



2. After the transient solution, the Newton's algorithm tries again for convergence and, if it fails, the transient simulation is extended for a larger amount of time, to further improve the initial iterate. Ultimately, the Newton's iteration converges to the steady-state solution.

Improving the robustness: transient method (II)

Species equations

$$\left\{ \rho \frac{\partial Y_k}{\partial t} = -\dot{m} \frac{\partial Y_k}{\partial x} + \frac{\partial}{\partial x} \left(\rho \mathcal{D}_k \frac{\partial Y_k}{\partial x} \right) + \dot{\Omega}_k \right.$$

We can proceed similarly to the steady-state case, by **discretizing the equations in space only (Method of lines)**. We obtain a system of ODEs (Ordinary Differential Equations) with Boundary conditions (BVP):

$$\frac{dY_{k,j}}{dt} = A_{k,j-1}Y_{k,j-1} + A_{k,j}Y_{k,j} + A_{k,j+1}Y_{k,j+1} - B_{k,j}$$

Of course we have a differential equation like the one above for each species in each point. We can solve this ODE system using one of the techniques we already studied for the 0D reacting systems. In general, the system is very stiff, because of the chemical reactions, so implicit methods (BDF methods) are mandatory.

Improving the robustness: transient method (III)

Let us write the system of ODEs in a compact form:

$$\frac{d\mathbf{y}}{dt} = \mathbf{F}(\mathbf{y})$$

We saw that according to BDF methods, at each time step we have to solve a system of algebraic non-linear equations, whose associated matrix \mathbf{A} is a simple function of the Jacobian matrix of the ODE system:

$$\left(\mathbf{I} - \sigma \mathbf{J}_{n+1}^{(m)}\right) \Delta \mathbf{y}_{n+1}^{(m)} = - \left[\mathbf{y}_{n+1}^{(m)} + \tilde{\mathbf{y}}_n - \sigma \mathbf{f}_{n+1}^{(m)} \right]$$

The diagram illustrates the mapping of terms from the boxed equation to the general linear system $\mathbf{Ax} = \mathbf{b}$. A central equation $\mathbf{Ax} = \mathbf{b}$ has three arrows pointing to its components: a red arrow from \mathbf{A} to $\mathbf{A} = (\mathbf{I} - \sigma \mathbf{J}_{n+1}^{(m)})$, a green arrow from \mathbf{x} to $\mathbf{x} = \Delta \mathbf{y}_{n+1}^{(m)}$, and a blue arrow from \mathbf{b} to $\mathbf{b} = -[\mathbf{y}_{n+1}^{(m)} + \tilde{\mathbf{y}}_n - \sigma \mathbf{f}_{n+1}^{(m)}]$.

$$\mathbf{Ax} = \mathbf{b}$$
$$\mathbf{A} = \left(\mathbf{I} - \sigma \mathbf{J}_{n+1}^{(m)}\right)$$
$$\mathbf{x} = \Delta \mathbf{y}_{n+1}^{(m)}$$
$$\mathbf{b} = - \left[\mathbf{y}_{n+1}^{(m)} + \tilde{\mathbf{y}}_n - \sigma \mathbf{f}_{n+1}^{(m)} \right]$$

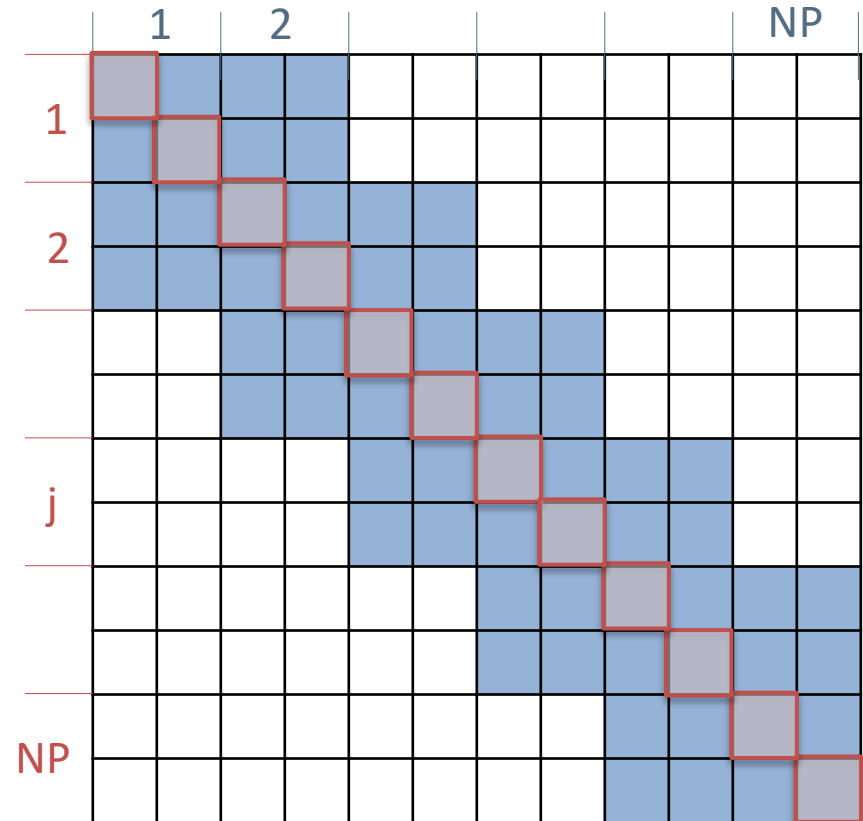
The superscript m in the equation above refers to the Newton's iteration, while the subscript n to the time step

Improving the robustness: transient method (III)

The matrix \mathbf{A} associated to the linear system resulting from the Newton's method has exactly the same sparsity structure of the Jacobian matrix associated to the non linear system we already discussed:

$$\mathbf{A} = \left(\mathbf{I} - \sigma \mathbf{J}_{n+1}^{(m)} \right)$$

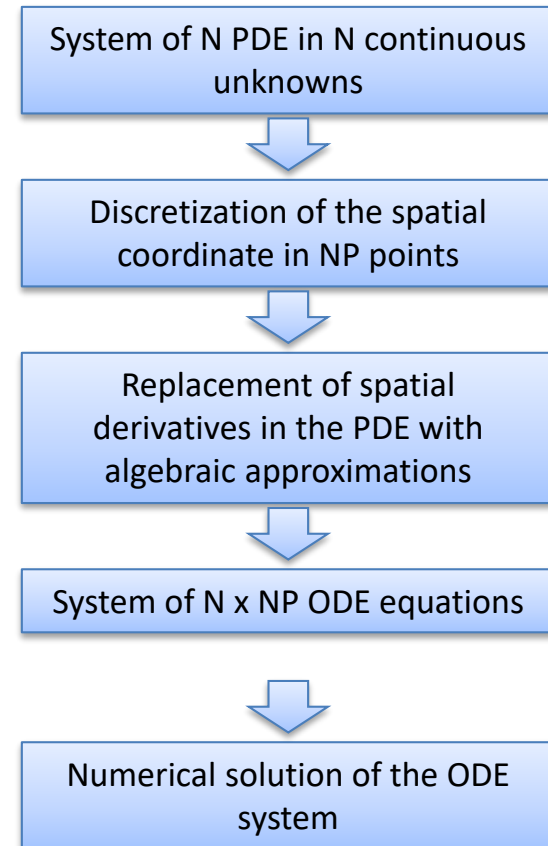
Indeed it is the sum of the identity matrix \mathbf{I} and the Jacobian matrix multiplied by a scalar σ which is a function of the time step



Example of sparsity pattern: $N = 2, NP = 6$

Method of lines

- I. The basic idea of the MOL is to replace the **spatial** (boundary value) derivatives with **algebraic approximations**.
- II. Once this is done, the spatial derivatives are no longer stated explicitly in terms of the spatial independent variables. Thus, only the initial value variable (typically time in a physical problem) remains. In other words, with only one remaining independent variable, we have a **system of ODEs** that approximate the original PDE.
- III. Once this is done, we can apply any integration algorithm for initial value ODEs to compute an approximate numerical solution to the PDE. Thus, one of the salient features of the MOL is the use of existing, and generally well established, numerical methods for ODEs.



Fully-coupled methods

In fully coupled (or global) algorithms all the equations are solved together

$$\frac{\partial \psi_{i,j}}{\partial t} = f_{i,j} \quad \text{System of } N \times NP \text{ ODEs}$$

Strong non linearity of reaction terms
High stiffness

Example: Backward Euler

$$\frac{\partial \Psi}{\partial t} = \mathbf{f} \quad \Rightarrow \quad \frac{\Psi^{(n+1)} - \Psi^{(n)}}{\Delta t} = \mathbf{f}^{(n+1)} \quad \Rightarrow \quad \Psi^{(n+1)} = \Psi^{(n)} + \Delta t \mathbf{f}^{(n+1)}$$

$$\mathbf{f}^{(n+1)} = \mathbf{f}^{(n)} + \frac{\partial \mathbf{f}^{(n)}}{\partial \Psi} (\Psi^{(n+1)} - \Psi^{(n)}) \quad \Rightarrow \quad \left[\mathbf{I} - \Delta t \frac{\partial \mathbf{f}^{(n)}}{\partial \Psi} \right] (\Psi^{(n+1)} - \Psi^{(n)}) = \Delta t \mathbf{f}^{(n)}$$

Fully coupled algorithms

- ☺ all the processes and their interactions are considered simultaneously
- ☺ natural way to treat problems with multiple stiff processes
- ☹ the resulting system of equations can be extremely large and the computational cost prohibitive

1. Introduction

Combustion and transport phenomena & laminar flames.

2. Numerical solution of 1D flames

a) Premixed laminar flames

- i. Burner stabilized unstretched (or flat) flame
 - Governing equations and modeling aspects
 - Numerical solution
- ii. **Freely-propagating unstretched (or flat) flame**
 - **Governing equations and modeling aspects**

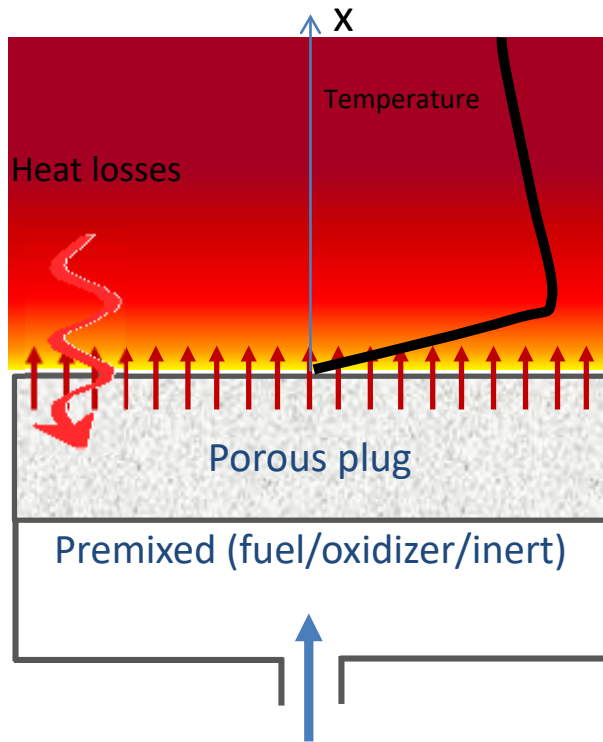
b) Counterflow diffusion flames

3. Multidimensional flames

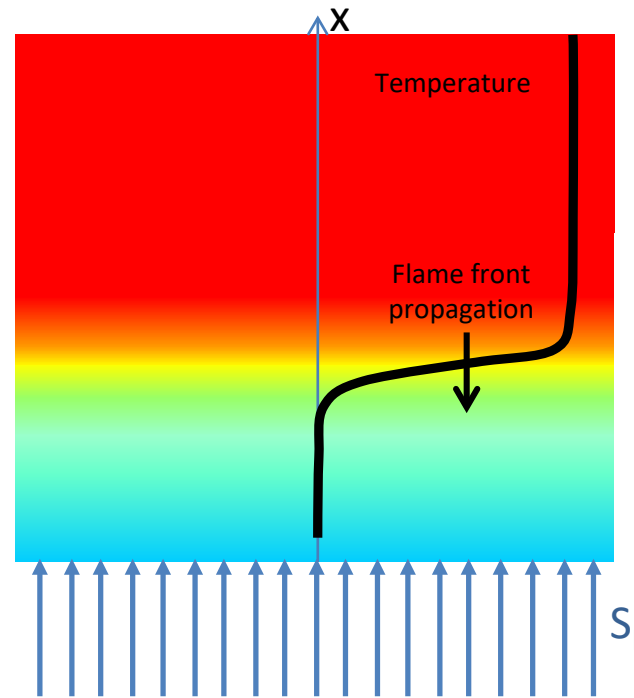
- a) Introduction and examples
- b) Governing equations
- c) Numerical algorithms for multidimensional flames
- d) The operator-splitting method

Premixed 1D flames

1. Burner Stabilized



2. Freely propagating unstretched flame



The propagation speed of the premixed flame with respect to the unburned gases is called the burning velocity or laminar flame speed S_L

The conservation equations are the same, but the **boundary conditions differ**:

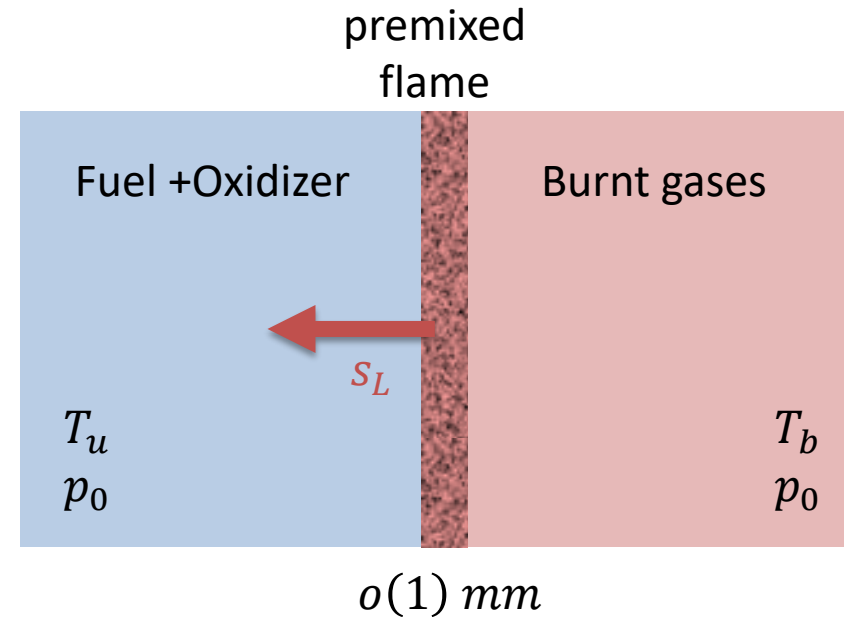
- For burner-stabilized flames the cold flow velocity (or mass flow rate) and composition are known, and vanishing gradients are imposed at the hot boundary.
- **For freely propagating flames it is an eigenvalue and must be determined as part of the solution [Smooke et al., Comb Sci and Tech 34:79 (1983)]**

The freely propagating unstretched flame

We shall consider the case of a one-dimensional (1D) laminar flame propagating into a premixed mixture of fuel and oxidizer (e.g., air and methane).

Important 1D simplifications

- Absence of mixture and velocity gradients ahead of the flame
- Absence of aerodynamic stretch and curvature
- Steady propagation

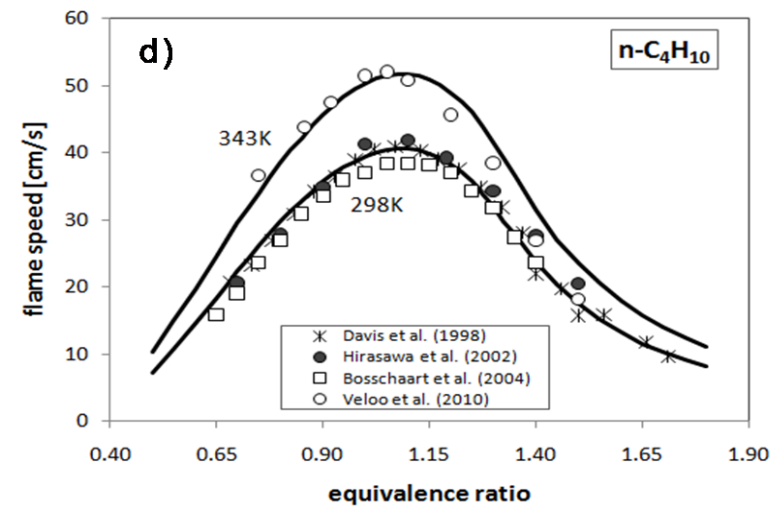
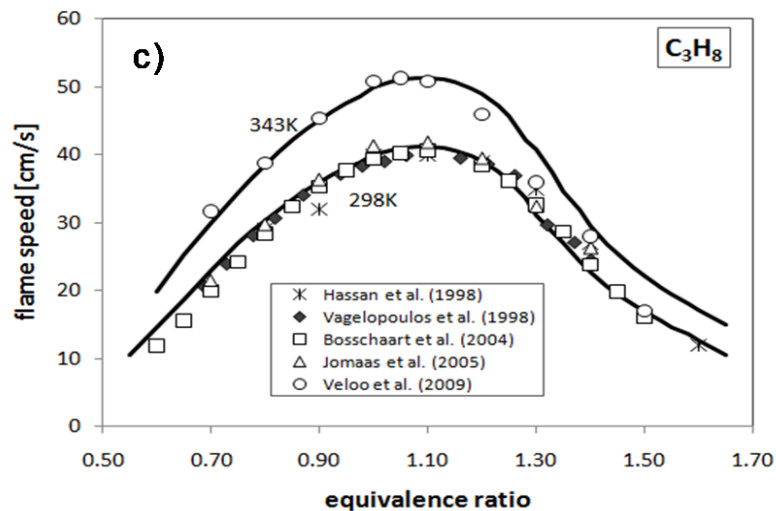
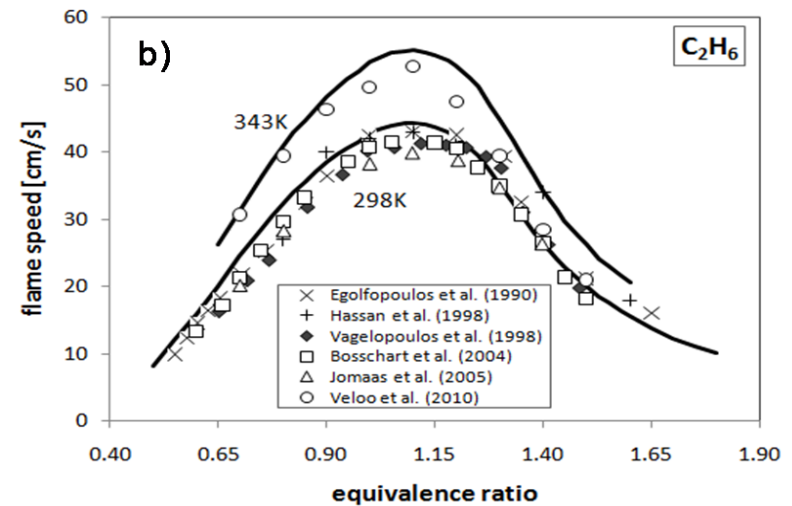
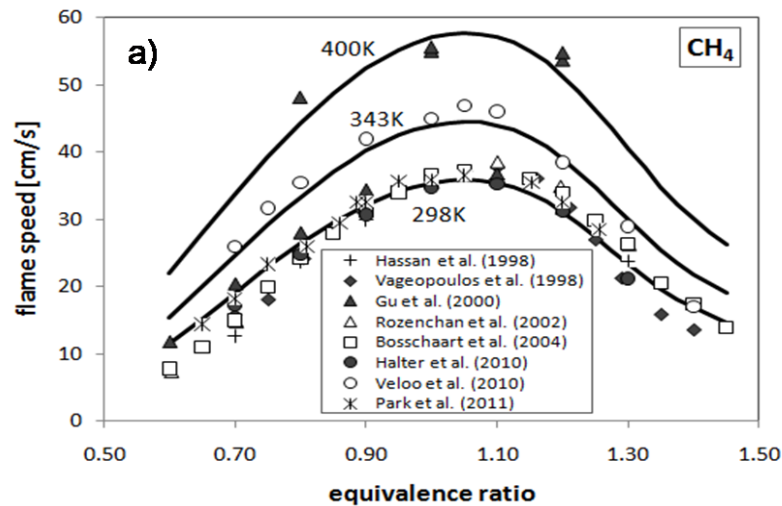


Even though there are simplifications, the main features of a premixed flames are retained:

- a thin interface propagating at $O(1) \text{ m/s}$
- pressure remains constant

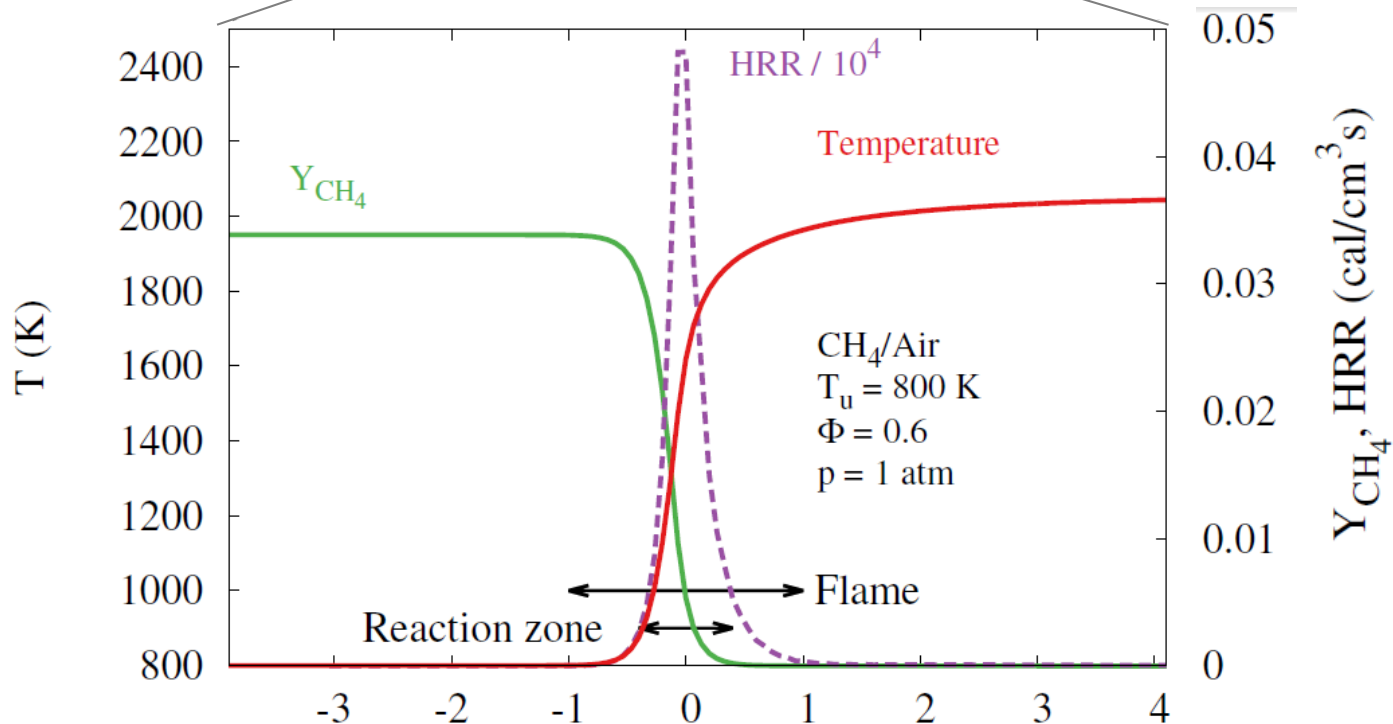
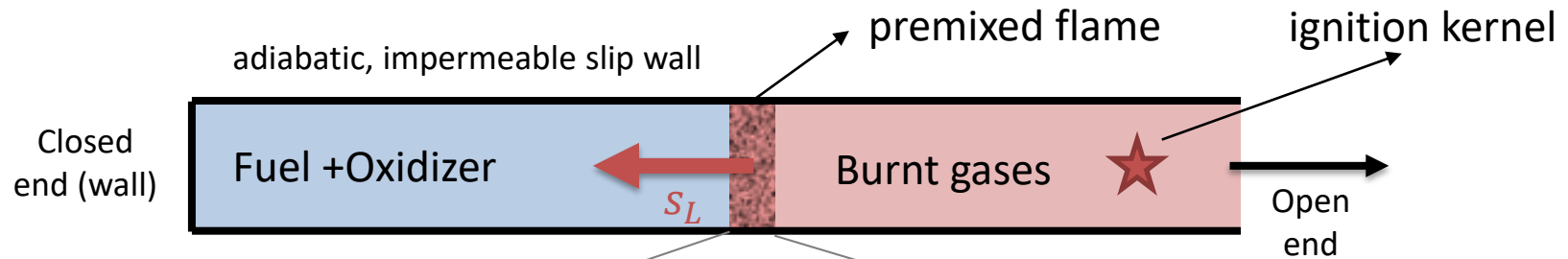
The 1D nature implies that the flame is “unstretched”, providing a reference condition to build databases of laminar flame speeds for various fuels (Egolfopoulos et al., 2014)

Laminar flame speed (I)

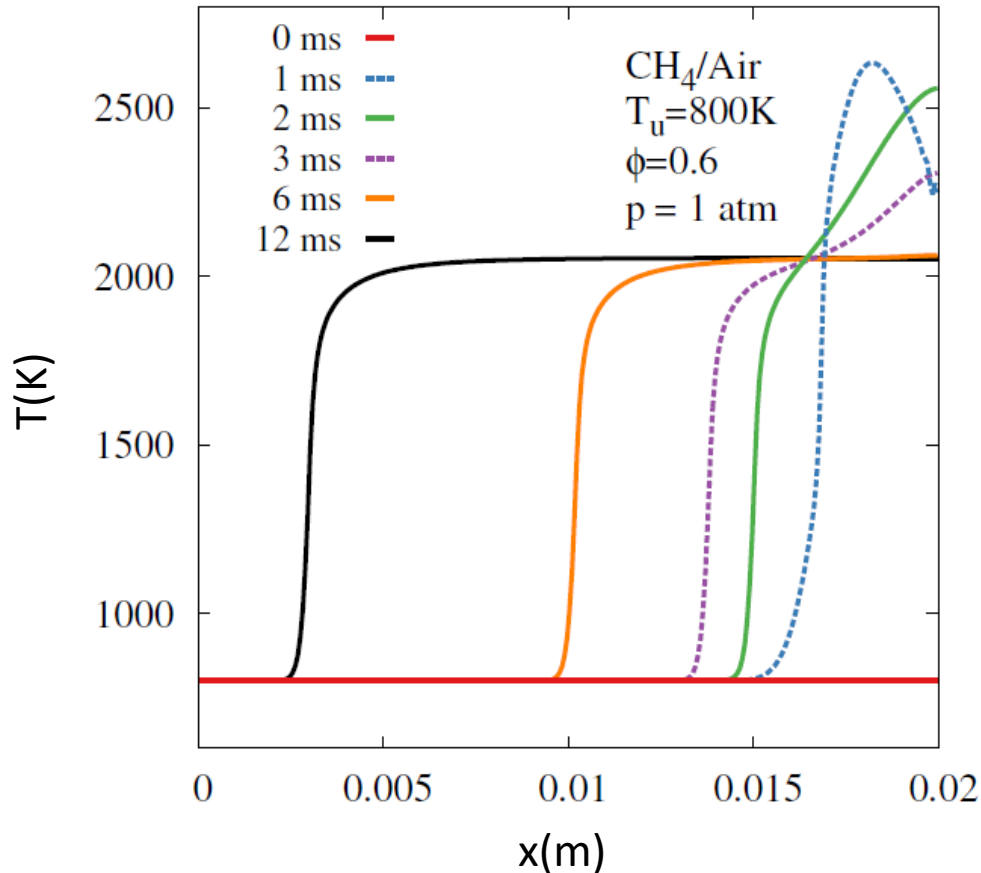


Ranzi, E., Frassoldati, A., Grana, R., Cuoci, A., Faravelli, T., Kelley, A.P., Law, C.K., *Hierarchical and comparative kinetic modeling of laminar flame speeds of hydrocarbon and oxygenated fuels* (2012) Progress in Energy and Combustion Science, 38 (4), pp. 468-501
DOI: 10.1016/j.peccs.2012.03.004

A flame-tube experiment (I)



A flame-tube experiment (II)



- A tube is filled with a quiescent mixture of methane and air at $T_u = 800 K$ and $1 atm$
- A source of energy is placed towards the open end causing the temperature to increase locally (ignition kernel)
- A flame develops and after a few ms, a premixed flame is established
- The flame propagates steadily right to left into the unburnt gases at a constant speed $s_L = 125 cm/s$

Governing equations (I)

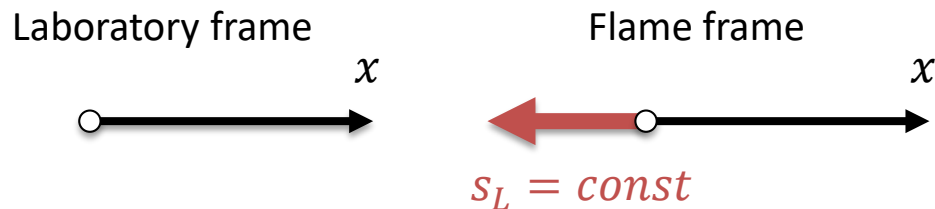
The conservation equations are the reactive Navier-Stokes equations where the x components and derivatives are retained.

$$\left\{ \begin{array}{ll} \frac{\partial \rho}{\partial t} + \frac{\partial}{\partial x}(\rho u) = 0 & \text{Mass conservation equation} \\ \frac{\partial \rho Y_k}{\partial t} + \frac{\partial}{\partial x}(\rho Y_k u) = -\frac{\partial}{\partial x}(\rho Y_k u_k) + \dot{\Omega}_k & k = 1, \dots, N \quad \text{Species transport equation} \\ \rho C_P \left(\frac{\partial T}{\partial t} + u \frac{\partial T}{\partial x} \right) = \frac{\partial}{\partial x} \left(\lambda \frac{\partial T}{\partial x} \right) - \rho \frac{\partial T}{\partial x} \sum_{k=1}^{N_S} C_{P,k} Y_k V_k + \dot{Q} & \text{Energy transport equation} \end{array} \right.$$

For reasons that will be clear shortly, there is no need to include the momentum equation to solve for the flame structure and the momentum equation serves the purpose of computing the dynamic pressure only.

Governing equations (II)

When the flame has settled, it propagates into quiescent, unburnt gases at a **constant speed** s_L , so that it is more advantageous to consider conservation equations written in an inertial frame of reference attached to the flame front



Recall that the Navier-Stokes equations are Galilean invariant, i.e., “the laws of motion are the same in all inertial frames”.

Of course, Galilean invariance with respect to a transformation of the reactive Navier-Stokes from the laboratory coordinate system to the flame’s assumes that the flame is moving at **constant** speed, i.e, past the transient.

Governing equations (III)

When written in the “flame frame”:

$$\left\{ \begin{array}{l} \rho u = \text{const} = \rho_u S_L = \dot{m} \\ \rho_u S_L \frac{\partial Y_k}{\partial x} = -\frac{\partial}{\partial x} (\rho Y_k u_k) + \dot{\Omega}_k \quad k = 1, \dots, N \\ \rho_u S_L \frac{\partial T}{\partial x} = \frac{\partial}{\partial x} \left(\lambda \frac{\partial T}{\partial x} \right) - \rho \frac{\partial T}{\partial x} \sum_{k=1}^{N_S} C_{P,k} Y_k V_k + \dot{Q} \end{array} \right.$$

The equations are formally equivalent to the burner stabilized flame. However there is a BIG difference!

The equations above are complemented with the equation of state and suitable models for transport properties and kinetics, which are functions of temperature, pressure and composition.

The equations above are solved numerically with suitable boundary conditions, numerical methods, and arbitrarily complex models for chemistry, thermodynamics, and reactions, yielding the solution to a one-dimensional, unstretched premixed flame.

The eigenvalue problem (I)

The **BIG difference** is the fact that the mass flow rate ($\rho_u s_L = \dot{m}$), i.e. the inlet velocity is unknown! We say the flame speed is an eigenvalue of the problem, i.e. an additional unknown

Flame speed “eigenvalue”

In order to solve for the flame “eigenvalue” s_L , the equation of conservation of mass is transformed in a first order ODE and discretized in agreement with the species and temperature equation:

$$\rho u = \text{const} = \rho_u s_L = \dot{m} \quad \longrightarrow \quad \frac{\partial \dot{m}}{\partial x} = 0 \quad \longrightarrow \quad \frac{\dot{m}_j - \dot{m}_{j-1}}{x_j - x_{j-1}} = 0$$

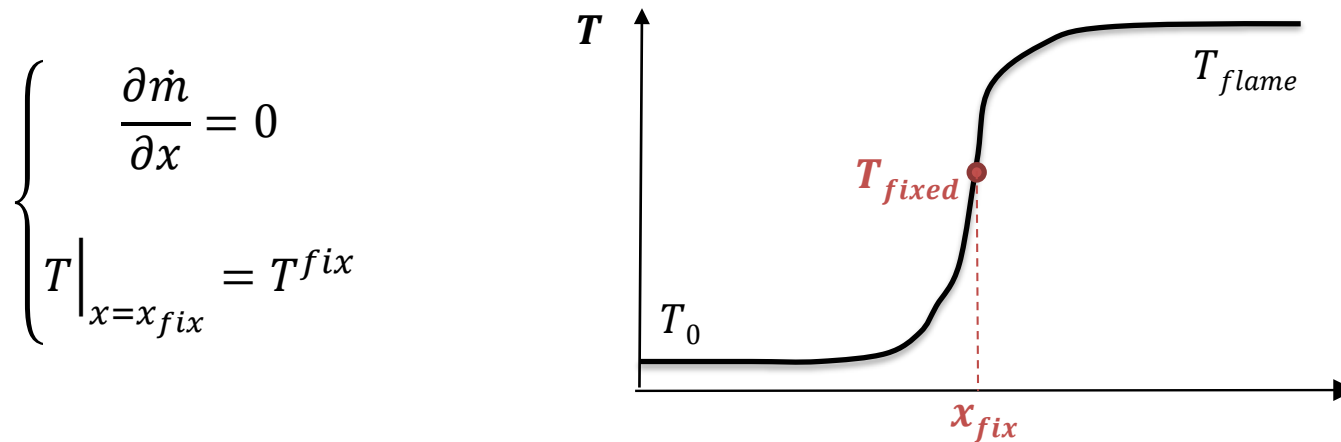
But what kind of boundary condition can we consider?

The most common solution is to **specify the temperature in one specific mesh point**. Thus, at this given point, temperature must satisfy two different conditions : the energy balance must be satisfied and the temperature must be equal to the specified temperature.

The eigenvalue problem (II)

For a freely propagating flame the mass flow rate \dot{m} (or, equivalently s_L) is an eigenvalue of the system and must be determined as a part of the solution [Smooke et al., CST 1983].

It is important to fix this point in such a way that the gradients tend to vanish at the inlet. Otherwise, the calculated s_L will be affected by heat loss at the boundary.



Usually the coordinate of the fixed point is placed in the middle of the computational domain and the fixed temperature value is the average between the unburnt gas temperature and the adiabatic temperature

Governing equations: summary

Governing equations	{	$\frac{\partial \dot{m}}{\partial x} = 0$	Mass conservation equation
		$\dot{m} \frac{\partial Y_k}{\partial x} = - \frac{\partial}{\partial x} (\rho Y_k u_k) + \dot{\Omega}_k \quad k = 1, \dots, N$	Species transport equation
		$\dot{m} \frac{\partial T}{\partial x} = \frac{\partial}{\partial x} \left(\lambda \frac{\partial T}{\partial x} \right) - \rho \frac{\partial T}{\partial x} \sum_{k=1}^{N_S} C_{P,k} Y_k V_k + \dot{Q}$	Energy transport equation

Boundary conditions	{	$\dot{m} Y_k^{inlet} = \dot{m} Y_k \Big _{x=0} - \rho \mathcal{D}_k \frac{dY_k}{dx} \Big _{x=0}$	{	$\frac{dY_k}{dx} \Big _{x=L} = 0$
		$T \Big _{x=0} = T^{inlet}$		$\frac{dT}{dx} \Big _{x=L} = 0$
		$T \Big _{x=x_{fix}} = T^{fix}$		

The momentum equation

The momentum equation may be solved (neglecting viscous stresses) to obtain the dynamic pressure field $p(x)$ across the flame:

$$\frac{\partial p}{\partial x} = -\rho u \frac{\partial u}{\partial x} = -\rho_u s_L \frac{\partial u}{\partial x}$$

$$p(x) - p_{in} = \rho_u s_L (u(x) - s_L)$$

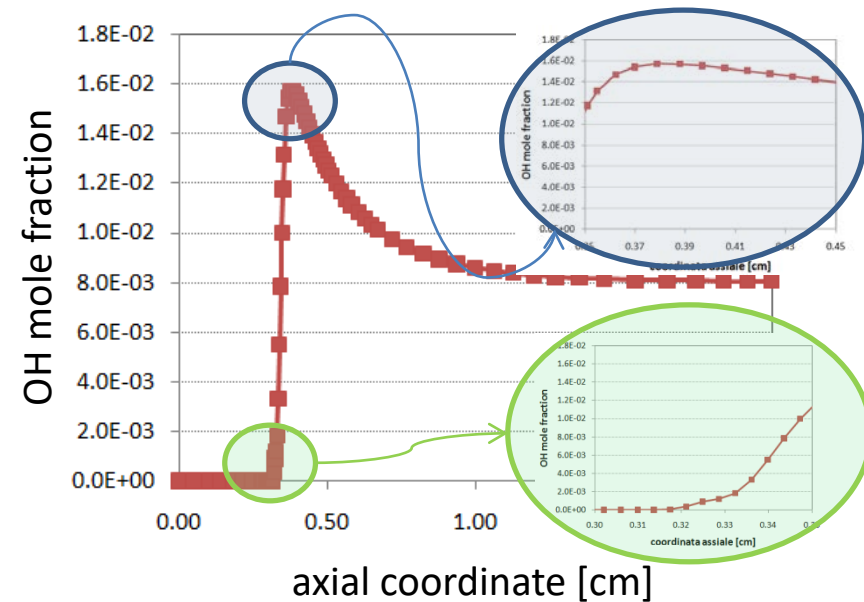
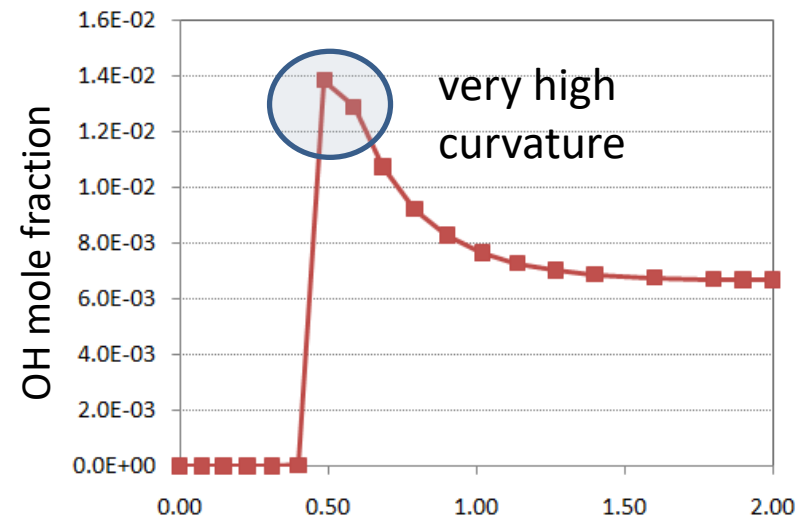
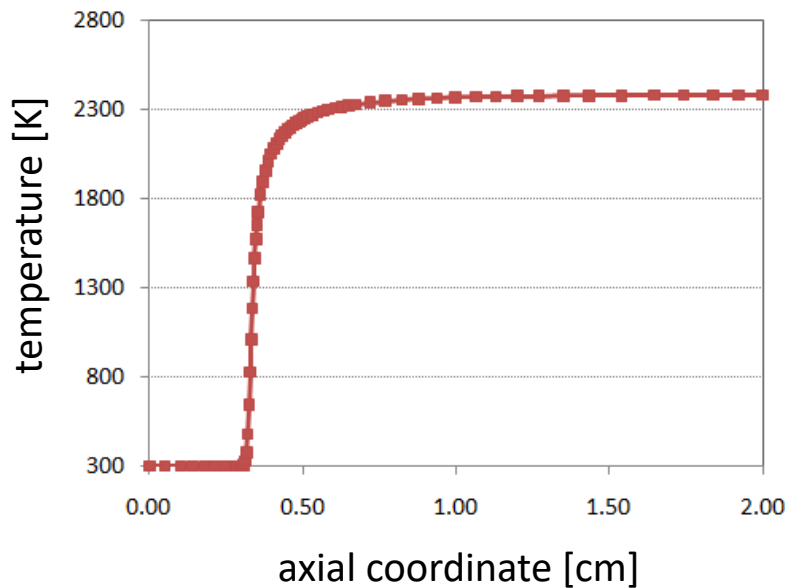
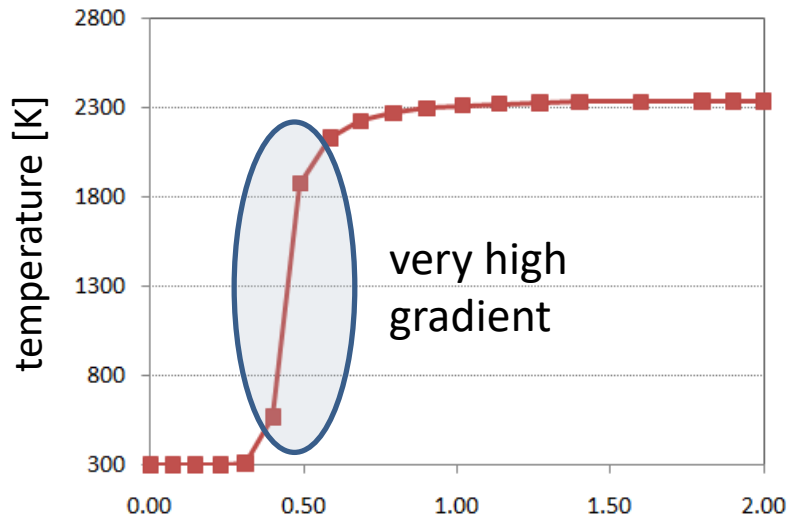
If changes in the molecular mass are neglected, $\frac{\rho}{\rho_u} = \frac{T}{T_u}$ and one may estimate the pressure difference across a propagating laminar premixed flame:

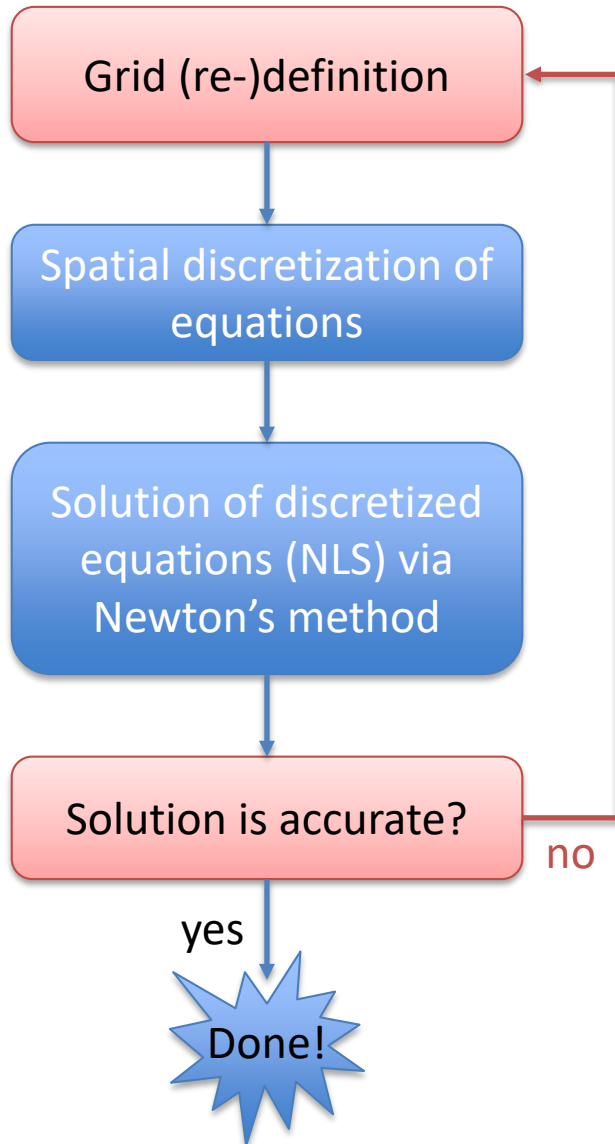
$$p_{out} - p_{in} \approx \rho_u s_L^2 \left(1 - \frac{T}{T_u}\right)$$

As a matter of example, take $\frac{T}{T_u} \sim 7$, $\rho_u = 1 \text{ kg/m}^3$, and $s_L = 0.5 \text{ m/s}$. Then,

$p_{out} - p_{in} = -1.5 \text{ Pa}$. Hence the pressure jump across flames is $o(1) \text{ Pa}$, the effect of which on density may be safely neglected.

Grid refinement (I)





Grid re-definition

1. Addition of new points

New points are added in locations where the gradient and the curvature of relevant variables are large

2. Adaptive refinement

No new points are added, but the position of existing points is redistributed (adapted) in order to better capture the high-gradient, high-curvature regions

Addition of new points (mesh refinement)

- The solution is initiated on a very coarse mesh (~ 10 *points*).
- Then a sequence of simulations on finer meshes is carried out. Based on the coarse-mesh solution, new mesh points are added in regions where finer mesh is required. The previous coarse-mesh solution is interpolated on the new finer mesh.
- In particular, mesh points are added in regions where the solution has high gradients and curvatures. The following conditions have to be met in every mesh point:

$$\left\{ \begin{array}{l} |\phi_j - \phi_{j-1}| \leq \delta_1 (\max \phi - \min \phi) \\ \left| \left(\frac{d\phi}{dx} \right)_j - \left(\frac{d\phi}{dx} \right)_{j-1} \right| \leq \delta_2 \left(\max \frac{d\phi}{dx} - \min \frac{d\phi}{dx} \right) \end{array} \right.$$

- In each of the subintervals where the constraints above are not satisfied, a new mesh point is placed. The δ_1 and δ_2 coefficients are user-specified input parameters. After determining a converged solution on the new fine mesh, the adaptation procedure is performed once again. A sequence of solutions on successively finer meshes is computed until the inequalities above are satisfied between all the mesh points.

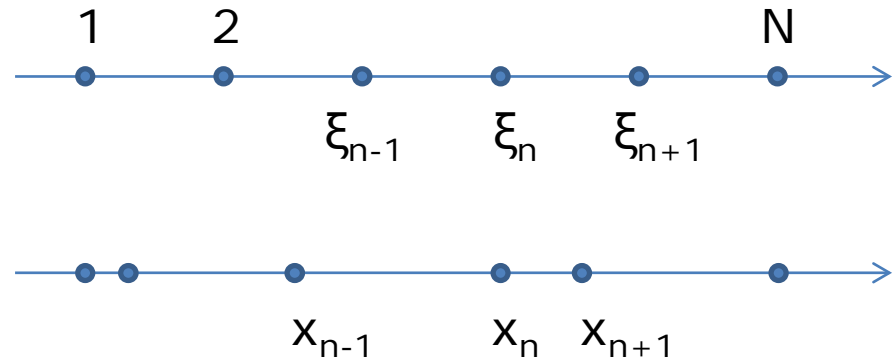
Adaptive grid refinement

The redistribution of the points is carried out on the idea that the product between each spatial interval and a suitable function weight W is the same for all the intervals of the grid:

$$W(x)\Delta x = \text{const}$$

In mathematical terms the redistribution is made by going to solve the following elliptical problem:

$$\begin{cases} W \frac{d^2 x}{d\xi^2} + \frac{dW}{d\xi} \frac{dx}{d\xi} = 0 \\ x(\xi = 1) = 0 \\ x(\xi = N_p) = L \end{cases}$$



The weight function must obviously be greater in areas where the gradient and the curvature of the profiles of the significant variables (in general the T) are higher:

$$W(x) = (1 + C_1^2 |k|) \sqrt{1 + C_2^2 \left(\frac{dT}{dx} \right)^2}$$

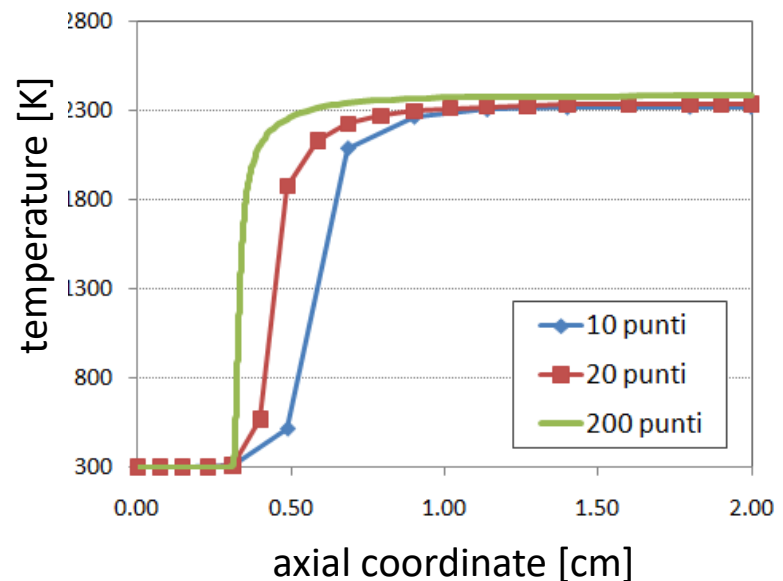
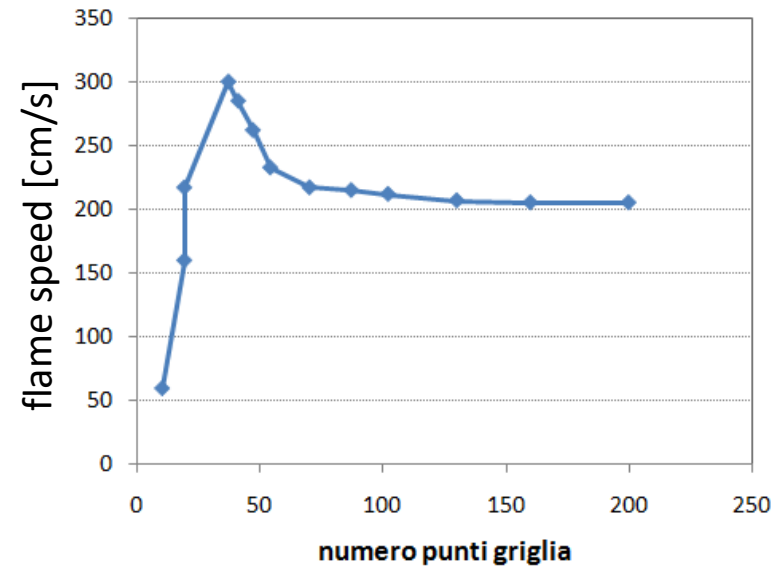
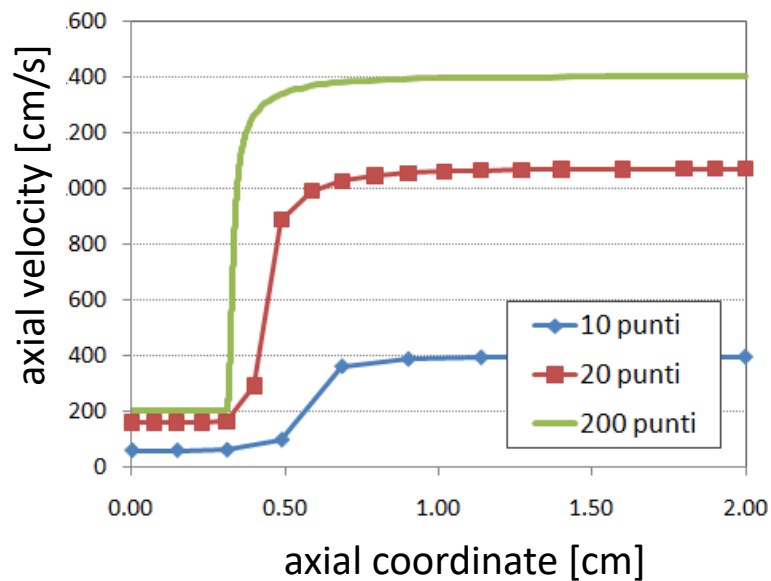
curvature

$$k = \frac{d^2 T}{dx^2} / \left(1 + \left(\frac{dT}{dx} \right)^2 \right)^{3/2}$$

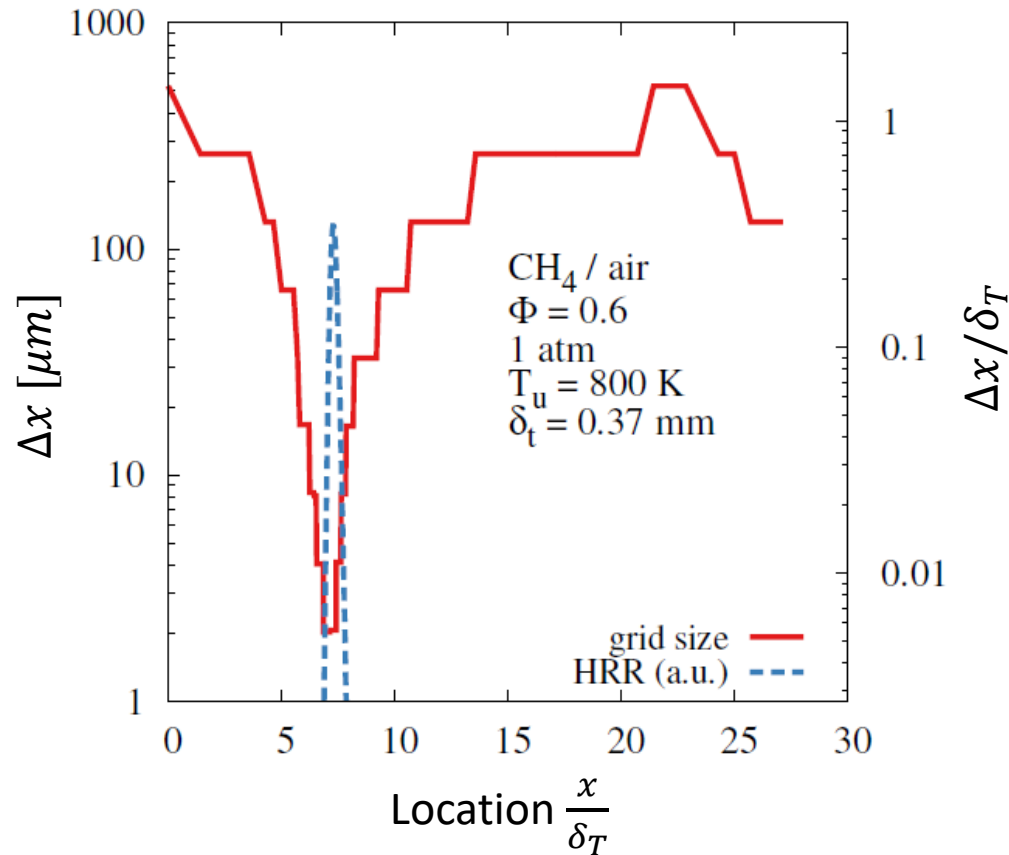
C_1 and C_2 are user-defined constants

Importance of grid refinement (I)

Example of a H₂/air flame at atmospheric pressure



Importance of grid refinement (II)



- The reaction zone poses the most strict requirements on grid size:

$$\frac{\Delta x}{\delta_T} \approx \frac{1}{100}$$

with physical size $\Delta x \approx 2 \mu m$.

- Outside of the reaction zone $\Delta x \approx 100 \mu m$ is acceptable.
- Mesh refinement is a mandatory strategy when simulating premixed flames.

1. Introduction

Combustion and transport phenomena & laminar flames.

2. Numerical solution of 1D flames

a) Premixed laminar flames

i. Burner stabilized unstretched (or flat) flame

- Governing equations and modeling aspects
- Numerical solution

ii. Freely-propagating unstretched (or flat) flame

- Governing equations and modeling aspects

b) Counterflow diffusion flames

3. Multidimensional flames

a) Introduction and examples

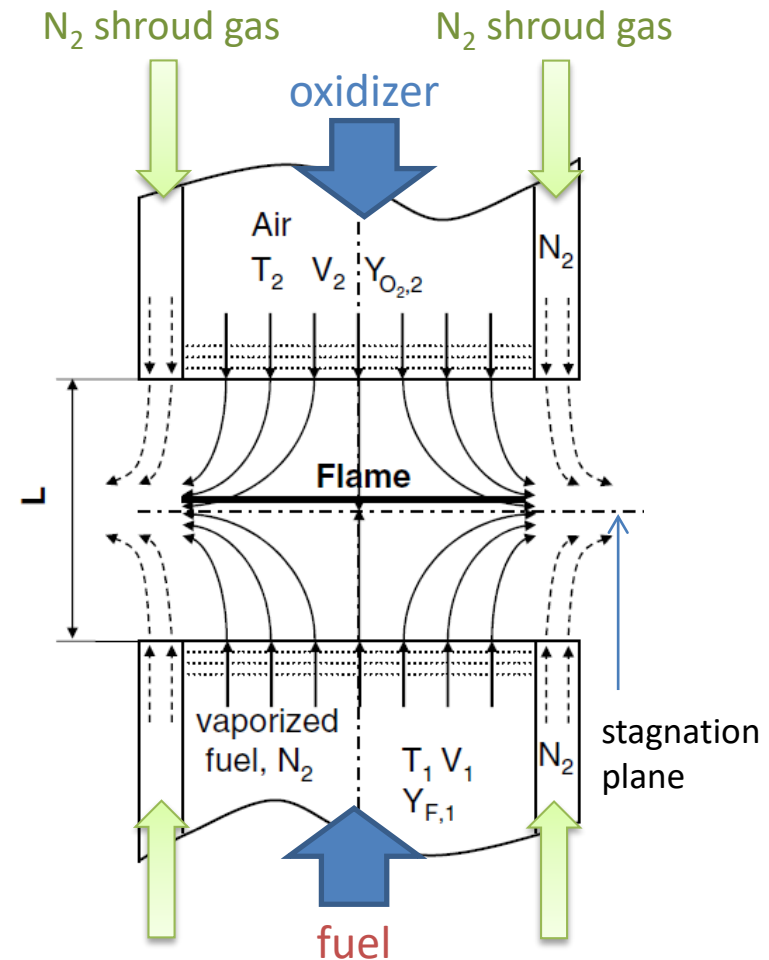
b) Governing equations

c) Numerical algorithms for multidimensional flames

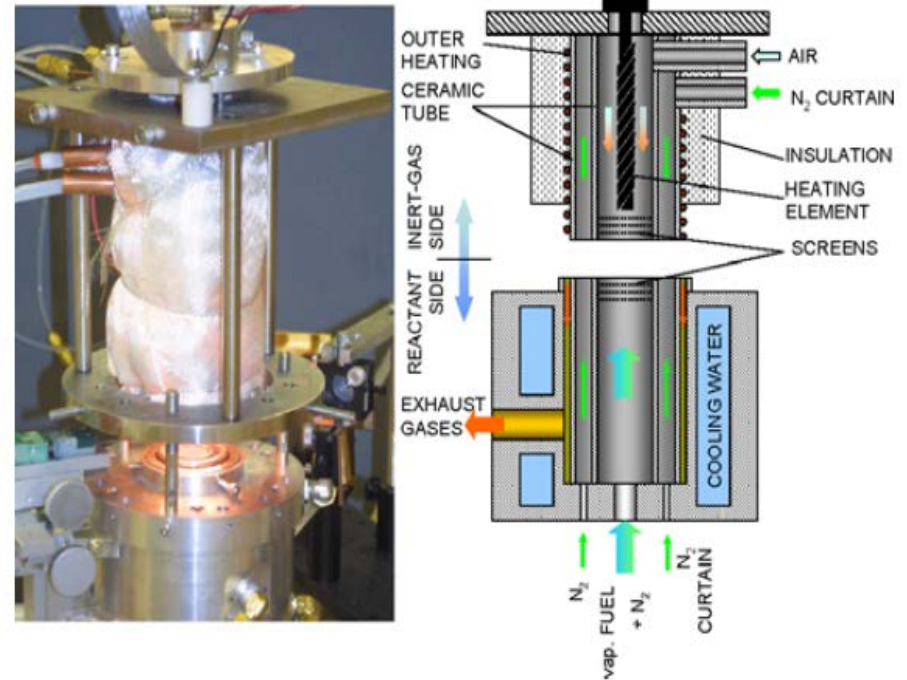
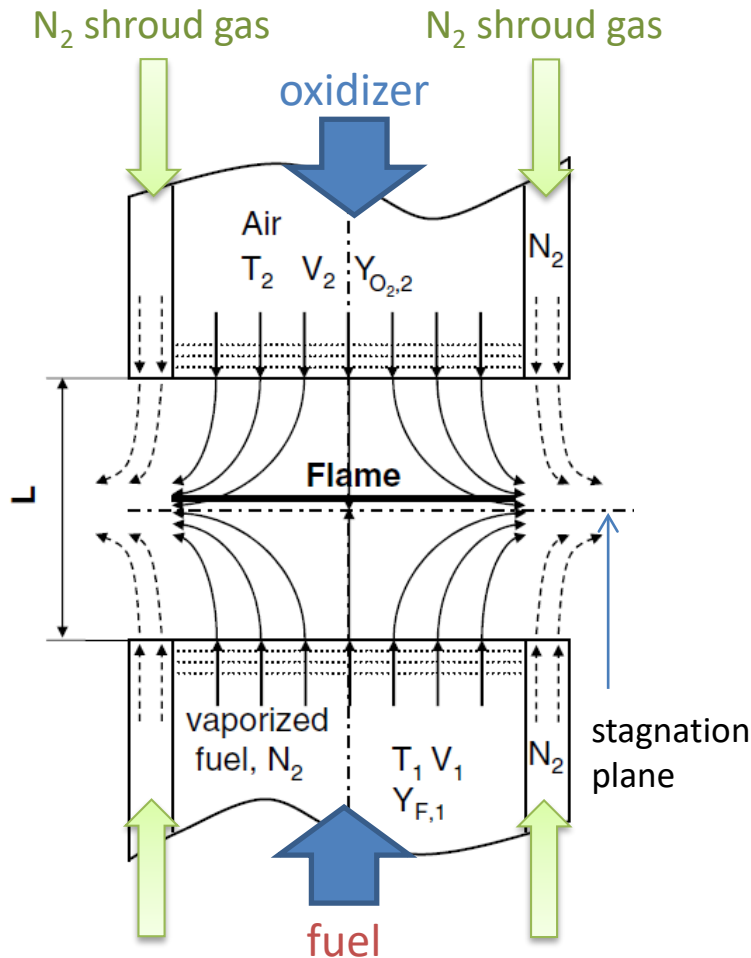
d) The operator-splitting method

Counterflow Diffusion Flames (I)

- The laminar one-dimensional counterflow flame configuration consists in a boundary value problem with parameter and describes the flow field in between opposing reactive jets.
- Counterflow flames are used to investigate ignition, extinction, and structure of non-premixed flames
- The one-dimensional counterflow flame is used to develop closure models for turbulent non-premixed combustion
- Often numerical solutions are compared to experiments
- Computations are numerically affordable



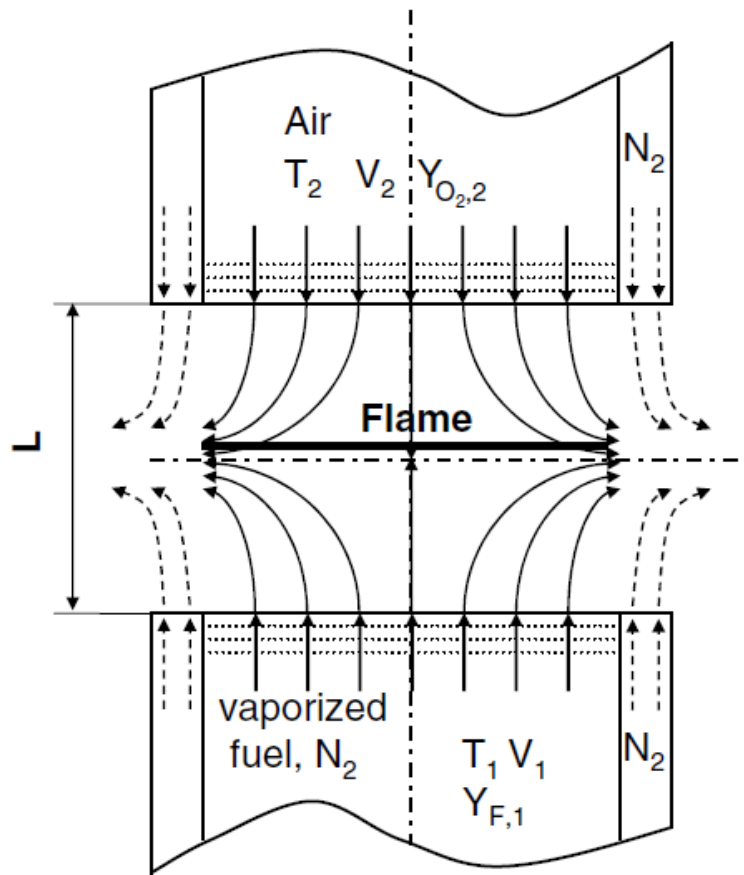
Counterflow Diffusion Flames (II)



A photograph of a counterflow burner and a sketch of the reactant flow in the ducts

T. Bieleveld et al., Proceedings of the Combustion Institute 32 (2009) 493–500

Counterflow Diffusion Flames (III)



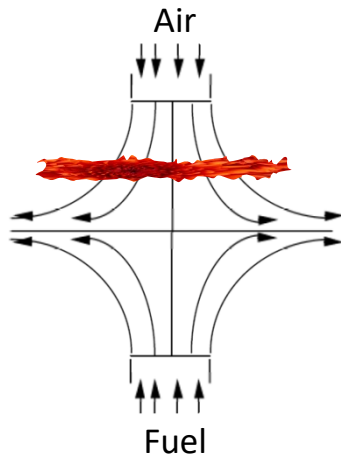
The opposed-flow geometry is an attractive experimental configuration, because the **flames are flat**, allowing for detailed study of the flame chemistry and structure.

Moreover, mathematically the 2D flow can be **reduced to 1D**.

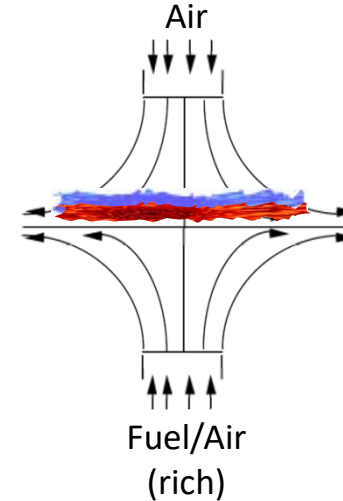
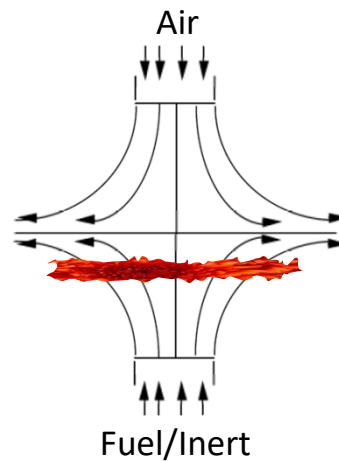
It leads to a significant simplification because all fluid properties are functions of the axial distance only. Kinetic studies can be performed using detailed mechanisms in a reasonable amount of time.

Types of counter-flow diffusion flames

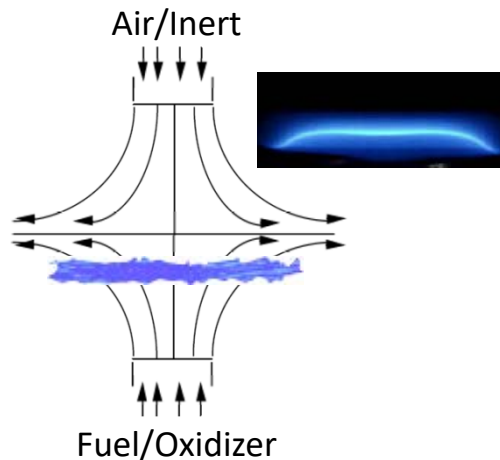
Non premixed flame configuration



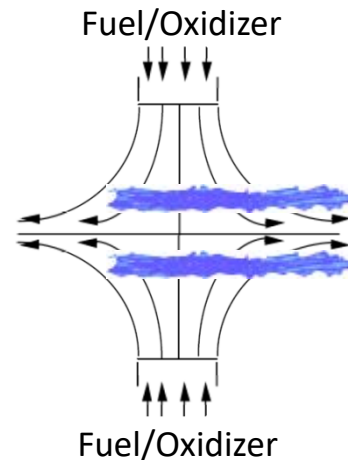
Partially premixed flame



Single premixed flame



Twin premixed flame



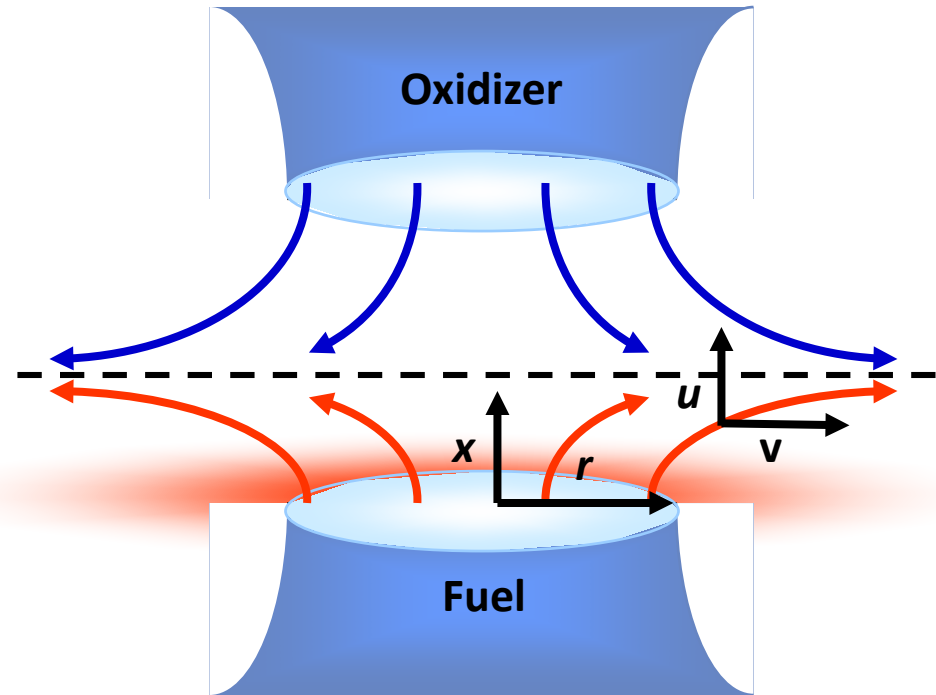
Counterflow diffusion flame mathematical model

Dotted line shows the stagnation plane (axial velocity $u = 0$)

The stagnation plane is approximately in the middle, depending on the momenta of the two streams

Usually, since the flame (if fuel is not largely diluted using an inert) requires more air than fuel by mass, the flame is formed on the oxidizer side of the stagnation plane.

The fuel diffuses (not convection) through the stagnation plane and forms a stoichiometric mixture.

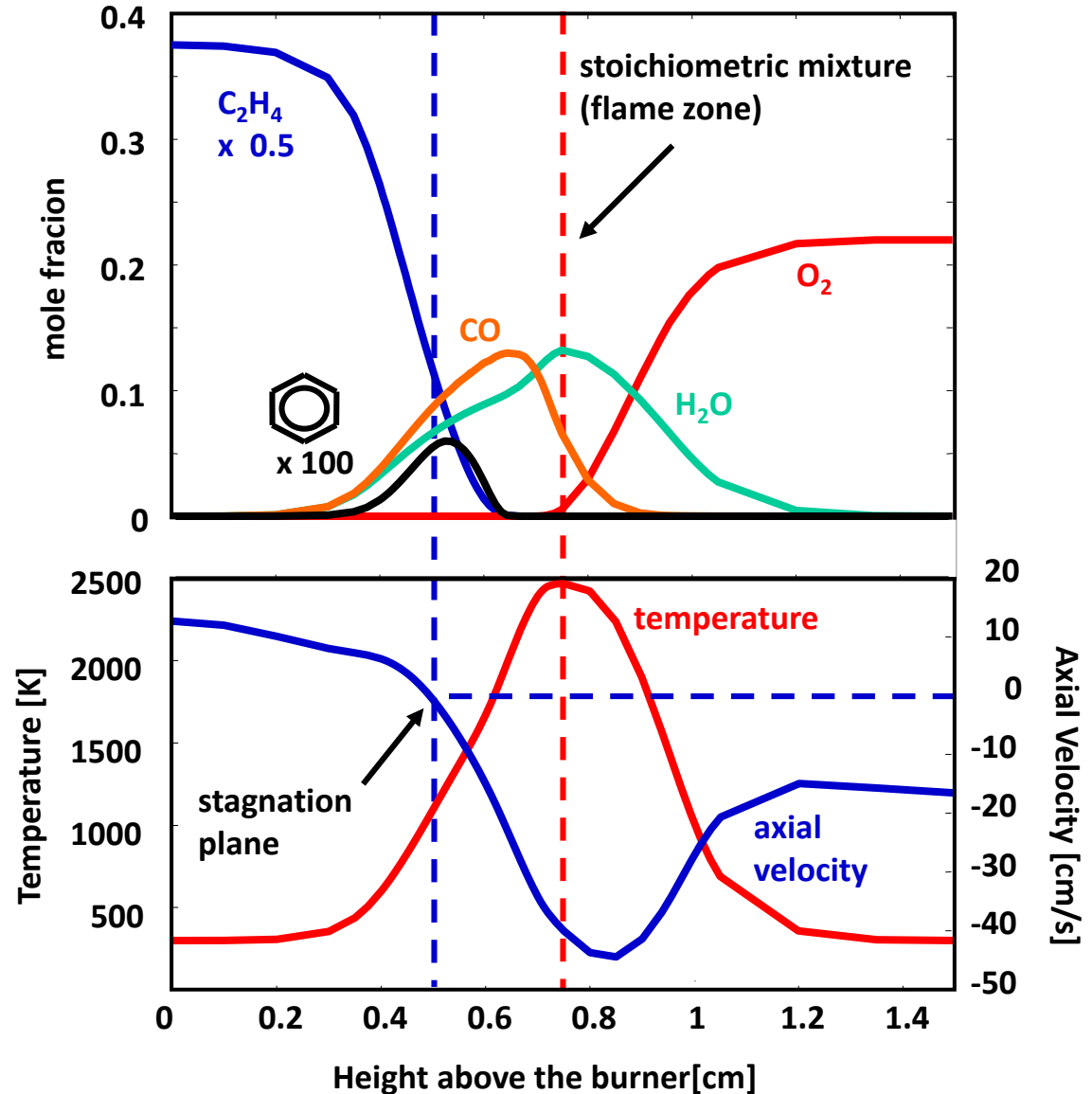


x, r : axial and radial coordinates

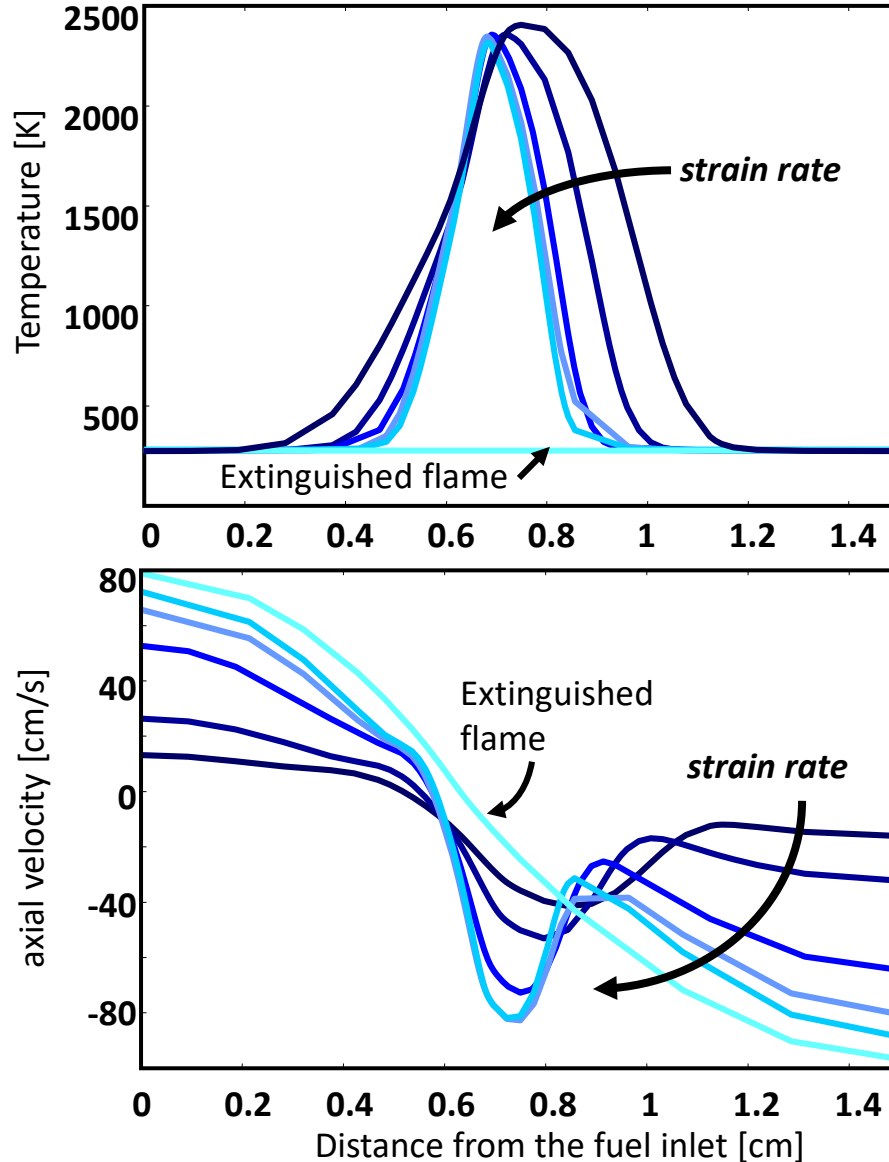
u, v : axial and radial velocities

Typical profiles in CFDF

- The Temperature peak corresponds to the stoichiometric mixture.
- Similarly, the products associated to complete oxidation (e.g. H_2O) have the peak value in the same position.
- In the rich side of the flame unburned hydrocarbons and partial oxidation products are observed.
- The maximum value of PAH is observed in the region of the stagnation plane.



Strain Rate in CFDF



The **strain rate** is a characteristic flow time.

Higher strain rates correspond to higher residence times of gases in the flame.

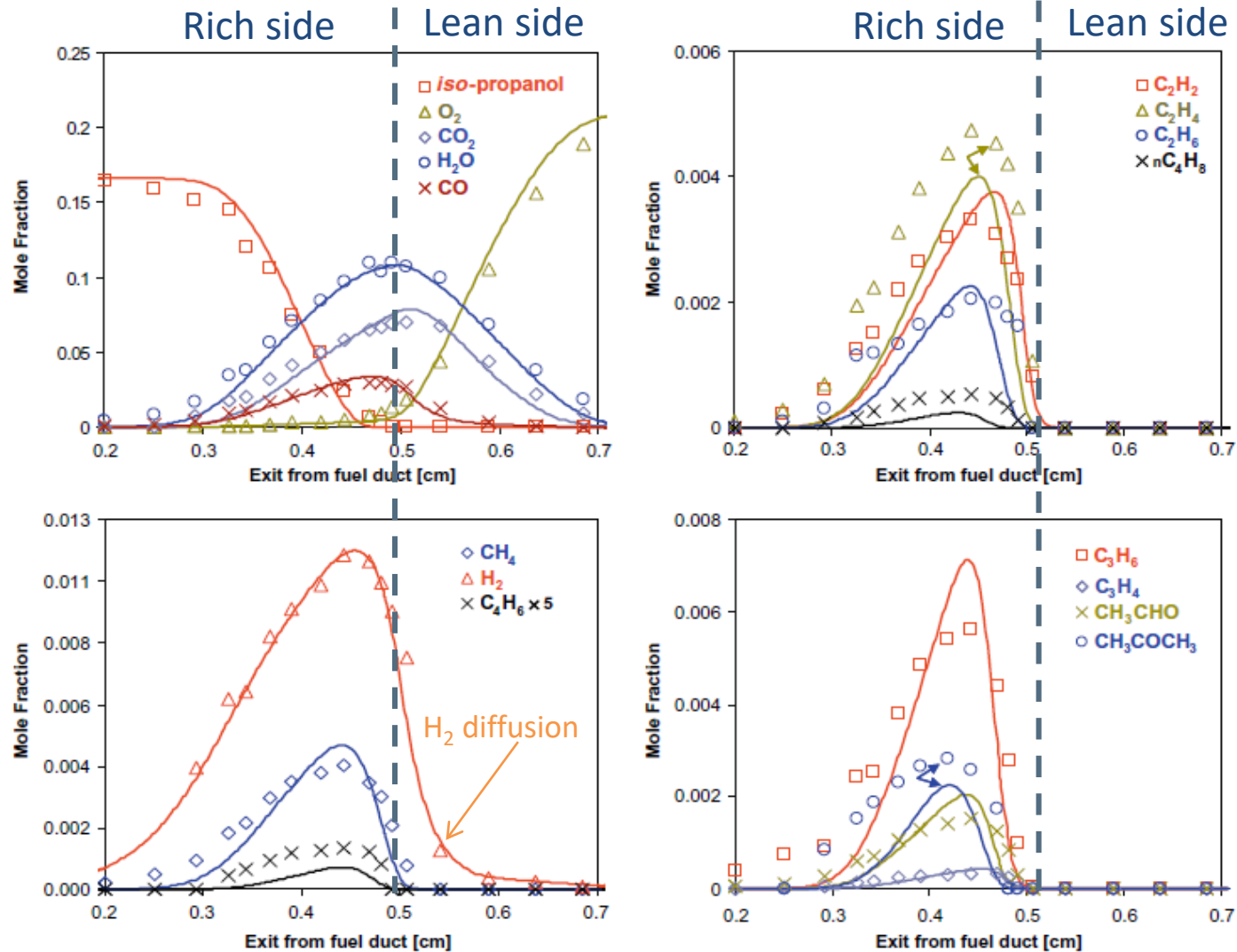
$$\text{Global strain rate: } K = \frac{2v_o}{v_o} \left(1 + \frac{v_c}{v_o} \left(\frac{\rho_c}{\rho_o} \right) \right)$$

$$a_s = \frac{2u_{ox}}{L} \left(1 + \frac{u_f}{u_{ox}} \sqrt{\frac{\rho_f}{\rho_{ox}}} \right)$$

Increasing the strain rate, the flame becomes thinner and eventually extinguishes

K. Seshadri and F.A. Williams, Structure and extinction of counterflow diffusion flames above condensed fuels, 1978]

Comparison with experimental data



A. Frassoldati, A. Cuoci, T. Faravelli, U. Niemann, E. Ranzi, R. Seiser, K. Seshadri, *An experimental and kinetic modeling study of n-propanol and iso-propanol combustion*, Combustion and Flame 157(1), 2-16 (2010)

Model assumptions

- Laminar flame
- Ideal gas
- Axial symmetry (2D flow)
- Steady-state conditions

Assuming:

- Temperature and composition (mass fractions) are only a function of the axial coordinate x , $T = T(x)$ and $Y_i = Y_i(x)$
- All physical properties only depend on the axial coordinate
- The axial velocity is also a function of the axial coordinate only: $u = u(x)$

The 2D problem is reduced to a 1D case, where the independent variable is the axial coordinate x .

$$\left\{ \begin{array}{ll} \frac{D}{Dt}(\rho \mathbf{u}) = 0 & \text{Continuity equation} \\ \rho \frac{D\mathbf{u}}{Dt} = -\nabla p + \nabla \cdot \mu \left(\nabla \mathbf{u} + \nabla \mathbf{u}^T - \frac{2}{3}(\nabla \cdot \mathbf{u})\mathbf{I} \right) + \rho \mathbf{g} & \text{Momentum equations} \\ \rho \frac{DY_i}{Dt} = \nabla \cdot (\rho \mathcal{D}_i \nabla Y_i) + \dot{\Omega}_i & \text{Species equations} \\ \rho C_P \frac{DT}{Dt} = \frac{Dp}{Dt} + \nabla \cdot \lambda \nabla T - \sum \rho \mathbf{u}_i^d Y_i C_{Pi} \cdot \nabla T + \dot{Q} & \text{Temperature equation} \end{array} \right.$$

Continuity equation

$$\frac{D}{Dt}(\rho u) = 0 \quad \longrightarrow \quad \nabla(\rho u) = 0 \quad \longrightarrow \quad \frac{\partial}{\partial x}(\rho u) + \frac{1}{r} \frac{\partial}{\partial r}(\rho v) = 0$$

Definitions

$$\frac{1}{r} \frac{\partial}{\partial r}(\rho v) = 2F(x) \quad \longrightarrow \quad \frac{\partial}{\partial r}(\rho v) = 2rF(x)$$

$$\int \frac{\partial}{\partial r}(\rho v) dr = \int 2rF(x) dr \quad \longrightarrow \quad \rho v = r^2 F(x) \quad \longrightarrow \quad \frac{v}{r} = F(x)$$

$$\frac{\partial v}{\partial r} = \frac{\partial}{\partial r}(rF(x)) \quad \longrightarrow \quad \frac{\partial v}{\partial r} = F(x) = \frac{v}{r}$$

$$\quad \longrightarrow \quad \frac{\partial}{\partial x}(\rho u) + 2\rho \frac{v}{r} = 0 \quad \longrightarrow \quad \frac{\partial}{\partial x}\left(\frac{\rho u}{2}\right) + \frac{\rho v}{r} = 0$$

$$U(x) \stackrel{\text{def}}{=} \frac{\rho u}{2} \quad G(x) \stackrel{\text{def}}{=} -\frac{\rho v}{r}$$

The continuity equation reduces to

$$\frac{dU}{dx} = G$$

Momentum equations (I)

The momentum equations can be written in cylindrical coordinates because of the 2D axisymmetric assumption. After some manipulations, considering that $v = v(x)$ and $\frac{\partial v}{\partial r} = \frac{v}{r}$, we have:

$$\left\{ \begin{array}{l} \rho \left(u \frac{\partial u}{\partial x} + v \frac{\partial u}{\partial r} \right) = -\frac{\partial P}{\partial x} + \mu \frac{2}{r} \frac{\partial v}{\partial x} + \frac{\partial}{\partial x} \left(\frac{4}{3} \mu \left(\frac{\partial u}{\partial x} - \frac{v}{r} \right) \right) \\ \rho \left(u \frac{\partial v}{\partial x} + v \frac{\partial v}{\partial r} \right) = -\frac{\partial P}{\partial r} + \frac{\partial}{\partial x} \left(\mu \frac{\partial v}{\partial x} \right) \end{array} \right.$$

which can be rewritten as:

$$\left\{ \begin{array}{l} \frac{\partial P}{\partial x} = -\rho u \frac{\partial u}{\partial x} + \mu \frac{2}{r} \frac{\partial v}{\partial x} + \frac{\partial}{\partial x} \left(\frac{4}{3} \mu \left(\frac{\partial u}{\partial x} - \frac{v}{r} \right) \right) \\ \frac{\partial P}{\partial r} = -\rho \left(u \frac{\partial v}{\partial x} + \frac{v^2}{r} \right) + \frac{\partial}{\partial x} \left(\mu \frac{\partial v}{\partial x} \right) \end{array} \right.$$

Momentum equations (II)

If we introduce the two variables $U(x) \stackrel{\text{def}}{=} \frac{\rho u}{2}$ and $G(x) \stackrel{\text{def}}{=} -\frac{\rho v}{r}$:

$$\begin{cases} \frac{\partial P}{\partial x} = -4U \frac{\partial}{\partial x} \left(\frac{U}{\rho} \right) - 2\mu \frac{\partial}{\partial x} \left(\frac{1}{\rho} \frac{\partial U}{\partial x} \right) + \frac{4}{3} \frac{\partial}{\partial x} \left(2\mu \frac{\partial}{\partial x} \left(\frac{U}{\rho} \right) + \frac{\mu}{\rho} \frac{\partial U}{\partial x} \right) \\ \frac{1}{r} \frac{\partial P}{\partial r} = \frac{\partial}{\partial x} \left(\frac{2U}{\rho} \frac{\partial U}{\partial x} \right) - \frac{3}{\rho} \left(\frac{\partial U}{\partial x} \right)^2 - \frac{\partial}{\partial x} \left(\mu \frac{\partial}{\partial x} \left(\frac{1}{\rho} \frac{\partial U}{\partial x} \right) \right) \end{cases}$$

It is evident that both $\frac{\partial P}{\partial x}$ and $\frac{1}{r} \frac{\partial P}{\partial r}$ are only a function of x only.

$$\frac{\partial P}{\partial x} = -4U \frac{\partial}{\partial x} \left(\frac{U}{\rho} \right) - 2\mu \frac{\partial}{\partial x} \left(\frac{1}{\rho} \frac{\partial U}{\partial x} \right) + \frac{4}{3} \frac{\partial}{\partial x} \left[2\mu \frac{\partial}{\partial x} \left(\frac{U}{\rho} \right) + \frac{\mu}{\rho} \frac{\partial U}{\partial x} \right]$$

$$\frac{1}{r} \frac{\partial P}{\partial r} = \frac{\partial}{\partial x} \left(\frac{2U}{\rho} \frac{\partial U}{\partial x} \right) - \frac{3}{\rho} \left(\frac{\partial U}{\partial x} \right)^2 - \frac{\partial}{\partial x} \left(\mu \frac{\partial}{\partial x} \left(\frac{1}{\rho} \frac{\partial U}{\partial x} \right) \right)$$

$$\Rightarrow \frac{\partial}{\partial x} \left(\frac{1}{r} \frac{\partial P}{\partial r} \right) = \frac{1}{r} \frac{\partial}{\partial r} \left(\frac{\partial P}{\partial x} \right) = 0$$

$$\frac{1}{r} \frac{\partial P}{\partial r} = H = \text{const} \quad \text{Eigenvalue of the system}$$

The radial momentum equation is satisfied by the eigenvalue

Momentum equations (III)

Since $\frac{dU}{dx} = G$, we can obtain from the radial momentum equation the following equation that is a function of x only:

$$\frac{1}{r} \frac{\partial P}{\partial r} = \frac{\partial}{\partial x} \left(\frac{2U}{\rho} \frac{\partial U}{\partial x} \right) - \frac{3}{\rho} \left(\frac{\partial U}{\partial x} \right)^2 - \frac{\partial}{\partial x} \left(\mu \frac{\partial}{\partial x} \left(\frac{1}{\rho} \frac{\partial U}{\partial x} \right) \right)$$

$$\begin{aligned} \frac{1}{r} \frac{\partial P}{\partial r} &= \frac{\partial}{\partial x} \left(\frac{2U}{\rho} \frac{\partial U}{\partial x} \right) - \frac{3}{\rho} \left(\frac{\partial U}{\partial x} \right)^2 - \frac{\partial}{\partial x} \left(\mu \frac{\partial}{\partial x} \left(\frac{1}{\rho} \frac{\partial U}{\partial x} \right) \right) \\ H &= \frac{\partial}{\partial x} \left(\frac{2U}{\rho} G \right) - \frac{3}{\rho} G^2 - \frac{\partial}{\partial x} \left(\mu \frac{\partial}{\partial x} \left(\frac{G}{\rho} \right) \right) \\ H &= \frac{\partial}{\partial x} \left(\frac{2U}{\rho} G \right) - \frac{3}{\rho} G^2 - \frac{\partial}{\partial x} \left(\mu \frac{\partial}{\partial x} \left(\frac{G}{\rho} \right) \right) \\ H + \frac{\partial}{\partial x} \left(\mu \frac{\partial}{\partial x} \left(\frac{G}{\rho} \right) \right) + \frac{3}{\rho} G^2 - 2 \frac{\partial}{\partial x} \left(\frac{UG}{\rho} \right) &= 0 \end{aligned}$$



$$\frac{\partial}{\partial x} \left(\mu \frac{\partial}{\partial x} \left(\frac{G}{\rho} \right) \right) - 2 \frac{\partial}{\partial x} \left(\frac{UG}{\rho} \right) + \frac{3}{\rho} G^2 + H = 0$$

$$\frac{d}{dx} \left[\mu \frac{d}{dx} \left(\frac{G}{\rho} \right) \right] - 2 \frac{d}{dx} \left(\frac{UG}{\rho} \right) + \frac{3}{\rho} G^2 + H = 0$$

Species conservation equations

$$\rho \frac{D\omega_i}{Dt} = -\nabla \cdot \mathbf{j}_i + \dot{\omega}_i$$

$$\rho \frac{DY_i}{Dt} = \rho v_r \frac{\partial Y_i}{\partial r} + (\rho \mathcal{D}_i \frac{\partial Y_i}{\partial x}) + \frac{1}{r} \frac{\partial (r \cdot j_{i,r})}{\partial r} - \frac{\partial j_{i,x}}{\partial x} + \dot{\omega}_i$$

Considering steady-state conditions and writing the equation in cylindrical coordinates:

$$\rho \left(u \frac{\partial Y_i}{\partial x} + v \frac{\partial Y_i}{\partial r} \right) = \frac{\partial}{\partial x} \left(\rho \mathcal{D}_i \frac{\partial Y_i}{\partial x} \right) \frac{1}{r} \frac{\partial}{\partial r} \left(r \rho \mathcal{D}_i \frac{\partial Y_i}{\partial r} \right) + \dot{\omega}_i$$

Since the mass fractions are a function of axial coordinate only:

$$\rho v_x \frac{d\omega_i}{dx} = \frac{d(\rho \omega_i V_{i,x})}{dx} - \frac{\partial}{\partial x} \left(\rho \mathcal{D}_i \frac{\partial Y_i}{\partial x} \right) + \dot{\omega}_i$$

After introducing the variable U :

$$2U \frac{d\omega_i}{dx} = \frac{d(\rho \omega_i V_{i,x})}{dx} + \dot{\omega}_i$$

$$2U \frac{\partial Y_i}{\partial x} = \frac{\partial}{\partial x} \left(\rho \mathcal{D}_i \frac{\partial Y_i}{\partial x} \right) + \dot{\omega}_i$$

Temperature equation

$$\rho C_P \frac{DT}{Dt} = \frac{Dp}{Dt} + \nabla \cdot \lambda \nabla T - \sum \rho \mathbf{u}_i^d Y_i C_{Pi} \nabla T + \dot{Q}$$

Considering steady-state conditions, writing the equation in cylindrical coordinates and accounting that the temperature is function of axial coordinate only:

$$\rho C_P u \frac{\partial T}{\partial x} = \frac{Dp}{Dt} + \frac{\partial}{\partial x} \left(\lambda \frac{\partial T}{\partial x} \right) - \sum \rho \mathbf{u}_i^d Y_i C_{Pi} \frac{\partial T}{\partial x} + \dot{Q}$$

If we consider negligible the Lagrangian derivative of pressure and we explicitly write the diffusion velocities:

$$\rho C_P u \frac{\partial T}{\partial x} = \frac{\partial}{\partial x} \left(\lambda \frac{\partial T}{\partial x} \right) + \sum \rho C_{Pi} \mathcal{D}_i \frac{\partial Y_i}{\partial x} \frac{\partial T}{\partial x} + \dot{Q}$$

After introducing the variable U :

$$2UC_P \frac{\partial T}{\partial x} = \frac{\partial}{\partial x} \left(\lambda \frac{\partial T}{\partial x} \right) + \sum \rho C_{Pi} \mathcal{D}_i \frac{\partial Y_i}{\partial x} \frac{\partial T}{\partial x} + \dot{Q}$$

Governing equations: summary

$$\left\{ \begin{array}{ll} \frac{dU}{dx} = G & \text{Continuity equation} \\ \frac{dH}{dx} = 0 & \text{Momentum equation (radial)} \\ \frac{d}{dx} \left(\mu \frac{d}{dx} \left(\frac{G}{\rho} \right) \right) - 2 \frac{d}{dx} \left(\frac{UG}{\rho} \right) + \frac{3}{\rho} G^2 + H = 0 & \text{Momentum equation (axial)} \\ 2U \frac{dY_i}{dx} = \frac{\partial}{\partial x} \left(\rho \mathcal{D}_i \frac{dY_i}{dx} \right) + \dot{\Omega}_i & \text{Species equations} \\ 2UC_p \frac{dT}{dx} = \frac{d}{dx} \left(\lambda \frac{dT}{dx} \right) + \sum \rho C_{pi} \mathcal{D}_i \frac{dY_i}{dx} \frac{dT}{dx} + \dot{Q} & \text{Temperature equation} \end{array} \right.$$

System of ODEs with boundary conditions (BVP)

Unknowns: U, H, G, Y_i, T

$$\rho v_x \omega_i + \rho \omega_i V_{i,x} = (\rho v_x \omega_i)$$

Boundary conditions

$$\text{Fuel side } x = 0 \left\{ \begin{array}{l} U|_{x=0} = \frac{\rho^f u^f}{2} \\ G|_{x=0} = 0 \\ \dot{m}Y_k|_{x=0} - \rho \mathcal{D}_k \frac{dY_k}{dx} \Big|_{x=0} = \dot{m}Y_k^f \\ T|_{x=0} = T^f \end{array} \right.$$

The radial inlet velocity is prescribed (through continuity) by setting G at the inlet. One reasonable choice (but only a “choice”) is $G = 0$ which corresponds to $v = 0$ at the inlets.

$$\text{Oxidizer side } x = L \left\{ \begin{array}{l} U|_{x=L} = \frac{\rho^{ox} u^{ox}}{2} \\ G|_{x=L} = 0 \\ \dot{m}Y_k|_{x=L} - \rho \mathcal{D}_k \frac{dY_k}{dx} \Big|_{x=L} = \dot{m}Y_k^{ox} \\ T|_{x=L} = T^{ox} \end{array} \right.$$

Boundary conditions

- The equation for G and H are first-order. The equation for U is second-order. The equations for T and Y_k are second-order.
- While two BCs may be specified for each of T and U , we are prescribing four BCs for G and U and G).
- Why is this the case? Recall the parameter $H = \text{const}$, which can be interpreted as an additional equation $\frac{dH}{dx} = 0$ (as it is actually implemented in discrete form)

Solution method

- The problem is again a boundary value problem with a parameter. Once discretized, the problem is solved as a non-linear system of equations (Newton's method).
- The algorithm alternates between: (a) re-gridding and (b) solving the system
- The cost scales with $o(NE^3)$ where $NE = NP \times (N + 4)$, where NP is the number of points and N is the number of species

1. Introduction

Combustion and transport phenomena & laminar flames.

2. Numerical solution of 1D flames

- a) Premixed laminar flames
 - i. Burner stabilized unstretched (or flat) flame
 - Governing equations and modeling aspects
 - Numerical solution
 - ii. Freely-propagating unstretched (or flat) flame
 - Governing equations and modeling aspects
- b) Counterflow diffusion flames

3. Multidimensional flames

- a) **Introduction and examples**
- b) Governing equations
- c) Numerical algorithms for multidimensional flames
- d) The operator-splitting method

An example: a naturally flickering flame (I)

Example of naturally flickering buoyancy-dominated diffusion flame



<https://www.youtube.com/watch?v=w5zWkSuYfIY>

Naturally flickering buoyancy-dominated diffusion flames exhibit natural flicker as a result of a buoyancy-induced flow instability, which leads to the formation of strong vortical motions that subsequently interact with the combusting regions of the flame.

Naturally occurring flickering flames are difficult to investigate experimentally because, even though the flickering frequency is well defined, there exist cycle-to-cycle variations. These variations lead to spatial and temporal averaging with a resulting loss in resolution.

An example: a naturally flickering flame (II)

Chrystie & Chung (2014) Combustion Science and Technology, 186:4-5, 409-420, DOI: 10.1080/00102202.2014.883202

Fuel stream

Composition: 100% C₃H₈

Temperature: 298 K

Velocity: 10 cm/s

Oxidizer stream

Composition: 21% O₂+79% N₂

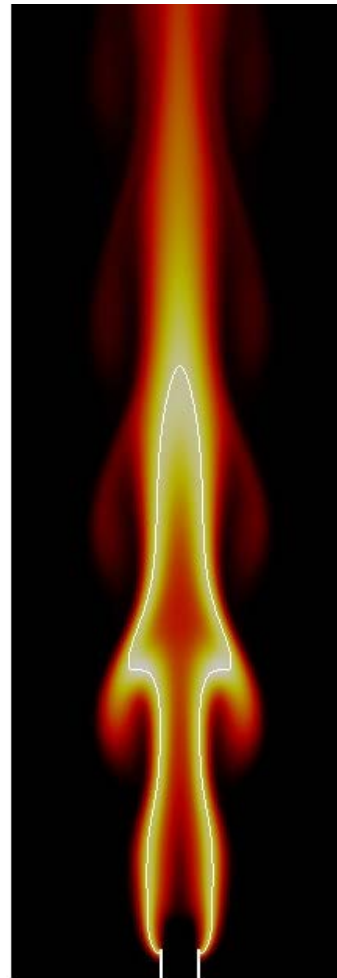
Temperature: 298 K

Velocity: 7 cm/s

Burner:

Diameter: 9 mm

Thickness: 0.8 mm

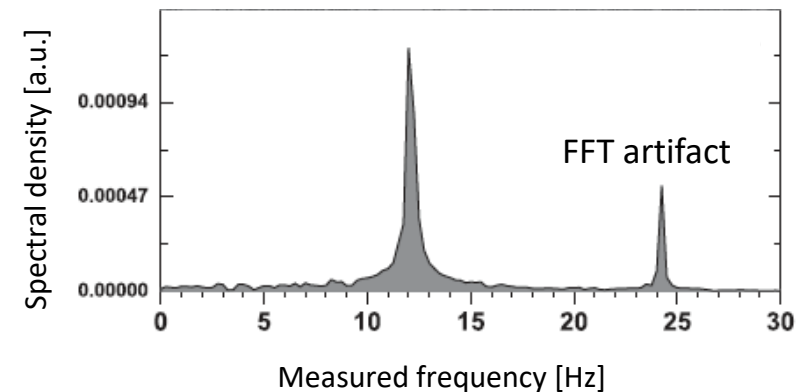


air fuel air

Under normal gravity conditions, laminar coflow diffusion flames have a well defined oscillation frequency f , which is inversely proportional to the square root of the burner diameter, D (in m):

$$f \sim \frac{1.5}{\sqrt{D}}$$

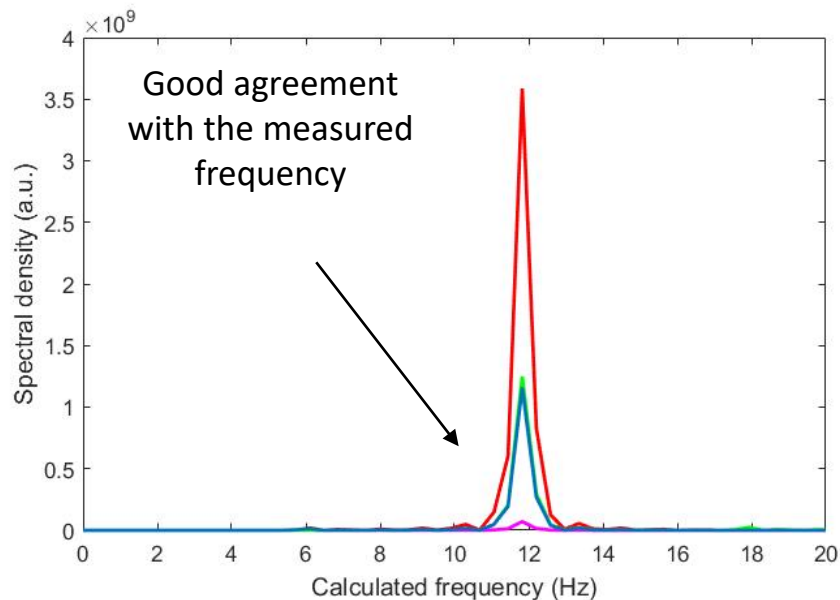
FFT decomposition of the frequencies (exp.)



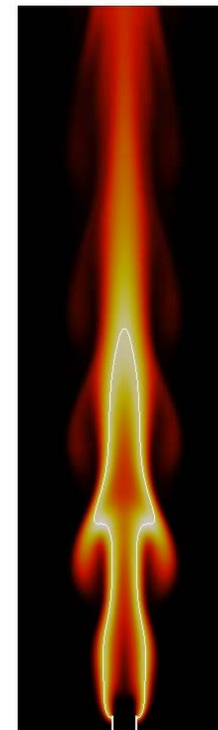
An example: a naturally flickering flame (III)

2D computational domain: 75 x 300 mm²
Number of cells: 58,000
Spatial discretization: 2nd order centered
Time integration: Cranck-Nicolson
ODE solver: OpenSMOKE++
Absolute tolerance: 1e-12
Relative tolerance: 1e-7
Linear solver: Sparse, MKL Pardiso

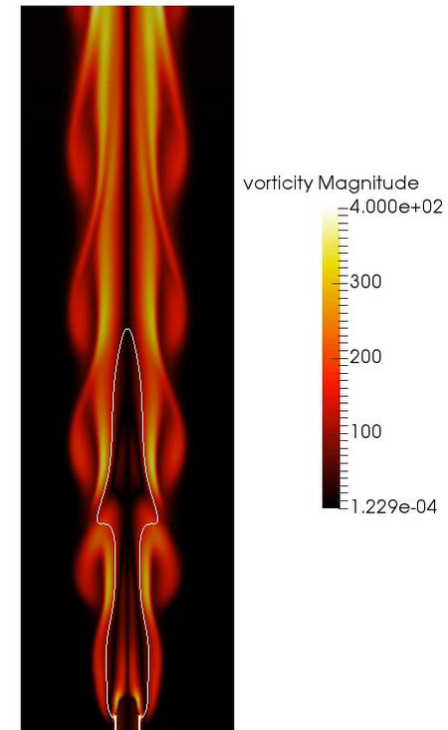
Kinetic mechanism: POLIMI_SOOT_2015
Soot model: discrete sectional method
Number of species: 210
Number of reactions: 10,800



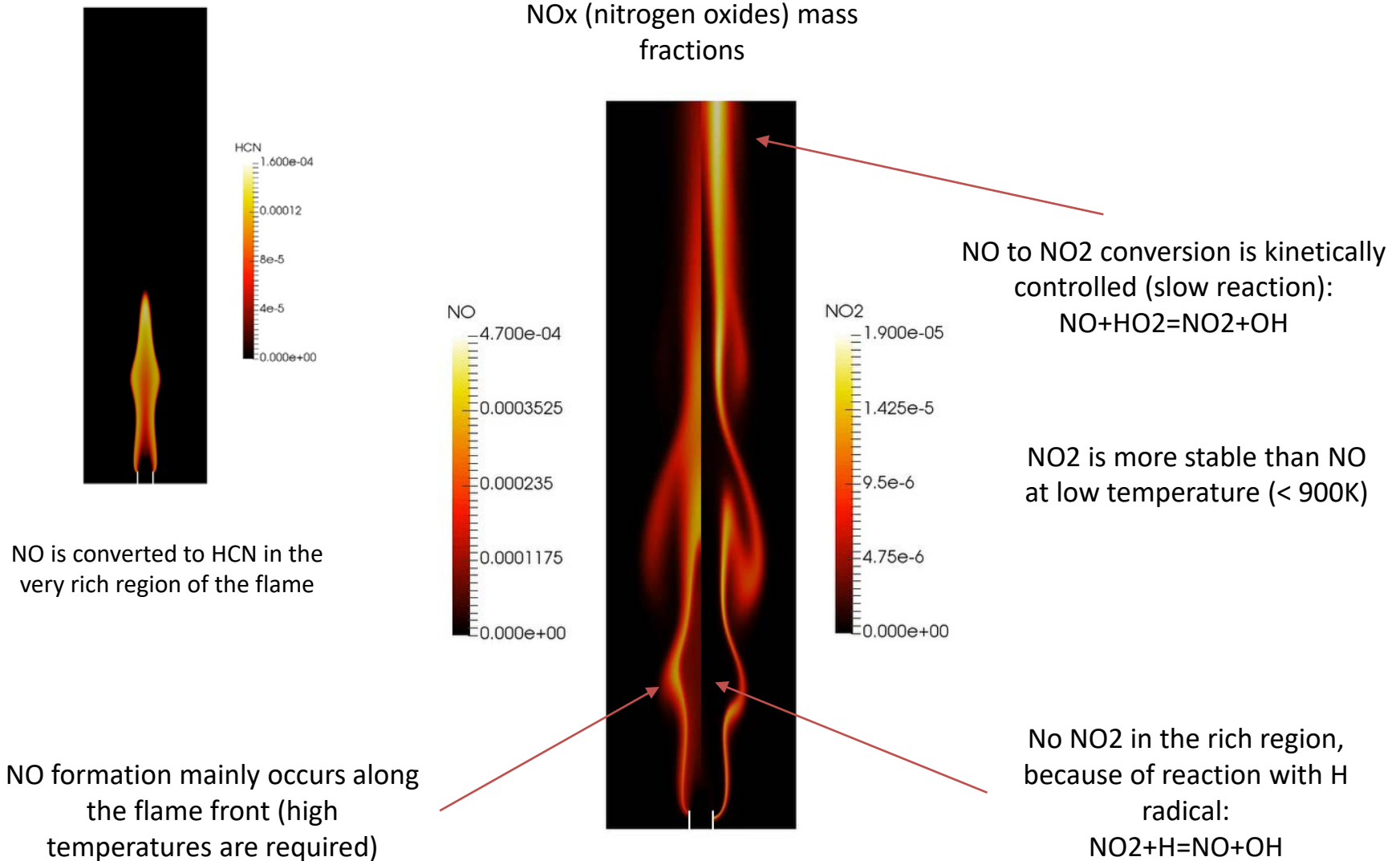
temperature



vorticity



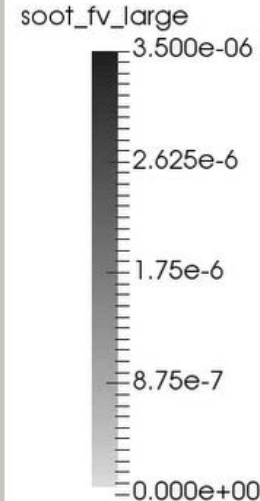
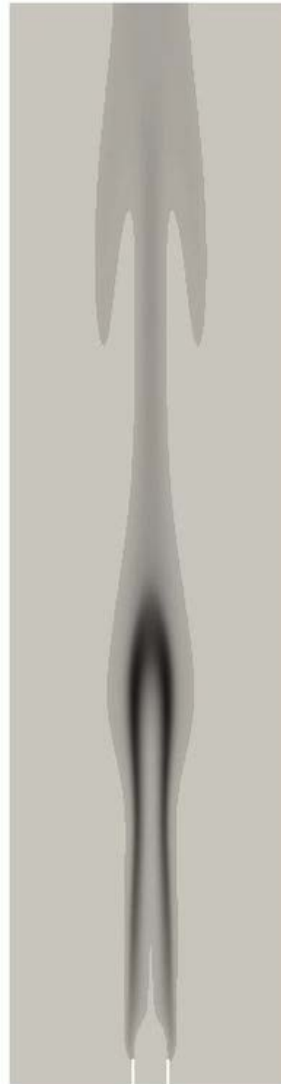
An example: a naturally flickering flame (IV)



An example: a naturally flickering flame (V)

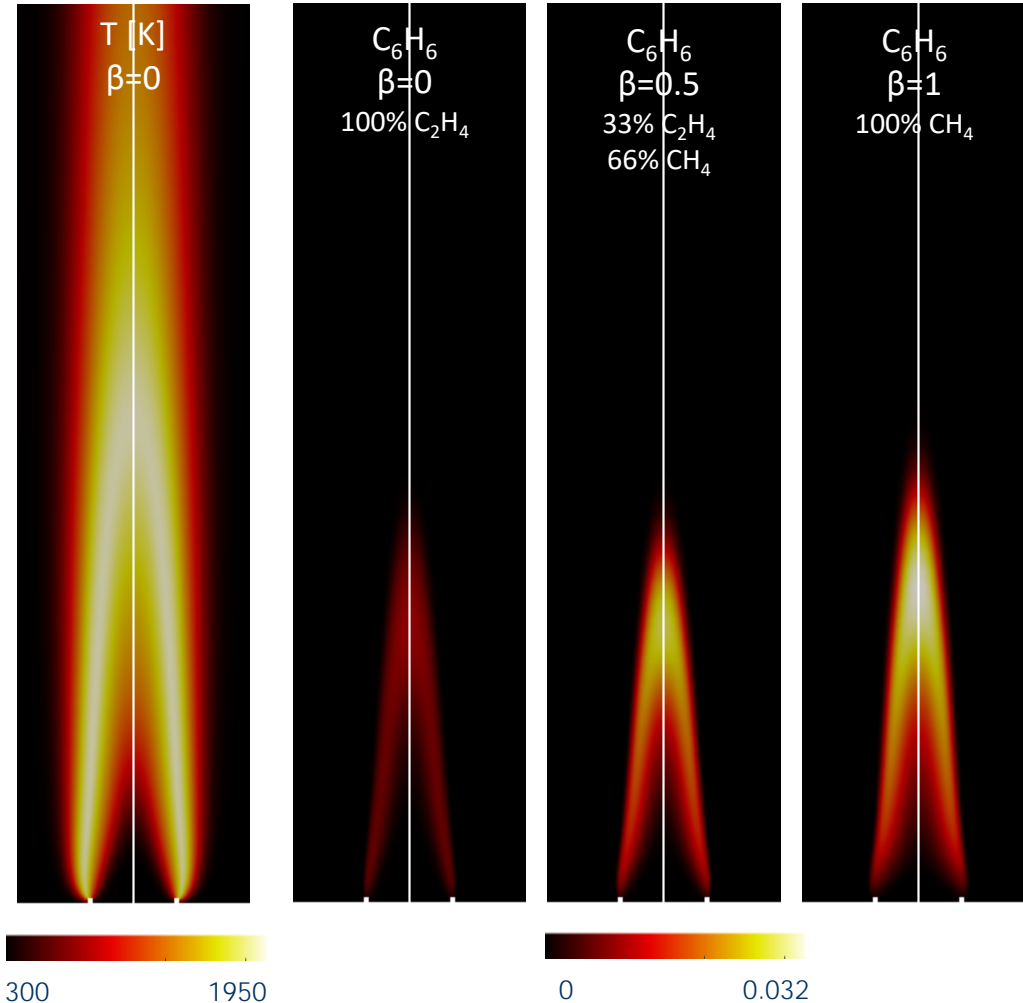
Soot volume fraction

- Soot oxidation occurs in this region
- Soot pockets are periodically released because of flame pinch-off
- The region of soot formation is not significantly affected by the flame flickering
- Formation of soot occurs along the rich side of the flame



Flame pinch-off is created by the presence of counter-rotating stream-wise vortices, that stretch and quench the flame

An example: C₂H₄/CH₄/N₂ coflow flames (I)



Flame details

Fuel: CH₄/C₂H₄

Air: O₂/N₂ (23.2%, 76.8% mass)

V_{fuel} : 12.52 cm/s

V_{air} : 10.50 cm/s

Fuel nozzle diameter: 11.1 mm

Chamber diameter: 110 mm

Computational domain

2D axisymmetric (55 x 200 mm)

Computational grid: ~25,000 cells

Discretization: 2nd order centered

Kinetic mechanism

POLIMI_HT1212:

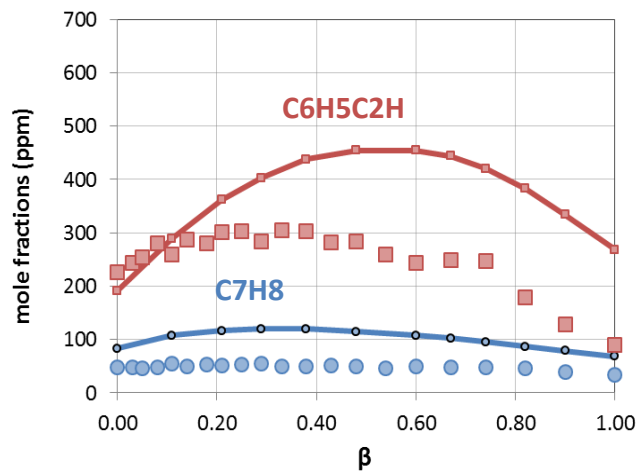
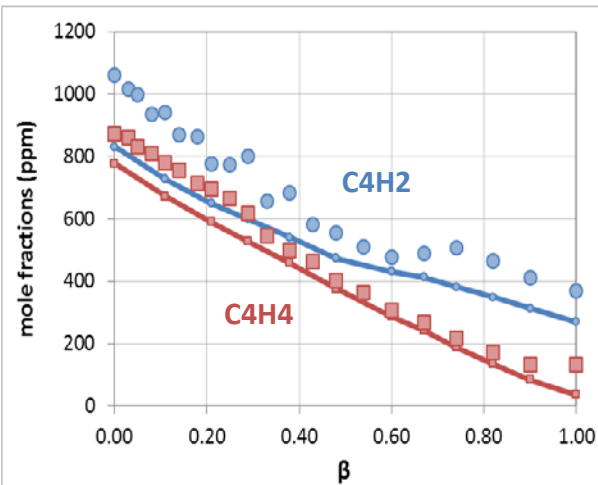
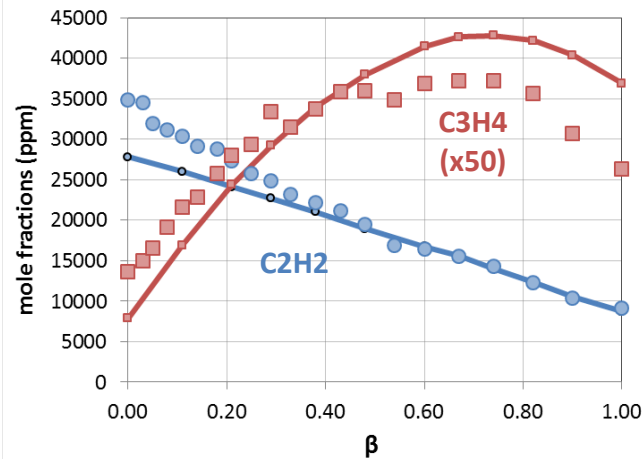
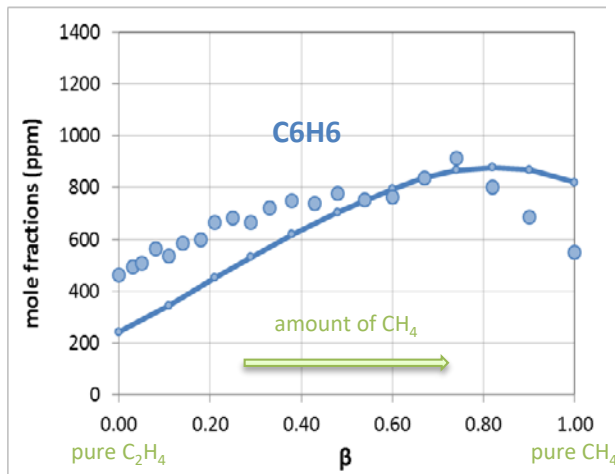
198 species, 6307 reactions

The concentrations of C₂H₄ and CH₄ are identified by the mixture parameter β :

$$\beta = \frac{X_{\text{C}_2\text{H}_4}}{X_{\text{CH}_4} + X_{\text{C}_2\text{H}_4}}$$

Cuoci A., Frassoldati A., Faravelli T., Ranzi E., *A computational tool for the detailed kinetic modeling of laminar flames: application to C₂H₄/CH₄ coflow flames.* Combustion and Flame, 160(5), p. 870-886 (2013)

An example: $C_2H_4/CH_4/N_2$ coflow flames (II)



The peak values (along the center-line) of mole fractions of several species are reported versus the β parameter and compared with the experimental measurements (points).

Experimental data from: J.F. Roesler, M. Martinot, C.S. McEnally, L.D. Pfefferle, J.L. Delfau, C. Vovelle, *Combustion and Flame*, 134 (2003) 249-260.

1. Introduction

Combustion and transport phenomena & laminar flames.

2. Numerical solution of 1D flames

- a) Premixed laminar flames
 - i. Burner stabilized unstretched (or flat) flame
 - Governing equations and modeling aspects
 - Numerical solution
 - ii. Freely-propagating unstretched (or flat) flame
 - Governing equations and modeling aspects
- b) Counterflow diffusion flames

3. Multidimensional flames

- a) Introduction and examples
- b) Governing equations**
- c) Numerical algorithms for multidimensional flames
- d) The operator-splitting method

Governing equation for multi-dimensional flows

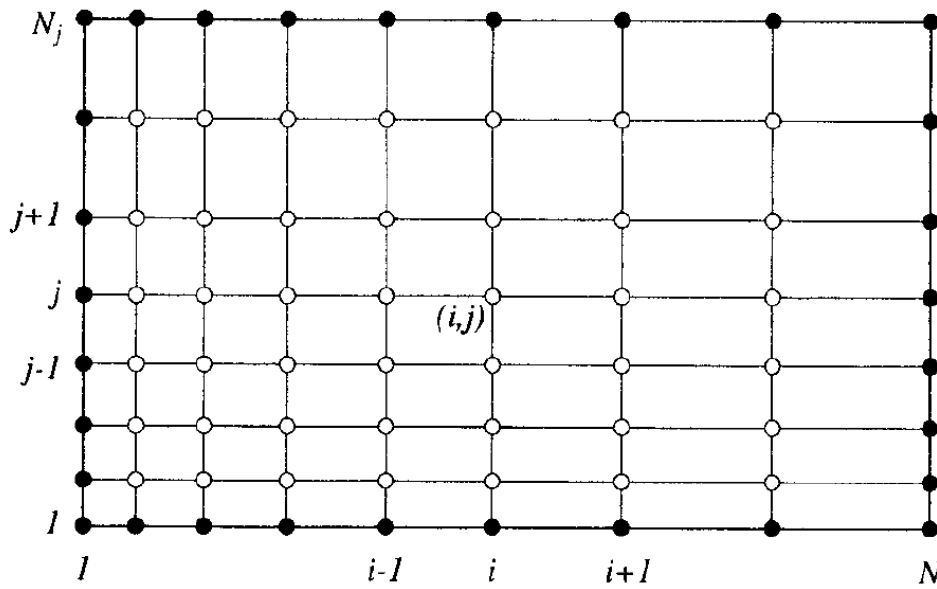
$$\left\{ \begin{array}{l} \frac{\partial \rho}{\partial t} + \nabla \cdot (\rho \mathbf{u}) = 0 \\[10pt] \frac{\partial(\rho \mathbf{u})}{\partial t} + \nabla \cdot (\rho \mathbf{u} \otimes \mathbf{u}) = -\nabla p + \nabla \cdot \mu \left(\nabla \mathbf{u} + \nabla \mathbf{u}^T - \frac{2}{3} (\nabla \cdot \mathbf{u}) I \right) + \rho \mathbf{g} \\[10pt] \rho \frac{\partial Y_i}{\partial t} + \rho \mathbf{u} \cdot \nabla Y_i = \nabla \cdot (\rho \mathcal{D}_i \nabla Y_i) + \dot{\Omega}_i \\[10pt] \rho C_P \frac{DT}{Dt} = \frac{Dp}{Dt} + \nabla \cdot \lambda \nabla T - \sum \rho \mathbf{u}_i^d Y_i C_{Pi} \cdot \nabla T + \dot{Q} \end{array} \right.$$

2D equations in Cartesian coordinates

$$\left\{ \begin{array}{l} \frac{\partial \rho}{\partial t} = -\frac{\partial}{\partial x}(\rho u) - \frac{\partial}{\partial y}(\rho v) \\ \rho \frac{\partial u}{\partial t} = -\rho u \frac{\partial u}{\partial x} - \rho v \frac{\partial u}{\partial y} - \frac{\partial P}{\partial x} + \frac{\partial}{\partial x} \left(\mu \frac{\partial u}{\partial x} \right) + \frac{\partial}{\partial y} \left(\mu \frac{\partial u}{\partial y} \right) + \mathcal{S}_x + \rho g_x \\ \rho \frac{\partial v}{\partial t} = -\rho u \frac{\partial v}{\partial x} - \rho v \frac{\partial v}{\partial y} - \frac{\partial P}{\partial y} + \frac{\partial}{\partial x} \left(\mu \frac{\partial v}{\partial x} \right) + \frac{\partial}{\partial y} \left(\mu \frac{\partial v}{\partial y} \right) + \mathcal{S}_y + \rho g_y \\ \rho \frac{\partial Y_i}{\partial t} = -\rho u \frac{\partial Y_i}{\partial x} - \rho v \frac{\partial Y_i}{\partial y} + \frac{\partial}{\partial x} \left(\rho \mathcal{D}_i \frac{\partial Y_i}{\partial x} \right) + \frac{\partial}{\partial y} \left(\rho \mathcal{D}_i \frac{\partial Y_i}{\partial y} \right) + \dot{\Omega}_i \\ \rho C_P \frac{\partial T}{\partial t} = -\rho C_P \left(u \frac{\partial T}{\partial x} + v \frac{\partial T}{\partial y} \right) + \frac{Dp}{Dt} + \frac{\partial}{\partial x} (\lambda T) - \frac{\partial}{\partial y} (\lambda T) + \dots \\ \dots + \sum \rho C_{Pi} \mathcal{D}_i \frac{\partial Y_i}{\partial x} \frac{\partial T}{\partial x} + \sum \rho C_{Pi} \mathcal{D}_i \frac{\partial Y_i}{\partial y} \frac{\partial T}{\partial y} + \dot{Q} \end{array} \right.$$

The method of lines (I)

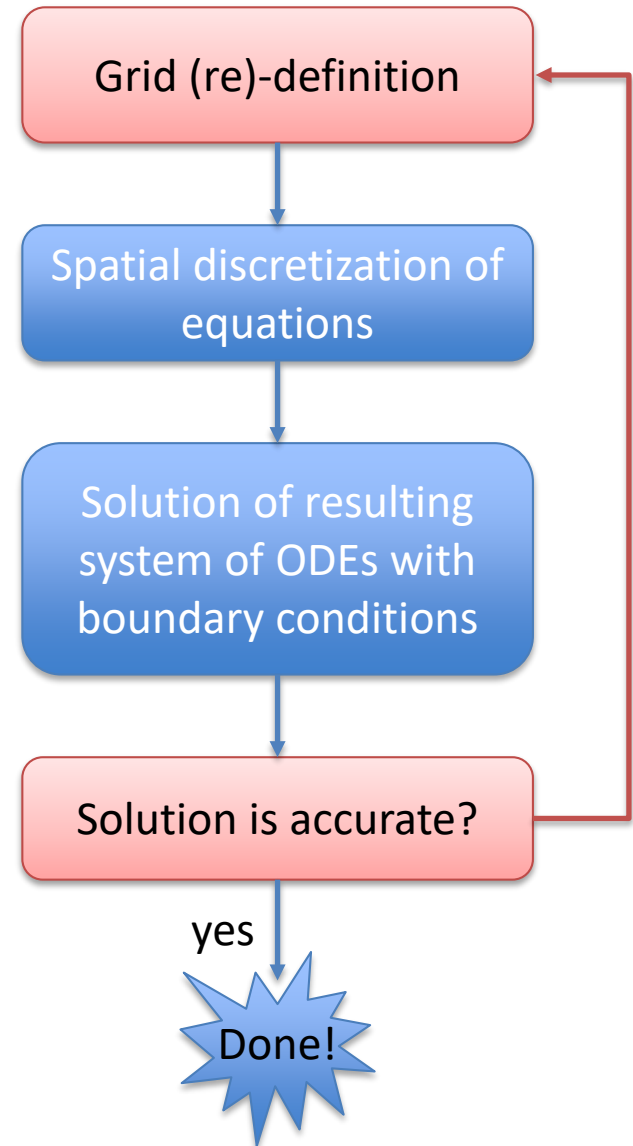
Structured orthogonal mesh in 2D (NP points)



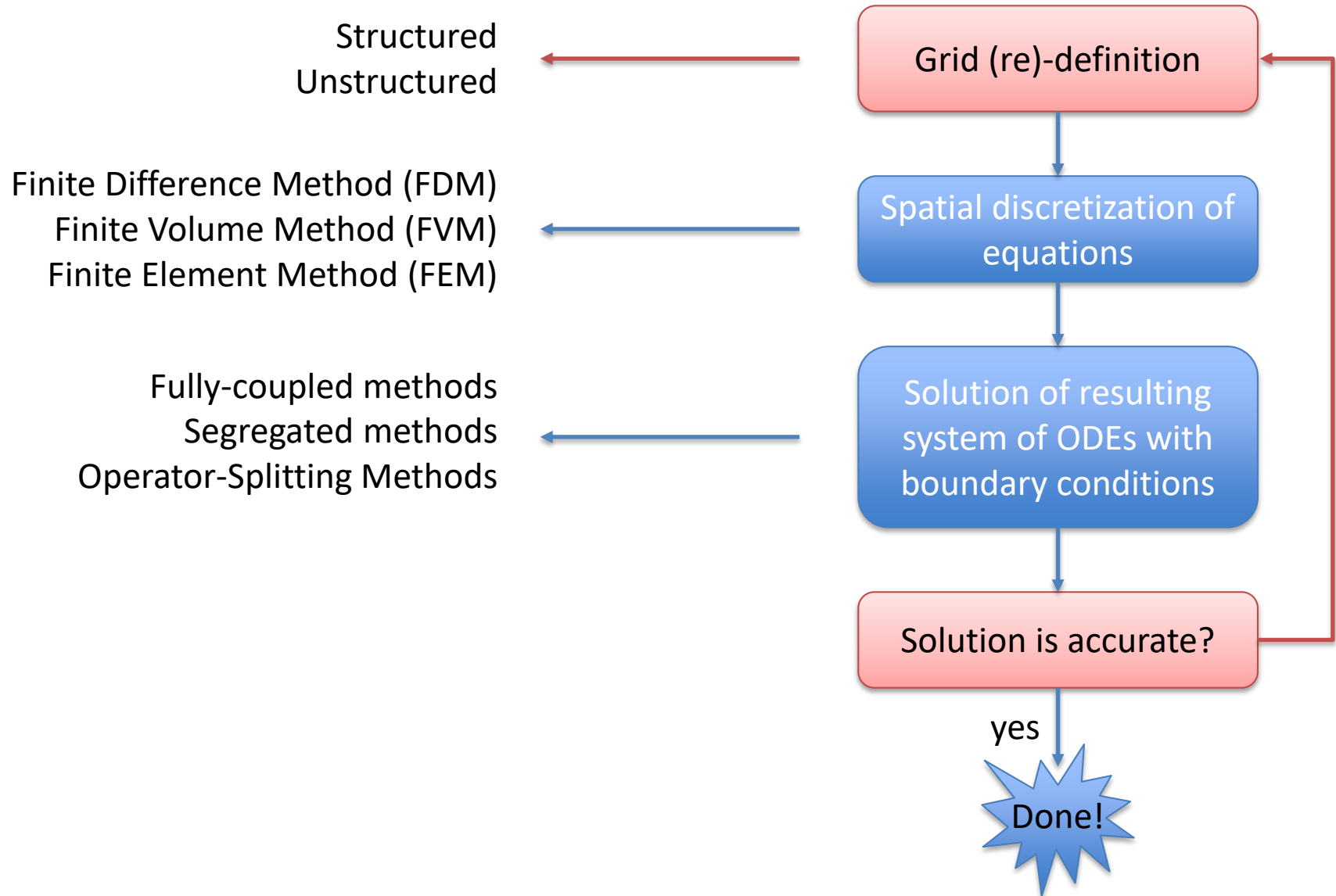
System of M Partial Differential Equations



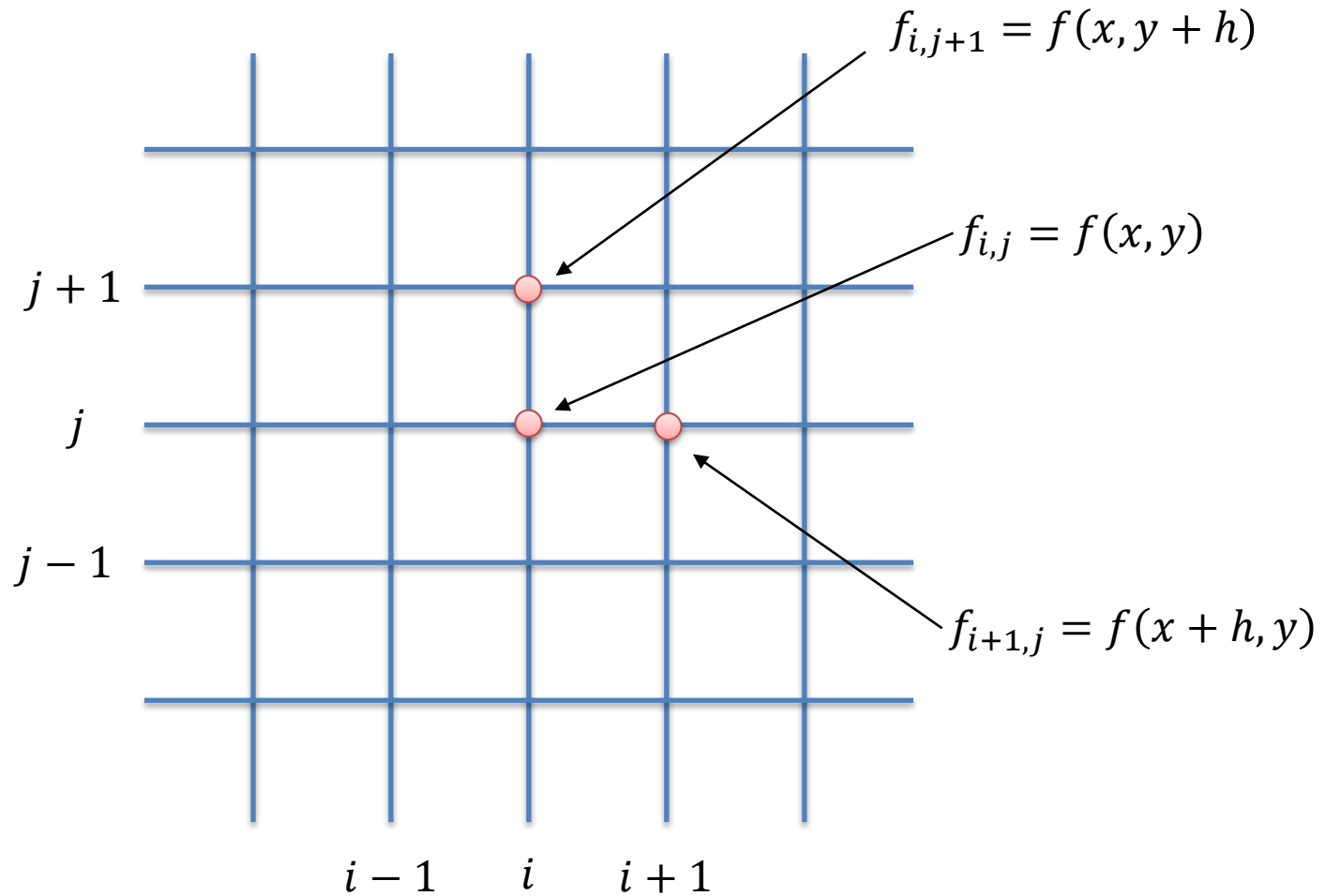
System of $M \times NP$ Ordinary Differential Equations with Boundary Conditions



The method of lines (I)



FDM: Structured orthogonal mesh in 2D



FDM: Discretization in space

Following the same procedure we adopted for the 1D cases, starting from the 2D advection-diffusion equation:

$$\frac{\partial f}{\partial t} + u \frac{\partial f}{\partial x} + v \frac{\partial f}{\partial y} = \Gamma \left(\frac{\partial^2 f}{\partial x^2} + \frac{\partial^2 f}{\partial y^2} \right)$$

we can easily obtain the corresponding finite-difference discretization:

$$\begin{aligned} \frac{\partial f_j}{\partial t} \approx & -u \frac{f_{i+1,j}^n - f_{i-1,j}^n}{2h} - v \frac{f_{i,j+1}^n - f_{i,j-1}^n}{2h} + \dots \\ & \dots + \Gamma \left(\frac{f_{i+1,j}^n - 2f_{i,j}^n + f_{i-1,j}^n}{h^2} + \frac{f_{i,j+1}^n - 2f_{i,j}^n + f_{i,j-1}^n}{h^2} \right) \end{aligned}$$

1. Introduction

Combustion and transport phenomena & laminar flames.

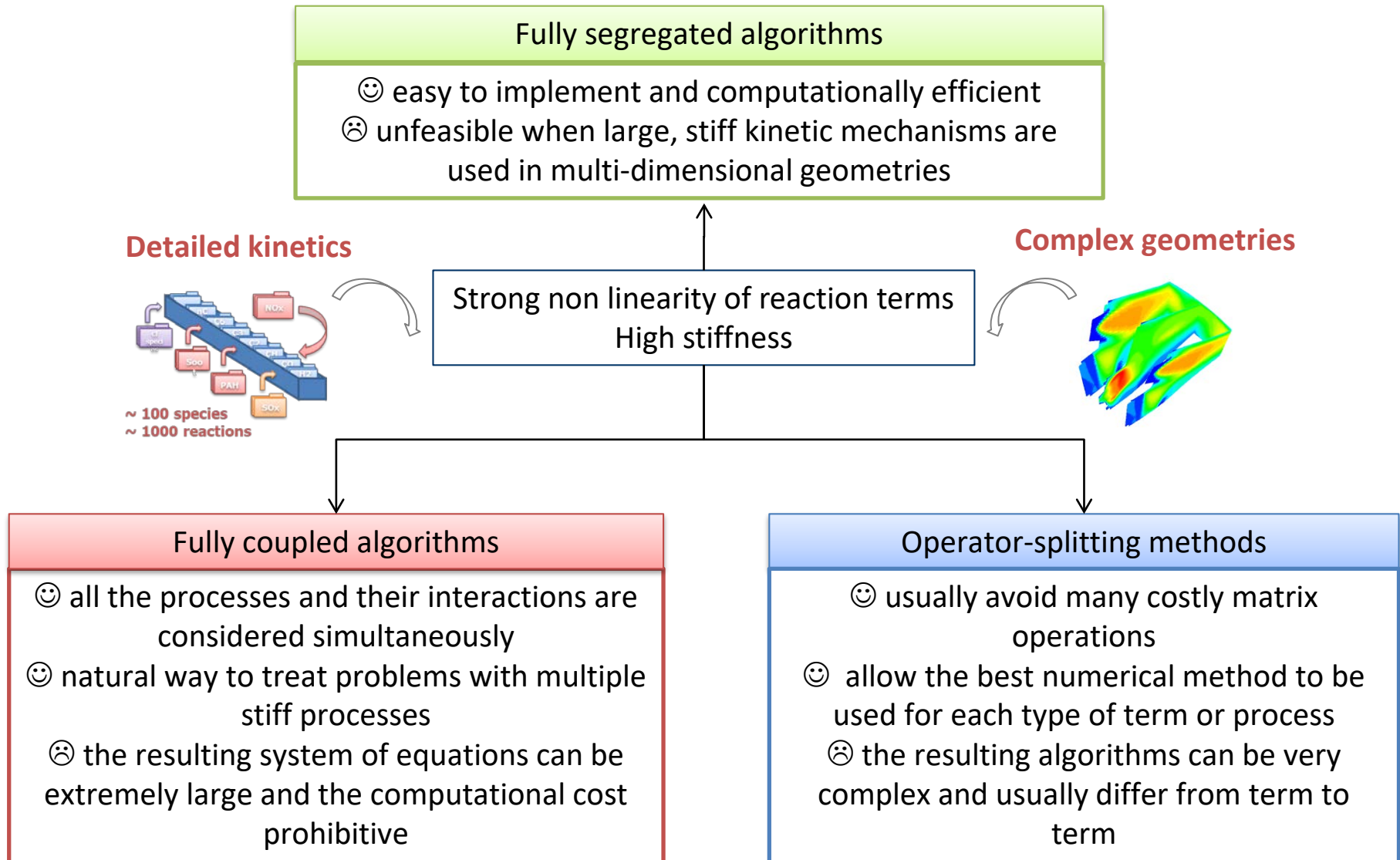
2. Numerical solution of 1D flames

- a) Premixed laminar flames
 - i. Burner stabilized unstretched (or flat) flame
 - Governing equations and modeling aspects
 - Numerical solution
 - ii. Freely-propagating unstretched (or flat) flame
 - Governing equations and modeling aspects
- b) Counterflow diffusion flames

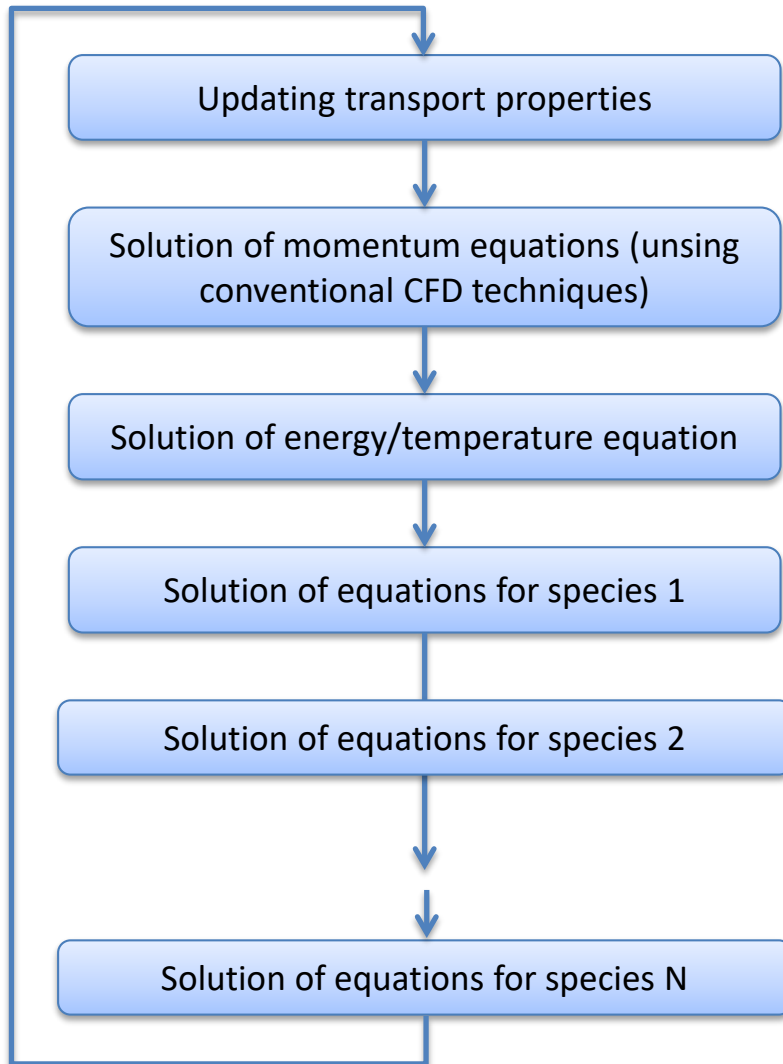
3. Multidimensional flames

- a) Introduction and examples
- b) Governing equations
- c) Numerical algorithms for multidimensional flames**
- d) The operator-splitting method

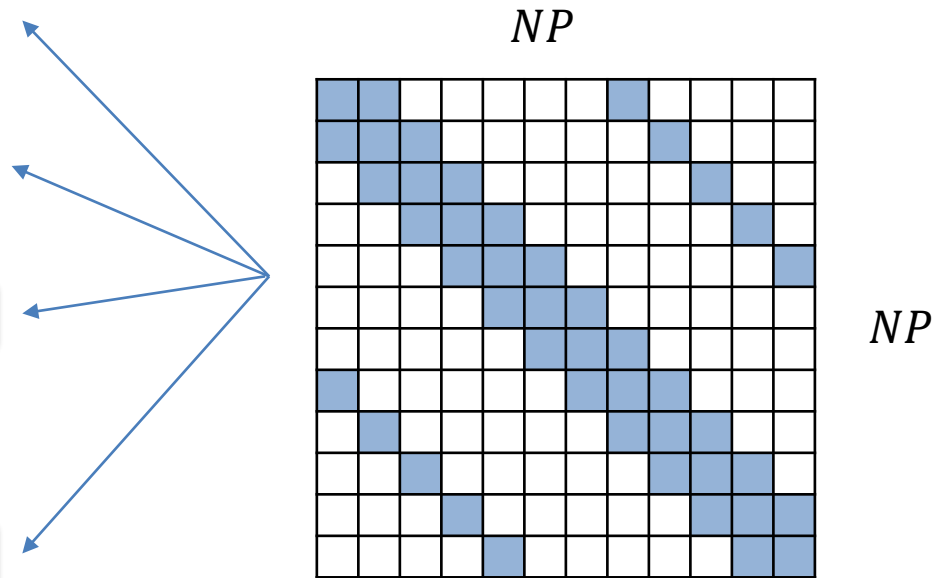
Methods for multi-dimensional reacting flows



Segregated approach

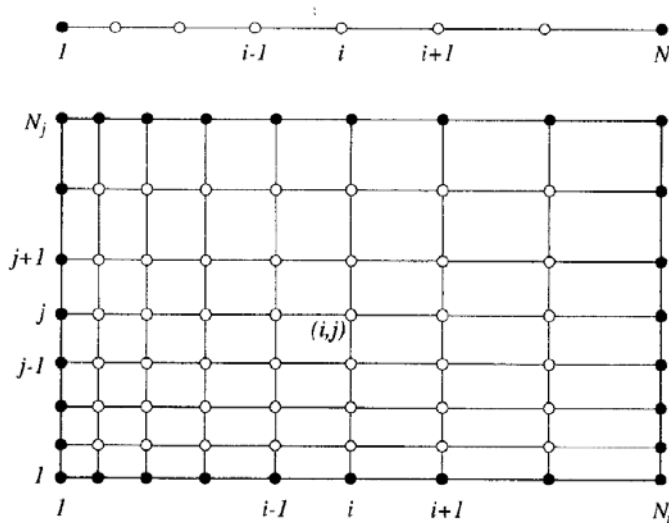


- usually does not work for stiff problems
- in laminar cases has strong issues about stability
- very easy to implement
- very low memory requirements
- It is a good approach for weakly non-linear, loosely coupled equations



Jacobian matrix sparsity pattern

Fully-coupled approach (I)



Example: 2D case

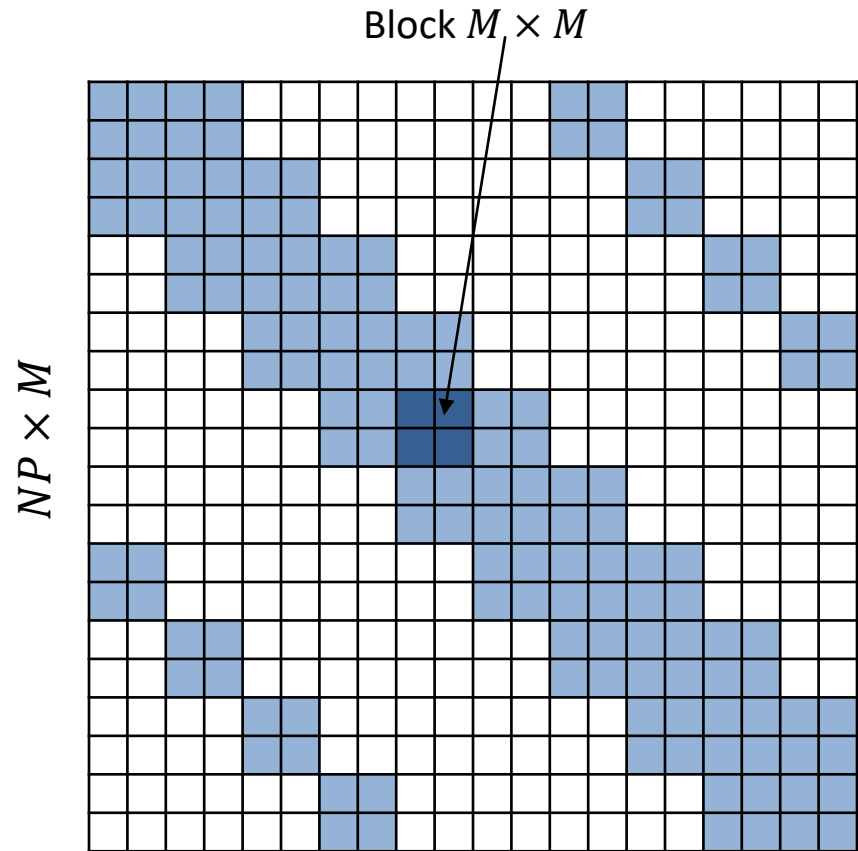
100 points x 100 points x 500 species $\sim 5,000,000$ eqs

Single block dimension $\sim 500 \times 500 = 250,000$

Example: 3D case

$(100 \text{ points})^3 \times 500 \text{ species} \sim 500,000,000$ eqs

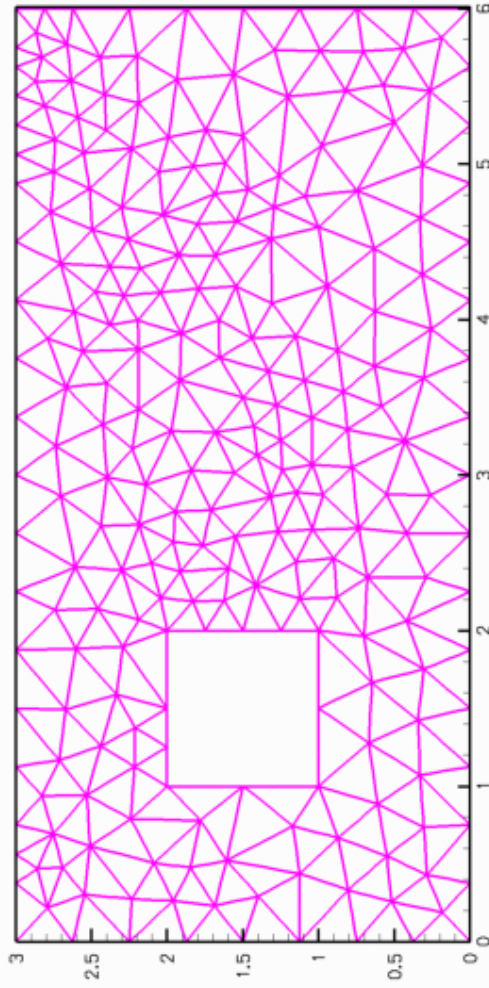
Single block dimension $\sim 500 \times 500 = 250,000$



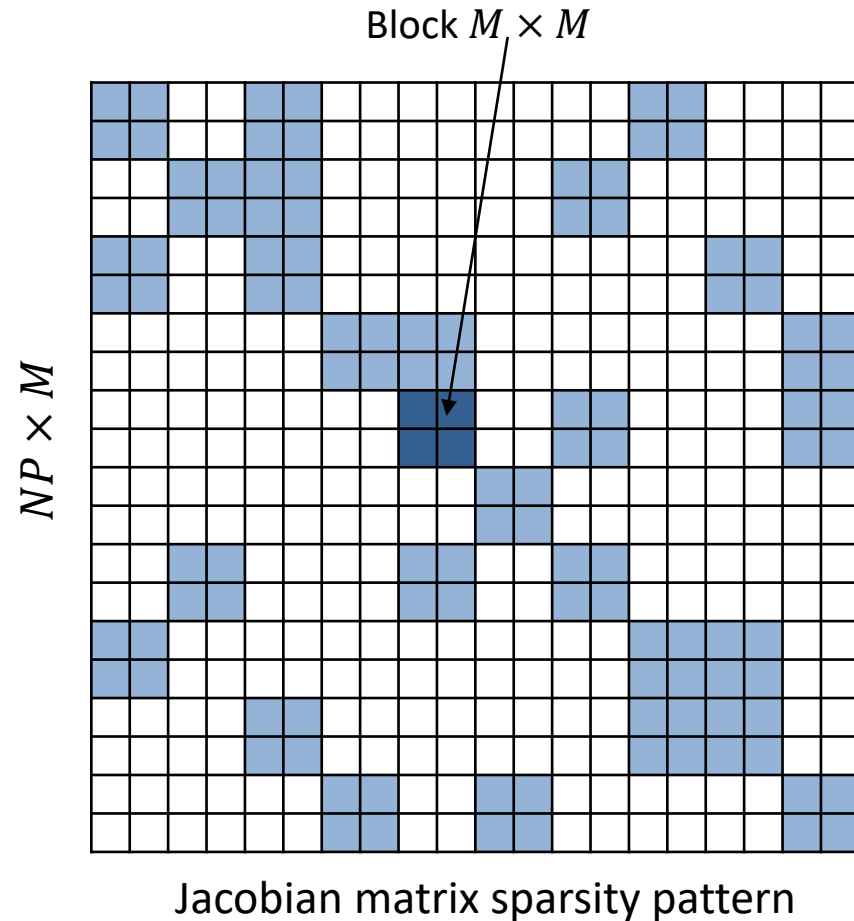
Jacobian matrix sparsity pattern

Fully-coupled methods are unsuitable for 3D (and in most cases also for 2D) when detailed kinetic mechanisms are employed

Unstructured meshes



Unstructured 2D mesh with
triangular cells



1. Introduction

Combustion and transport phenomena & laminar flames.

2. Numerical solution of 1D flames

- a) Premixed laminar flames
 - i. Burner stabilized unstretched (or flat) flame
 - Governing equations and modeling aspects
 - Numerical solution
 - ii. Freely-propagating unstretched (or flat) flame
 - Governing equations and modeling aspects
- b) Counterflow diffusion flames

3. Multidimensional flames

- a) Introduction and examples
- b) Governing equations
- c) Numerical algorithms for multidimensional flames
- d) The operator-splitting method**

Operator-splitting methods (I)

$$\frac{\partial \Psi}{\partial t} = \mathbf{f} \quad \Rightarrow \quad \frac{\partial \Psi}{\partial t} = \mathbf{f}_1 + \mathbf{f}_2 + \mathbf{f}_3 + \cdots + \mathbf{f}_M$$

Oran, Boris, *Numerical simulation of reactive flows*, Cambridge University Press (2001)

The right hand side function \mathbf{f} has been broken into M different (constituent) processes

$$\begin{cases} \Delta \Psi_1^n = \Delta t \mathbf{f}_1^n \\ \Delta \Psi_2^n = \Delta t \mathbf{f}_2^n \\ \Delta \Psi_3^n = \Delta t \mathbf{f}_3^n \\ \dots \\ \Delta \Psi_M^n = \Delta t \mathbf{f}_M^n \end{cases}$$

$$\mathbf{f} = \mathbf{f}_1 + \mathbf{f}_2 + \mathbf{f}_3 + \cdots + \mathbf{f}_M$$

convection diffusion reaction

Each function in the set \mathbf{f} contributes some amount to the overall change in Ψ during the numerical time step

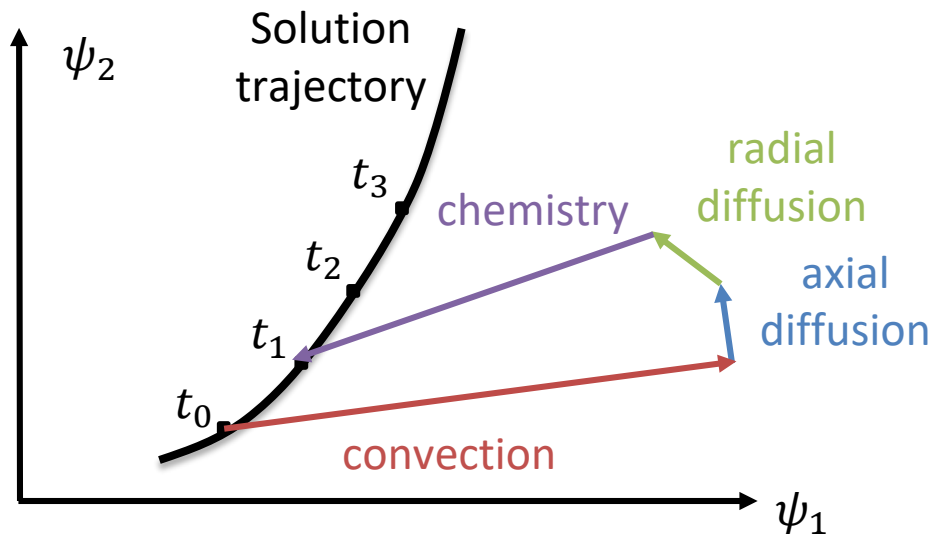
$$\Psi^{n+1} = \Psi^n + \sum_{m=1}^M \Delta \Psi_m^n$$

The solution for the new values Ψ^{n+1} is found by summing all of the partial contributions

Operator-splitting methods (II)

Each process is simulated individually and the results are combined together

- ✓ allow the best numerical method to be used for each type of term or process (modular simulation paradigm)
- ✓ Parallel architectures can be better exploited
- ✓ the time step must be chosen carefully, in order to avoid instabilities (stability is not guaranteed)
- ✓ Less strain on computational resources, but more efforts on the part of the modeler

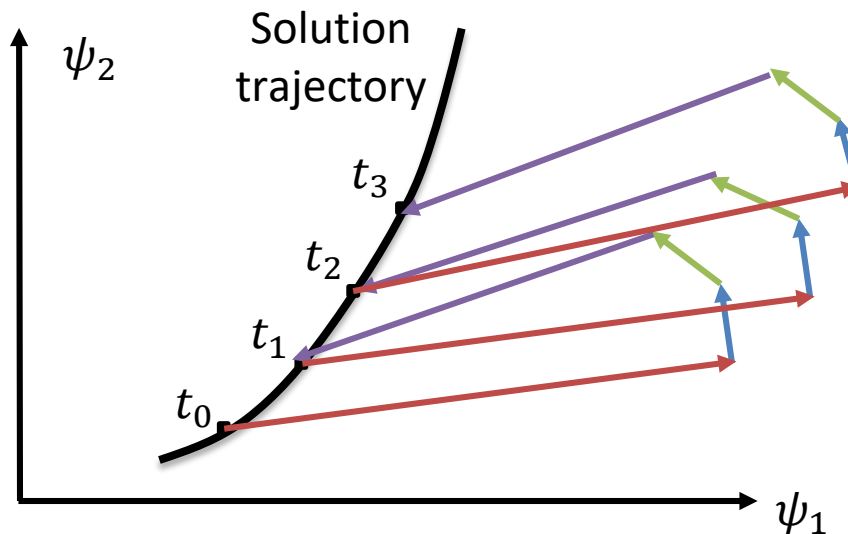


Adapted from: **Oran, Boris**, *Numerical simulation of reactive flows*, Cambridge University Press (2001)

Operator-splitting methods (III)

Each process is simulated individually and the results are combined together

- ✓ allow the best numerical method to be used for each type of term or process (modular simulation paradigm)
- ✓ Parallel architectures can be better exploited
- ✓ the time step must be chosen carefully, in order to avoid instabilities (stability is not guaranteed)
- ✓ Less strain on computational resources, but more efforts on the part of the modeler



Adapted from: **Oran, Boris**, *Numerical simulation of reactive flows*, Cambridge University Press (2001)

In steady-state conditions, each loop closes perfectly since the solution does not change

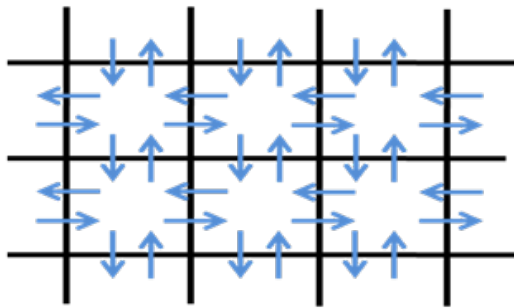
Operator-splitting method: a naïve implementation (I)

$$\frac{d\psi}{dt} = \mathbf{M} + \mathbf{S}$$

Transport
(convection + diffusion)
Chemistry
(reactions)

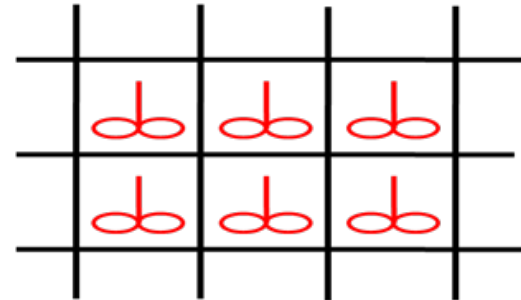
$$\begin{cases} \Delta\psi_1^n = \Delta t \mathbf{M}^n \\ \Delta\psi_2^n = \Delta t \mathbf{S}^n \end{cases}$$

Transport step (Δt)



$$\frac{d\psi}{dt} = \mathbf{M}$$

Chemical step (Δt)

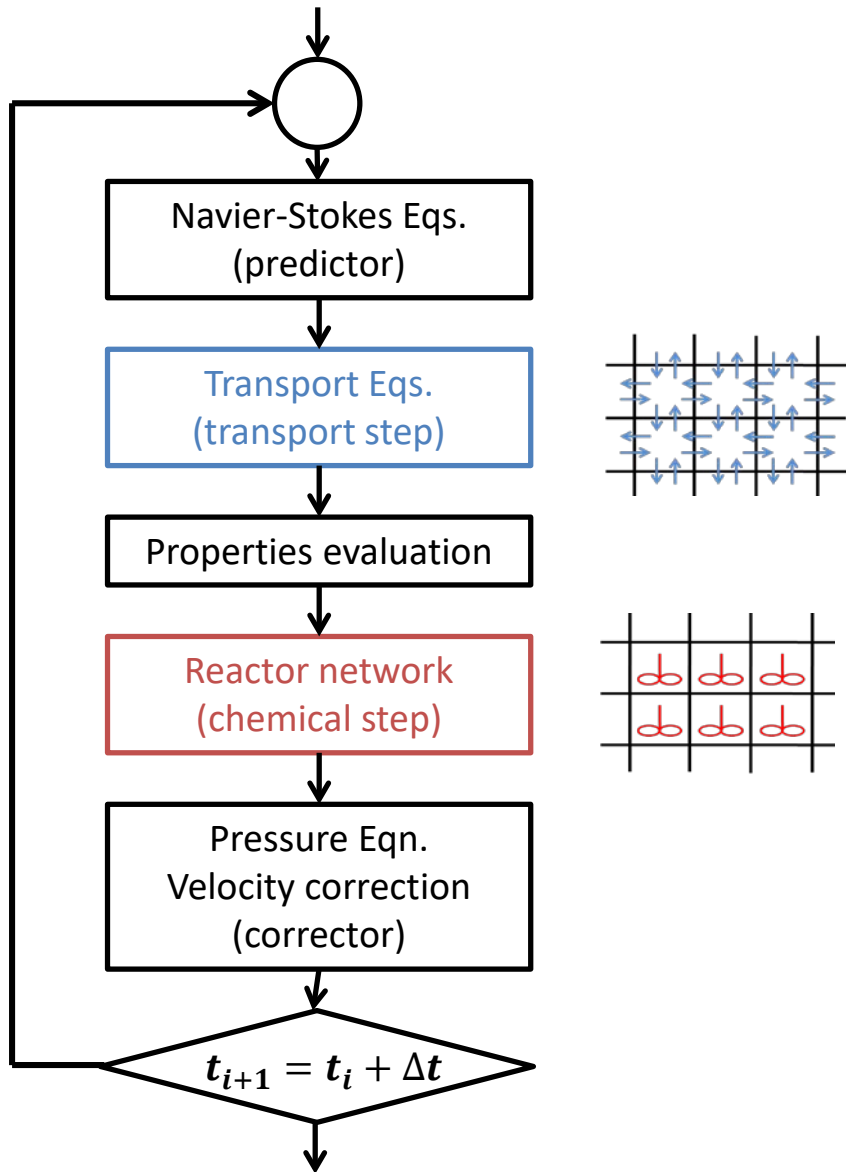


$$\frac{d\psi}{dt} = \mathbf{S}$$

Strang, *On the construction and comparison of difference schemes*. SIAM Journal of Numerical Analysis, 5, p. 506-517 (1968)

Ren, Pope, *Second-order splitting schemes for a class of reactive systems*. Journal of Computational Physics, 227 p. 8165-8176 (2008)

Operator-splitting method: a naïve implementation (II)



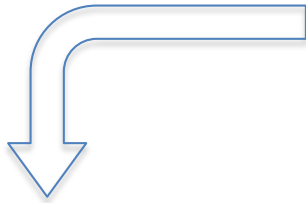
Navier-Stokes equations are solved using one of the conventional techniques adopted in CFD of non reactive flows (SIMPLE, PISO, projection algorithm, etc.)

The transport (convection + diffusion) equations, weakly non linear, can be solved using a **segregated approach**. Linearization is usually adopted

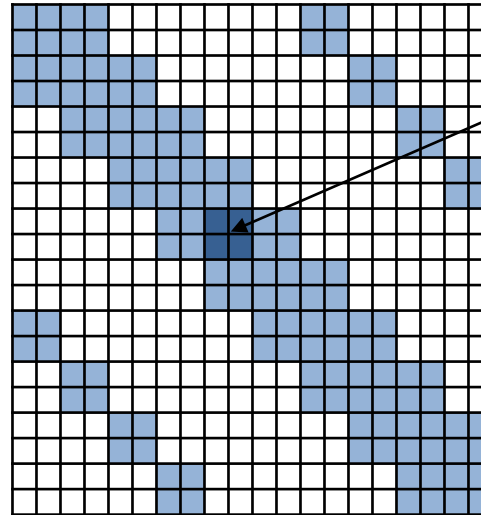
The chemical step corresponds to the solution of **NP independent ODE systems** with IC (i.e. NP independent batch reactors). Here we can exploit **fully-coupled methods**

Operator-splitting = segregated + fully-coupled (I)

Transport step

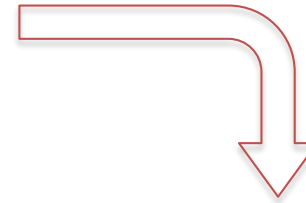


$NP \times M$

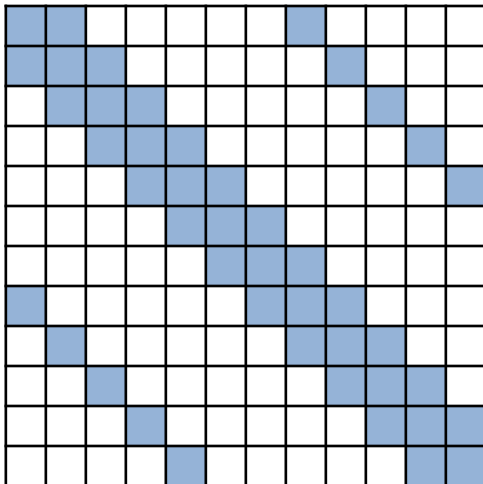


Block $M \times M$

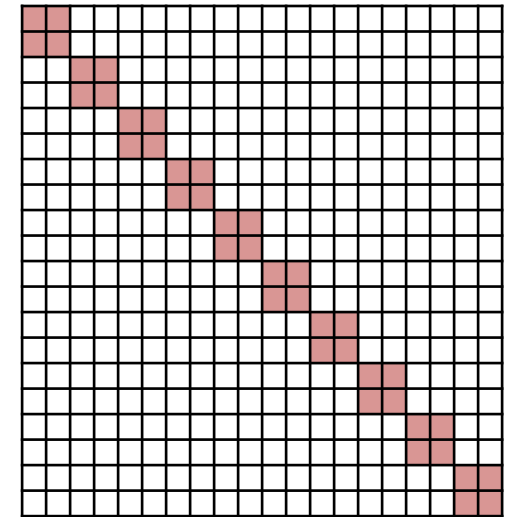
Chemical step



NP



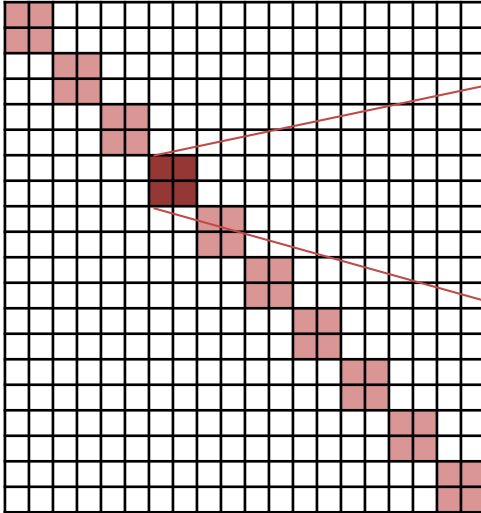
Solution of $N+1$ ODE systems
with size NP



Solution of NP ODE systems
with size $(N+1)$

Operator-splitting = segregated + fully-coupled (II)

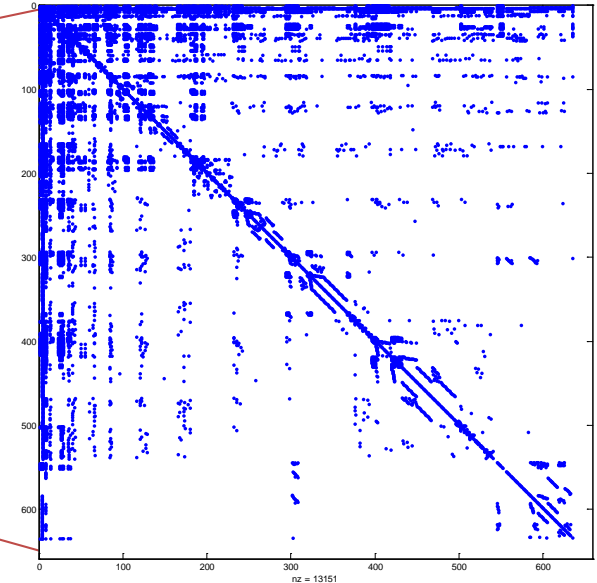
Chemical step



Solution of NP ODE systems
with size (N+1)

The chemical steps is equivalent
to the solution of NP
independent batch reactors:

$$\begin{cases} \rho \frac{dY_i}{dt} = \dot{\Omega}_i \\ \rho C_P \frac{dT}{dt} = \dot{Q} \end{cases}$$



Thus we can use exactly the
same numerical techniques we
discussed/presented for 0D
reacting systems, including the
possibility to exploit the
sparsity pattern of local
Jacobian matrices

Strang method (2nd order)

System of ODEs with boundary conditions

$$\frac{d\boldsymbol{\psi}}{dt} = \underbrace{\mathbf{M}(\boldsymbol{\psi}, \boldsymbol{\varphi}(\boldsymbol{\psi}), t)}_{\text{convection + diffusion}} + \underbrace{\mathbf{S}(\boldsymbol{\psi}, \boldsymbol{\varphi}(\boldsymbol{\psi}))}_{\text{chemistry}}$$

$\boldsymbol{\psi}$ Primary variables (mass fractions and composition)

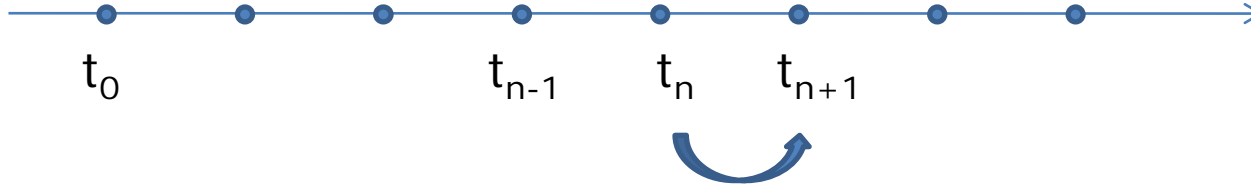
Usually \mathbf{S} is not an explicit function of time

$\boldsymbol{\varphi}(\boldsymbol{\psi})$ Secondary variables (transport properties, kinetic constants, etc.)

\mathbf{M} can be an explicit function of time through time-varying boundary conditions

1. Usually \mathbf{S} is a stiff operator
2. Usually $\boldsymbol{\varphi}(\boldsymbol{\psi})$ the evaluation of secondary variables is computationally expensive

Strang method (2nd order) (I)



Sub-step 1: chemistry integration (chemical step)

$$\begin{cases} \frac{d\boldsymbol{\Psi}^{(a)}}{dt} = \mathbf{S}(\boldsymbol{\Psi}^{(a)}, \boldsymbol{\varphi}(\boldsymbol{\Psi}^{(a)})) \\ \boldsymbol{\Psi}^{(a)}(t_n) = \boldsymbol{\Psi}(t_n) \end{cases} \quad t \in \left[t_n; t_n + \frac{\Delta t}{2} \right]$$

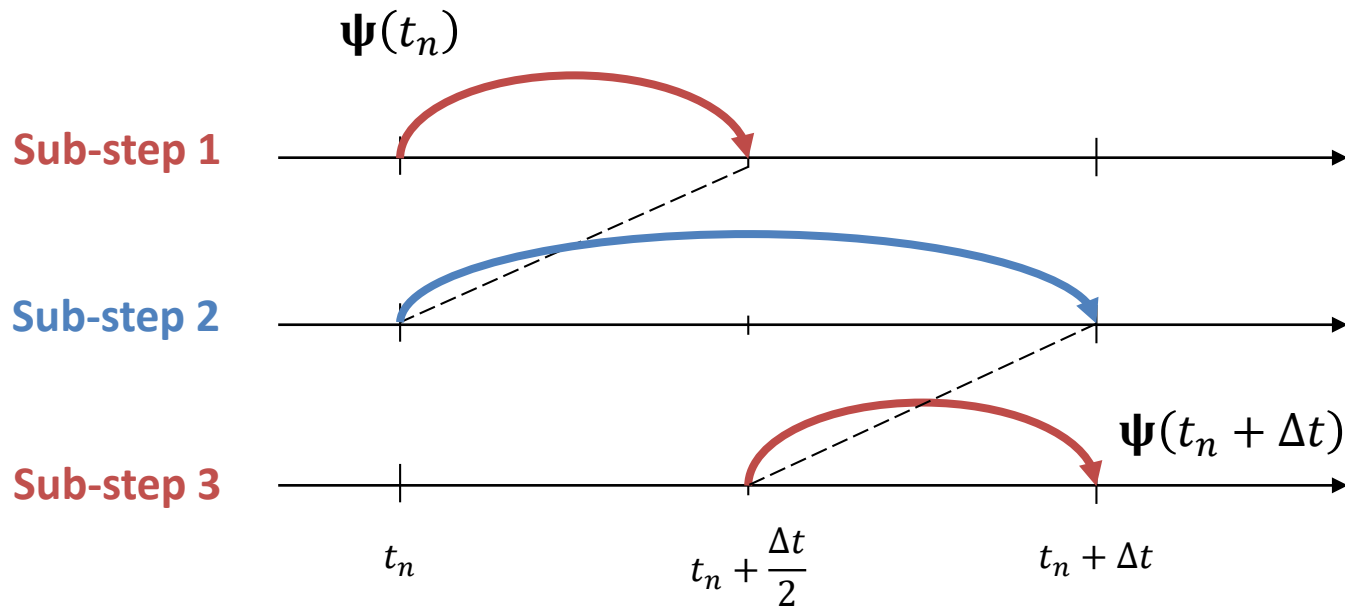
Sub-step 2: transport integration (transport step)

$$\begin{cases} \frac{d\boldsymbol{\Psi}^{(b)}}{dt} = \mathbf{M}(\boldsymbol{\Psi}^{(b)}, \boldsymbol{\varphi}(\boldsymbol{\Psi}^{(b)}), t) \\ \boldsymbol{\Psi}^{(b)}(t_n) = \boldsymbol{\Psi}^{(a)}\left(t_n + \frac{\Delta t}{2}\right) \end{cases} \quad t \in [t_n; t_n + \Delta t]$$

Strang method (2nd order) (II)

Sub-step 3: chemistry integration (chemical step)

$$\begin{cases} \frac{d\boldsymbol{\Psi}^{(a)}}{dt} = \mathbf{S}\left(\boldsymbol{\Psi}^{(a)}, \boldsymbol{\varphi}(\boldsymbol{\Psi}^{(a)})\right) \\ \boldsymbol{\Psi}^{(a)}\left(t_n + \frac{\Delta t}{2}\right) = \boldsymbol{\Psi}^{(b)}(t_n + \Delta t) \end{cases} \quad t \in \left[t_n + \frac{\Delta t}{2}; t_n + \Delta t\right]$$



Improving the efficiency (I)

Sub-step 2.a: Prediction

$$\begin{cases} \frac{d\Psi^{(p)}}{dt} = \mathbf{M}(\Psi^{(p)}, \boldsymbol{\varphi}^{(0)}, t) \\ \Psi^{(p)}(t_n) = \Psi^{(a)}\left(t_n + \frac{\Delta t}{2}\right) \end{cases}$$

Only 1 calculation of secondary variables

$$\boldsymbol{\varphi}^{(0)} = \boldsymbol{\varphi}\left(\Psi^{(a)}\left(t_n + \frac{\Delta t}{2}\right)\right)$$

Sub-step 2.b: Correction

$$\begin{cases} \frac{d\Psi^{(c)}}{dt} = \frac{1}{2}\mathbf{M}(\Psi^{(c)}, \boldsymbol{\varphi}^{(0)}, t) + \frac{1}{2}\mathbf{M}(\Psi^{(c)}, \boldsymbol{\varphi}^{(p)}, t) \\ \Psi^{(c)}(t_n) = \Psi^{(a)}\left(t_n + \frac{\Delta t}{2}\right) \end{cases}$$

Only 1 calculation of secondary variables

$$\boldsymbol{\varphi}^{(p)} = \boldsymbol{\varphi}\left(\Psi^{(p)}(t_n + \Delta t)\right)$$

Improving the efficiency (II)

Sub-step 2.b: Correction

The step correction can also be formulated differently, although more expensive in terms of calculation time:

$$\varphi^{(p)} = \varphi^{(0)} + (\psi^{(p)} - \psi^{(0)}) \nabla_r \varphi \Big|_{\psi=\psi^{(0)}}$$

To evaluate the $\nabla_r \varphi \Big|_{\psi=\psi^{(0)}}$ term numerically (through incremental ratios) it is necessary to calculate the secondary variables at least $N + 1$ times

Ren Z., Pope S.B., “Second order splitting schemes for a class of reactive systems”, Journal of Computational Physics, 227 (2008) 8165-8176

Linearization of transport step

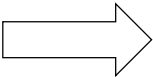
Sub-step 2: Linearization

The transport term can alternatively be linearized around the initial condition:

$$M_i(\Psi, \varphi(\Psi), t) \approx M_i(\Psi^{(0)}, \varphi^{(0)}, t) + \sum_k \frac{\partial M_i}{\partial \psi_k} (\psi_k - \psi_k^0) + \sum_k \sum_j \frac{\partial M_i}{\partial \varphi_j} \frac{\partial \varphi_j}{\partial \psi_k} (\psi_k - \psi_k^0)$$

$$M_i(\Psi, \varphi(\Psi), t) \approx M_i(\Psi^{(0)}, \varphi^{(0)}, t) + \sum_k \left[\frac{\partial M_i}{\partial \psi_k} + \sum_j \frac{\partial M_i}{\partial \varphi_j} \frac{\partial \varphi_j}{\partial \psi_k} \right] (\psi_k - \psi_k^0)$$

$$M_i(\Psi, \varphi(\Psi), t) \approx M_i^{(0)} + \sum_k D_{ik}^{(0)} (\psi_k - \psi_k^0) \quad D_{ik}^{(0)} \stackrel{\text{def}}{=} \frac{\partial M_i}{\partial \psi_k} + \sum_j \frac{\partial M_i}{\partial \varphi_j} \frac{\partial \varphi_j}{\partial \psi_k}$$


$$\left\{ \begin{array}{l} \frac{d\psi_i^{(b)}}{dt} = M_i^{(0)} + \sum_k D_{ik}^{(0)} (\psi_k - \psi_k^0) \\ \psi_i^{(b)}(t_n) = \psi_i^{(a)} \left(t_n + \frac{\Delta t}{2} \right) \end{array} \right.$$

The advantage is that now we have a system of linear ODEs

However, the calculation of matrix $D_{ik}^{(0)}$ can be expensive

Training Session 3 (optional)

- using the freely-propagating flame model to estimate the laminar flame speed of a fuel in air at different equivalence ratios
- getting familiar with the numerical solution of 1D problems via fully-coupled methods
- getting familiar with the concept of grid refinement